MICROCOPY RESOLUTION TEST CHART

NATIONAL BUREAU OF STANDARDS-1963-A

AFWAL-TR-84-2007

GC-FTIR OF JET FUELS

Mr. J.R. Cooper
Dr. L.T. Taylor

DEPARTMENT OF CHEMISTRY
VIRGINIA POLYTECHNIC INSTITUTE AND STATE UNIVERSITY
BLACKSBURG, VIRGINIA 24061-0699

February 1984

Final Report for Period 15 July 1982 - 15 August 1983
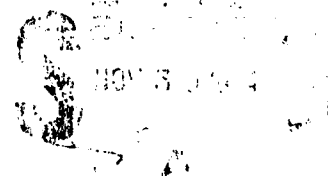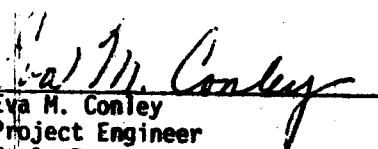
AD-A148 272

84 11 29 005

NOTICE

When Government drawings, specifications, or other data are used for any purpose other than in connection with a definitely related Government procurement operation, the United States Government thereby incurs no responsibility nor any obligation whatsoever, and the fact that the Government may have formulated, furnished, or in any way supplied the said drawings, specifications, or other data, is not to be regarded by implication or otherwise as in any manner licensing the holder of any other person or corporation, or conveying any rights or permission to manufacture, use, or sell any patented invention that may in any way be related thereto.

This report has been reviewed by the Office of Public Affairs (ASD/PA) and is releasable to the National Technical Information Service (NTIS). At NTIS, it will be available to the general public, including foreign nations.

This technical report has been reviewed and is approved for publication.

Eva M. Conley
Project Engineer
Fuels Branch
Fuels and Lubrication Division
Aero Propulsion Laboratory

Arthur V. Churchill
Chief, Fuels Branch
Fuels and Lubrication Division
Aero Propulsion Laboratory

FOR THE COMMANDER

R. D. SHERRILL
Chief, Fuels and Lubrication Division
Aero Propulsion Laboratory

"If your address has changed, if you wish to be removed from our mailing list or if the addressee is no longer employed by your organization, please notify AFWAL/POSF, WPAFB, OH 45433 to help us maintain a current mailing list."

Copies of this report should not be returned unless return is required by security considerations, contractual obligations, or notice on a specific document.

REPORT DOCUMENTATION PAGE	READ INSTRUCTIONS BEFORE COMPLETING FORM

1. REPORT NUMBER	2. GOVT ACCESSION NO.	3. RECIPIENT'S CATALOG NUMBER
AFWAL-TR-84-2007	AD-A148272	

4. TITLE *(and Subtitle)*	5. TYPE OF REPORT & PERIOD COVERED
GC-FTIR OF JET FUELS	Final July 1982 - August 1983
	6. PERFORMING ORG. REPORT NUMBER

7. AUTHOR(s)	8. CONTRACT OR GRANT NUMBER(s)
John R. Cooper Larry T. Taylor	F33615-82-C-2258

9. PERFORMING ORGANIZATION NAME AND ADDRESS	10. PROGRAM ELEMENT, PROJECT, TASK AREA & WORK UNIT NUMBERS
Department of Chemistry Virginia Polytechnic Institute & State University Blacksburg, VA 24061-0699	PE 62203F Project 3048 W.U. 30480531

11. CONTROLLING OFFICE NAME AND ADDRESS	12. REPORT DATE
Aero Propulsion Laboratory (AFWAL/POSF) Air Force Wright Aeronautical Laboratories (AFSC) Wright-Patterson Air Force Base, Ohio 45433	February 1984
	13. NUMBER OF PAGES
	143

14. MONITORING AGENCY NAME & ADDRESS(if different from Controlling Office)	15. SECURITY CLASS. (of this report)
	Unclassified
	15a. DECLASSIFICATION/DOWNGRADING SCHEDULE

16. DISTRIBUTION STATEMENT *(of this Report)*

Approved for public release; distribution unlimited

17. DISTRIBUTION STATEMENT *(of the abstract entered in Block 20, if different from Report)*

18. SUPPLEMENTARY NOTES

19. KEY WORDS *(Continue on reverse side if necessary and identify by block number)*

Fourier Transform Infrared Spectrometry   Jet Fuels
Gas Chromatography   Model Compounds
Detection Limits
Identification Limits

20. ABSTRACT *(Continue on reverse side if necessary and identify by block number)*

The successful interfacing and utilization of fused silica capillary (GC) columns with Fourier transform infrared spectrometry (FTIR) can introduce difficulties not usually encountered with lower efficiency (higher capacity) GC columns. Recognition of these difficulties, however, can lead to refinement of a GC-FTIR detection system which can analyze complex samples with low nanogram detection limits. Chromatographic and spectrometric considerations include lightpipe temperature, choice of same introduction, column concentration dynamic range capability, infrared data acquisition rate and spectral

DD ₁ FORM ₇₃ 1473   EDITION OF 1 NOV 65 IS OBSOLETE

S/N ratio. These parameters as they relate to capillary GC-FTIR method development are discussed.

GC-FTIR spectrometric "identification limits" for sixteen model compounds which represent both polar and non-polar functionalities have been established employing optimized chromatographic-spectrometric parameters for complex mixture analysis. Identification was considered positive when the spectral search routines correctly matched the known compound "on-the-fly" spectrum to a library file spectrum. Various experimental factors leading to successful compound identification are discussed. Linear absorbance/concentration relationships for each model compound are reported from IR data collected.

The GC-FTIR analysis of a complex sample is presented in an effort to explain these problems.

PREFACE

TABLE OF CONTENTS

LIST OF ILLUSTRATIONS

LIST OF ILLUSTRATIONS (cont.)

LIST OF ILLUSTRATIONS (cont.)

LIST OF TABLES

LIST OF TABLES (cont.)

LIST OF TABLES (cont.)

SECTION I

SCOPE OF THE PROJECT

The goals for this research involved four basic tasks: (1) optimize
the Gas Chromatograph/Fourier Transform Infrared Spectrometry
(GC/FTIR) experiment insofar as gas chromatographic separation, FTIR
detector, lightpipe cell and mode of injection are concerned, (2)
determine the qualitative detection limits and the specific compound
computer search identification limits for select model compounds of
widely differing functionality using the best GC/FTIR system, (3)
identify organic oxygen, nitrogen and sulfur functionalities in up to
ten fuel samples to be provided by the Air Force and (4) concentrate the
heteroatom components of the fuel samples by liquid chromatography prior
to their analysis by GC/FTIR.

1

SECTION II
TECHNICAL DISCUSSION

A. BACKGROUND

The advent of modern FTIR spectrometers offers improvements
and advantages over conventional dispersive infrared spectrophoto-
meters for detecting eluting components from a gas chromatograph(1).
Increased optical throughput, rapid-scanning of the IR region and
dedicated high-speed computers make possible routine high-resolution
infrared spectra.

While use of packed GC columns with FTIR detection can
provide valuable information(2,3) highly complex samples may require
the separating capability of capillary columns. The use of capillary
columns with FTIR, however, introduces interface considerations due
to lightpipe (broadening of peaks) and transfer line dead volume
(loss of chromatographic resolution). Initially, capillary GC/FTIR
analyses were generally confined to support coated open tubular
(SCOT) columns. The SCOT column provided more efficiency than a
packed column and also needed sample loading(4). Low FTIR detection
limits using SCOT columns have been reported(5) as well as their
applications in the analysis of environmental pollutants(6) and
peppermint oil(7) with FTIR detection.

GC/FTIR analyses with wall coated open tubular (WCOT)
capillary columns have also been demonstrated. Sample sizes for WCOT
are smaller than for SCOT columns but their efficiency is better than
the support coated column. Early work by Azarraga(8) and later by
Shafer et. al.(9) showed that the use of wide bore WCOT (glass)
capillary columns with FTIR detection was feasible. In this regard,
wide bore WCOT glass columns have been employed with FTIR to separate
and analyze complex samples such as priority pollutants(10) and
diesel fuel(11).

Despite the excellent separating capability of wide bore
WCOT glass columns (0.5-0.7 mm i.d.), more narrow fused silica
columns (0.2-0.35 mm i.d.) offer several advantages(12). Equally
narrow glass columns can also give better efficiency than wide bore
glass WCOT columns, but narrow fused silica columns provide added
efficiency plus greater flexibility and durability. Fused silica
columns, for example, can be inserted through transfer lines

2

resulting in a near zero dead volume path to the infrared lightpipe. Such fused silica columns are available with a stationary phase film thickness of 1 micron and can handle 500 ng per component (recommended limit) without displaying column over-loading characteristics(13). For the work reported here, a column with a μm film thickness was used to alleviate potential "concentration dynamic range" problems. For complex samples such as the jet fuel presented here, high concentrations of homologous alkanes may cause column overloading while minor components do not. A relatively thick film (1 μm) should be more appropriate for such concentration "chemically" dynamic samples. At least one example of a capillary separation somewhat limited by column concentration or "chemical" dynamic range has been presented in the literature with FTIR detection(6). A related discussion with reference to both thin (0.2-0.3 μm) and thick (0.8-1.2 μm) stationary films has also recently been given(14).

Proper optimization of capillary GC/FTIR conditions and parameters is frequently more critical when using narrow columns since FTIR scan rates must coincide with very narrow peak widths (on the order of seconds) and detection limits must lie in the low nanogram range. Although several reports have discussed the on-line coupling of fused silica WCOT columns with FTIR(14-16), the overall capability of fused silica column efficiency combined with low nanogram FTIR detection limits may not have been most clearly represented.

In this work, we report the application of fused silica capillary GC/FTIR to the separation and analysis of a complex jet fuel sample. An indication of the low level of measured FTIR detection is represented by performing quantitative studies on standard compounds similar to the components found in the "real" complex sample. Also discussed will be the effects of make-up gas, lightpipe temperature, and interferometer scan velocity with respect to FTIR sensitivity and chormatographic resolution. Efforts to establish computer search, specific compound identification limits for a wide variety of compounds will also be described.

3

B. OPTIMIZATION OF GC-FTIR APPROACH

1. Instrumentation

A Varian 3700 gas chromatograph with on-column injector
fitted for fused silica columns was interfaced to an external Nicolet
7000 lightpipe bench. The IR beam from a Nicolet 6000 FTIR was
brought out to the external bench via appropriate optics. A 1.5 mm
i.d. x 40 cm gold-coated lightpipe was operated at 230°C. A narrow
range liquid-nitrogen cooled mercury-cadmium-telluride (MCT) detector
(5000-700 cm^{-1} with a detectivity of 4×10^{10}) was used. A dry
nitrogen purge was available for both optics and lightpipe bench.

2. Spectral Parameters

Interferograms (2048 point) were taken resulting in 8 cm^{-1}
spectra. Twelve data scans were co-added (on-the-fly) resulting
in a data acquisition time frame of one file (12 data scans) per 1.08
seconds. A rapid interferometer velocity of 2.22 cm/sec (actual)
facilitated the fast data acquisition. The 3 mm diameter IR beam (at
focus on the KBr window of the lightpipe) resulted in adequate energy
throughput. All computer spectral search routines were performed
with Nicolet software utilizing an Environmental Protection Agency
(EPA) vapor phase library which contained 3310 spectra (reduced to 16
cm^{-1} resolution). A more in-depth discussion of the library search
routine can be found in the literature(17).

3. Sample and Capillary GC Conditions

A complex jet fuel sample was separated on a 60 meter x
0.33 mm i.d. DB-5 (chemically bonded; equivalent to SE-54) fused
silica column capable of 3010 plates per meter for C_{13} at K'=5.1.
The film thickness for the DB-5 was 1 μm. A jet fuel sample
(VN-77-11) was diluted 10x in chloroform and 0.5 μl of solution
injected using on-column injection. A linear flow velocity of 33

4

cm/sec helium was used with total gas flow through the 40 cm IR cell being 8 mL/min via nitrogen make-up gas. Preservation of chromatographic resolution was aided by insertion of the column through the transfer line (200°C) up to the IR cell entrance. The temperature program was 60°C for 5 min with a 4°C/min increase to 180°C.

4. GC Resolution versus FTIR Sensitivity

Variation of certain parameters (both spectrometric and chromatographic) may have a drastic influence on final results when performing a narrow bore capillary column GC/FTIR experiment. Data acquisition rate is one of these. Typical high resolution capillary GC separations can result in peak widths of only several seconds. With regard to such widths, several infrared absorbance "readings" of the complex sample component as it passes through the lightpipe are desirable. Too slow a data acquisition rate would obviously distort the true chromatographic resolution as well as create the possibility of not recording infrared data when the sample would be at its highest concentration in the lightpipe. A much faster data acquisition rate (i.e. files/second) may increase the chances of determining the sample component at the point of highest concentration in the lightpipe, however signal-to-noise ratio (S/N), may suffer enough to result in diminishing returns since fewer scans would be co-added. A compromise must be sought, therefore, between rapid data acquisition and a reasonable FTIR signal-to-noise ratio. We feel such an acquisition rate of ~1 file/second along with 12 coadded scans fulfills this reasonable compromise.

Figure 1 is a FTIR reconstructed chromatogram showing a portion of the separated jet fuel. The IR region 3150-2850 cm^{-1} was used in the reconstruction. This chromatogram follows closely the FID chromatogram (Figure 2) generated by using only FID detection. We feel that comparison of FID direct and FTIR reconstructed chromatograms may be more appropriate in determining dead volume contributions rather than an in-series FID trace (preceded by the
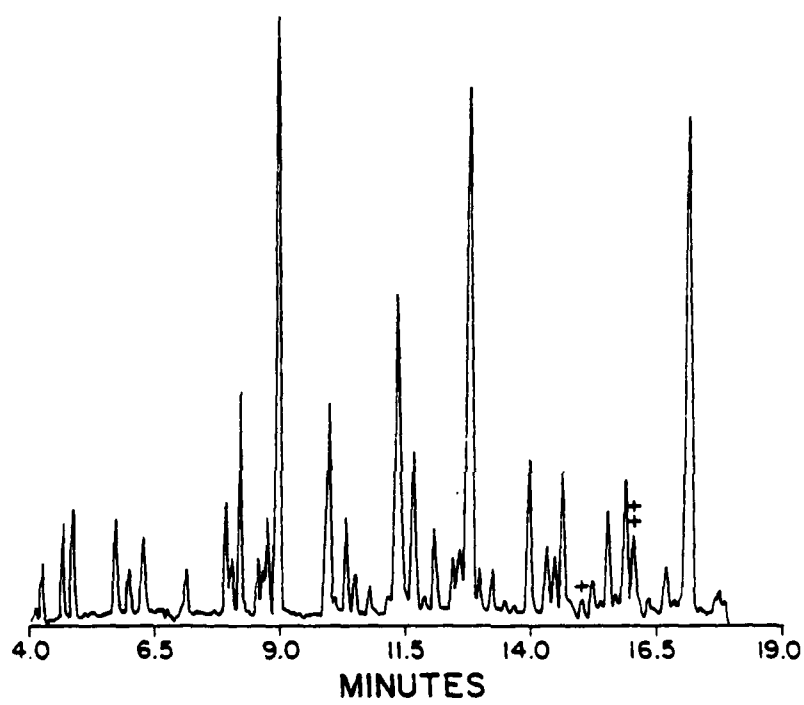
Figure 1.   FTIR reconstructed chromatogram: 3150-2850cm^{-1}
VN-77-11 Jet Fuel.

6
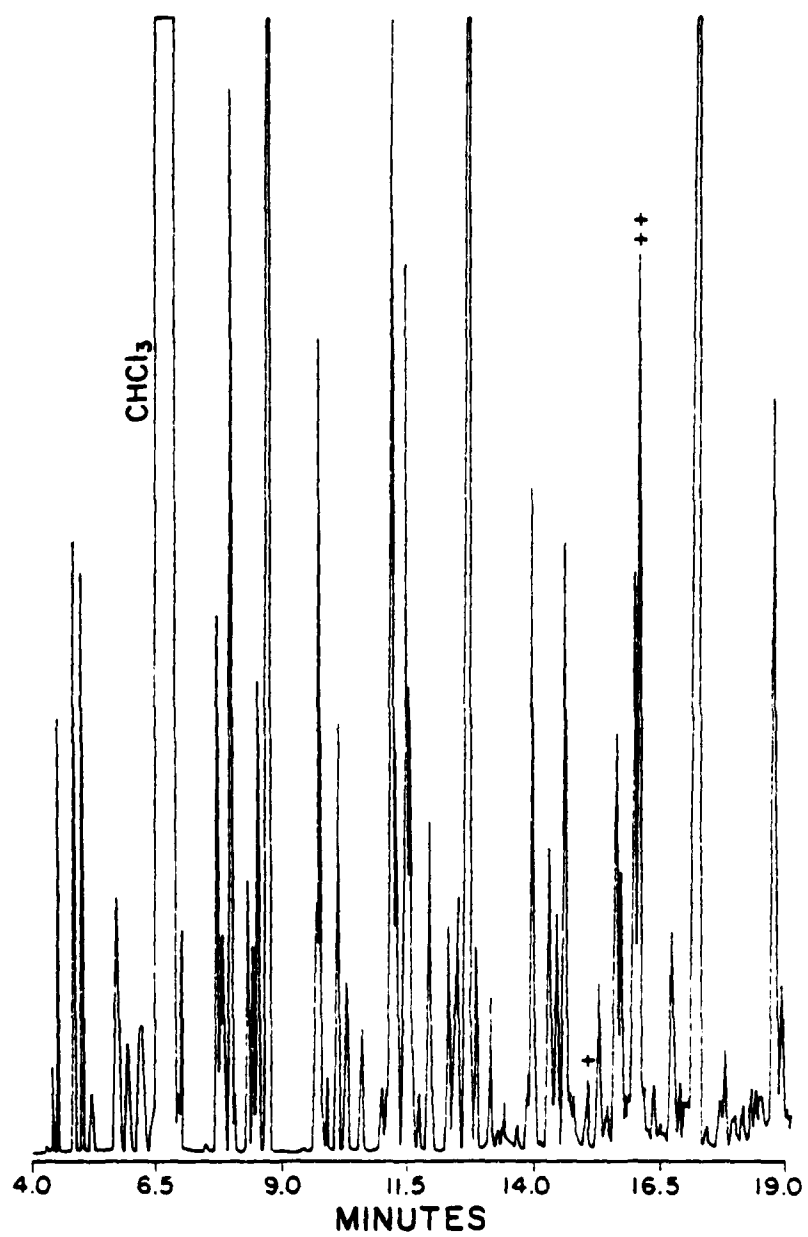
Figure 2. FID trace (direct), VN-77-11 Jet Fuel

7

lightpipe) since return transfer line dead-volume may contribute to additional degradation of (FID) chromatographic resolution.

While an increase in make-up gas may retain resolution through the system to the FID, infrared sensitivity would surely suffer. For a total gas (He + N_2) flow through the GC/FTIR system of 8 mL/min, chromatographic resolution appears to be reasonably preserved while sensitivity has not been grossly compromised. While a lower make-up gas flow would have increased the sensitivity, chromatographic resolution would have been degraded and co-elution of closely spaced components would then become more likely.

The following data illustrate these points for two make-up gas flow rates. Two standard compounds (n-nonane and cyclohexyl acetate) were run under the same conditions except for make-up flow which was 6 mL/min and 8 mL/min. For n-nonane, peak width decreased from 7 files to 6 files, respectively, (14.3% change). For cyclohexyl acetate, the peak width decreased from 9 to 7 files, respectively, (22.2% change). While the residence time through the lightpipe decreased, it was not without sacrifice of FTIR signal intensity. Maximum intensity for both n-nonane (0.0234 to 0.0196 absorbance units, 16.2% change) and cyclohexyl acetate (0.0403 to 0.0321 absorbance units, 20.4% change) decreased upon going to the faster make-up flow. Again, while a significant increase in infrared sensitivity can be realized by decreasing the make-up gas flow rate through the lightpipe, coelution of components will become more likely. Azarraga and Potter have also shown the importance of make-up gas optimization as related to infrared sensitivity and chromatographic resolution. Their example shows significant changes in sensitivity and resolution for total gas flow rates through the lightpipe of 2 mL/min and 15 mL/min for a lightpipe volume of 0.8 mL(6).

The following example also illustrates the relationship between make-up gas flow and infrared sensitivity. Since the injected sample is diluted in chloroform, a solvent peak can be expected in the chromatogram. To flush the solvent through the lightpipe a 20 mL/min gas flow was actuated at the start of the

8

chloroform elution to prevent excessive peak tailing. Figure 3, a Gram-Schmidt reconstruction of the entire infrared region, illustrates the sensitivity increase at point A as the 20 mL/min purge is closed and 8 mL/min make-up resumed.

Several reports, including Grob and Grob(18), have stated that on-column injection may be the best way to introduce a sample for GC separation. In this regard Grob and Grob cite at least five drawbacks for the evaporation (heated injector) process. Drawbacks included sample discrimination related to the boiling point of sample component(s), possible sample decomposition due to contact with an injector at elevated temperatures and quantitative discrimination may occur with sample components showing an increasing tendency to be absorbed. The attempt, therefore, to compare, quantitatively, experimental GC/FTIR sensitivities with other reports in the literature would certainly be complicated by injector design, accuracy, and reliability assuming all other parameters, such as injector temperature, are held constant.

In the present work, an on-column injector was used for both standards and complex sample. A standard 13-component mixture was prepared and unambiguously identified by comparison with EPA library file spectra. The same rapid data acquisition rate and lightpipe temperature were used as previously described in order to simulate the actual S/N which would be encountered in the jet fuel separations. Figures 4 and 5 show "on-line" the infrared sensitivity for n-nonane (40 ng) and cyclohexyl acetate (40 ng).

5.   Quantitative Data From Jet Fuel Spectra

It was of interest to determine minor component concentrations for a complex fuel which exhibited a wide concentration dynamic range. Sample FTIR spectra were taken from the capillary GC separation eluded to earlier. The annotated peaks in Figures 1 and 2 correspond to these minor sample components. Figure 6 represents the on-line FTIR spectrum of the earlier eluting component (+). Being devoid of FTIR absorbances in all regions

9
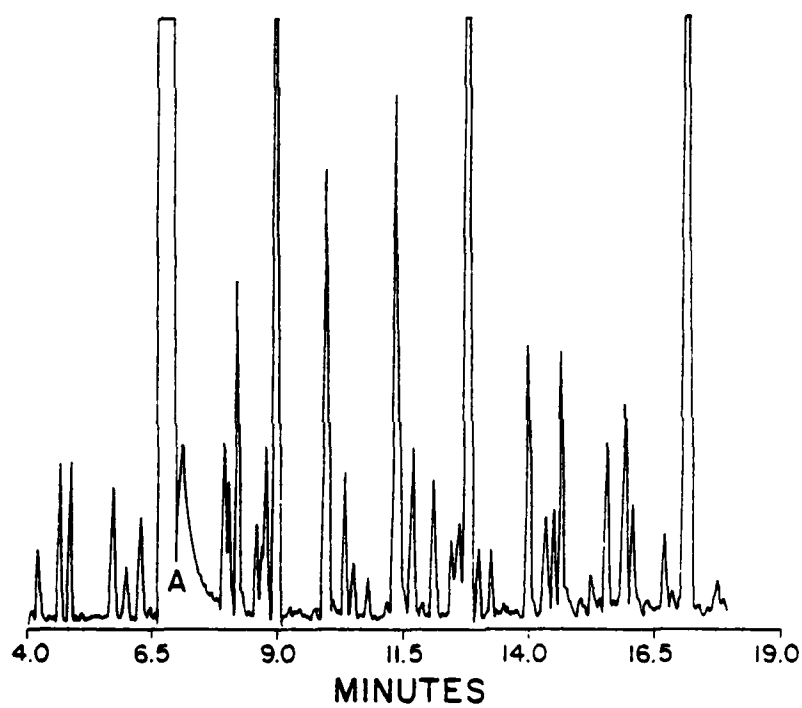
Figure 3. FTIR Gram-Schmidt reconstructed chromatogram VN-77-11
Jet Fuel.

10
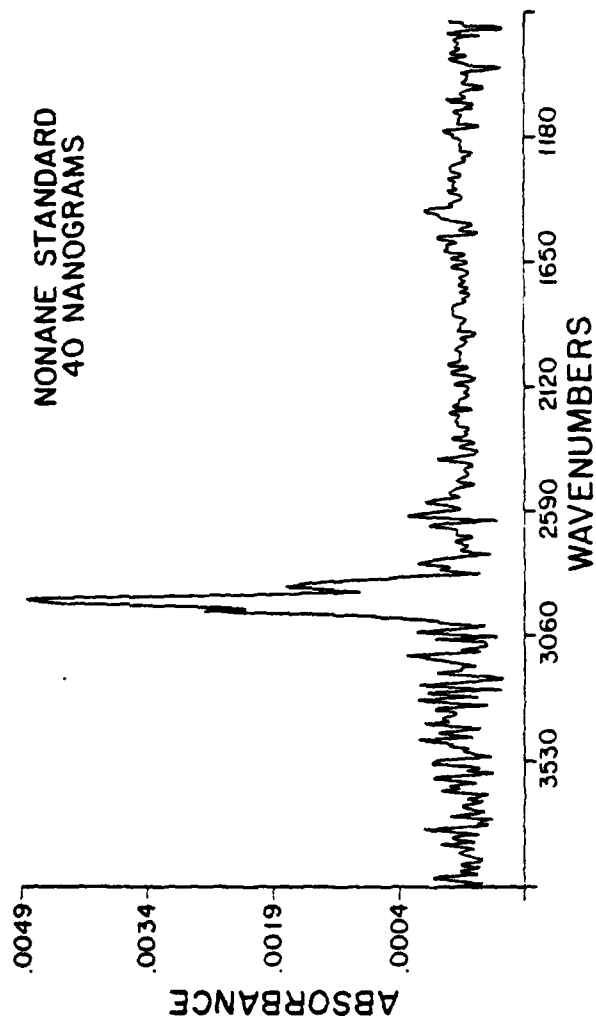
Figure 4. n-Nonane standard; FTIR file spectrum; 40 ng.

11
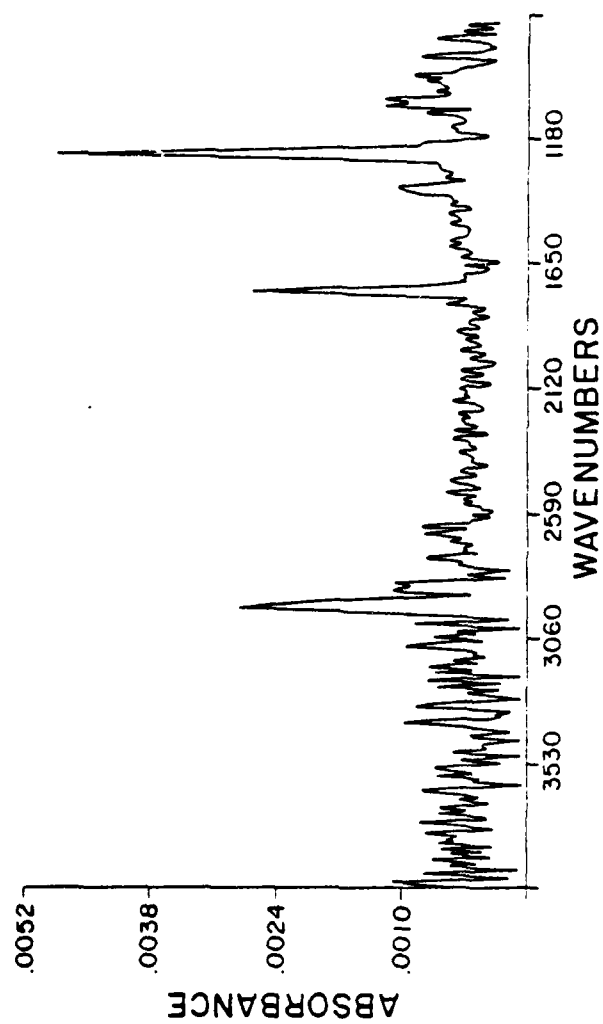
Figure 5. Cyclohexyl acetate standard; FTIR file spectrum; 40 ng.

12
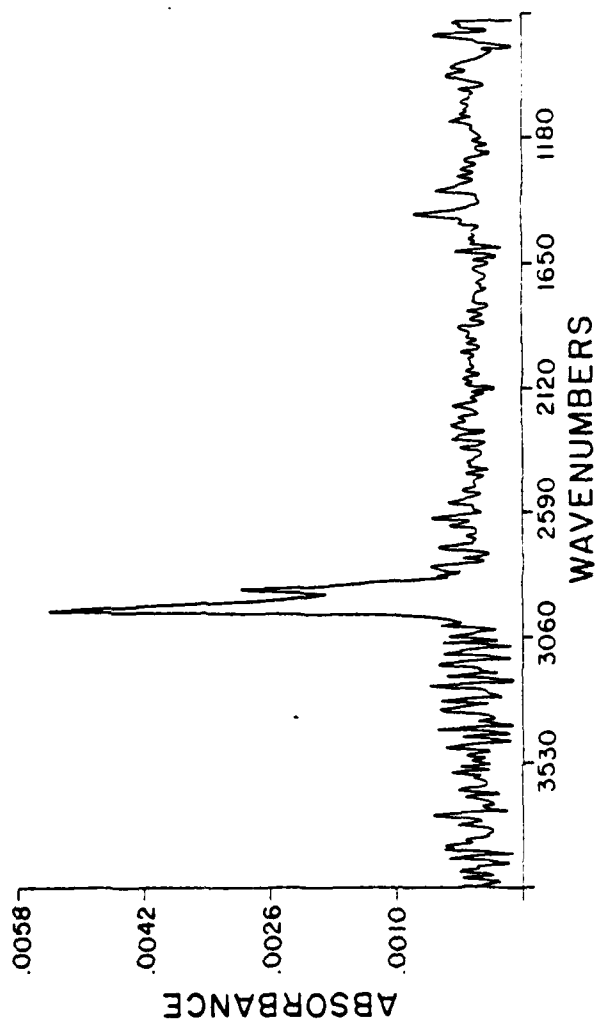
Figure 6. FTIR file spectrum (+); VN-77-11.

13

except the aliphatic carbon-hydrogen stretching region, the species
is undoubtedly an alkane functionality, possibily of a cyclic nature.
Quantitation of unknown sample components should be done by
comparison with standard compounds of the same or near the same
functionality. For example, an attempt to equate the strong
absorption of certain polar compounds containing carbon-oxygen bands
(around 1200 cm-^{1}) to other stretching and bending vibrational modes
would certainly not be appropriate. By comparing the spectra in
Figures 4 and 6, which appear to be of the same general compound
type, one can estimate the concentration of this minor component to
be approximately 40 ng. In like manner m-xylene, the other minor
component (++), was found to be present in the jet fuel at an approx-
imate concentration of 400 ng, Figure 7 (see also Figure 1 and 2). A
m-xylene standard was included in the 13 component standard mixture
described previously in order to determine this concentration level.

The use of available library search routines can, of
course, be helpful in determining compound identification. Table 1
lists results from a spectral search routine for the m-xylene compcn-
ent.   The 400-720 cm-^{1} region (corresponding to the MCT detector
cutoff) was eliminated from consideration. A "match value" of 945
indicates a reasonable match compared with the second, third, etc.
choices. The first column of numbers in Table 1 is the EPA vapor
phase file location for the 16 cm-^{1} library spectrum. The next
column of numbers to the right indicates how well the sample
spectrum matches the EPA library file. Typical values range from
50 to 2000 depending on the S/N. As a general rule, a "good" match
is tentatively assumed when the first match equals about one-half
the second match value (second choice). A match value of zero
indicates a perfect match. A search algorithm which uses a least-
squares approach was employed(17).

Infrared library spectral searching should not be the sole
criteria for compound identification since only a relatively small
number of all volatile organic compounds may be included in the

14

FILE SPECTRUM
VN 77-11 JET FUEL
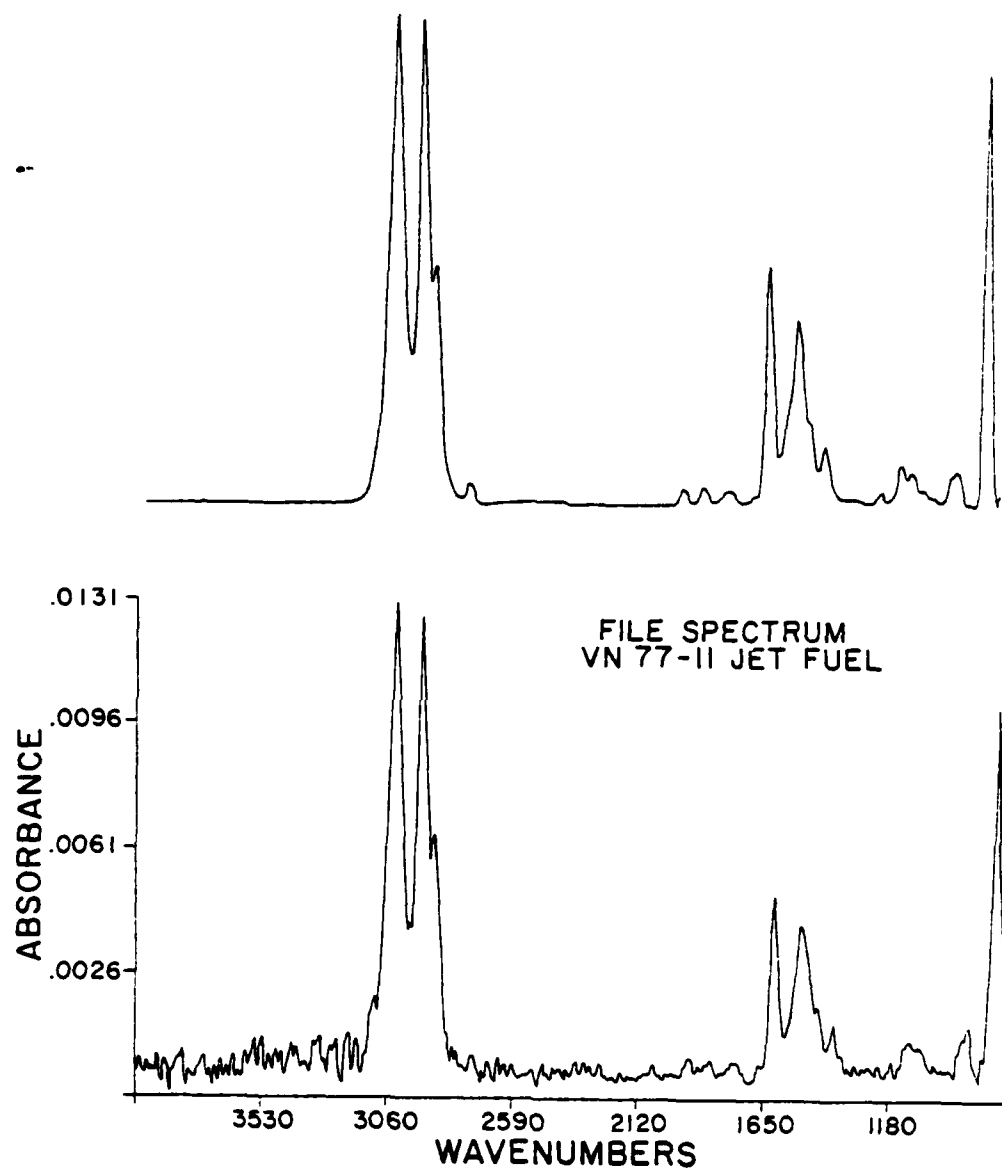
Figure 7. FTIR file spectrum (++); VN-77-11.

library. Other factors such as boiling point and chromatographic retention time should be considered. Spectral searching results can, however, give a good qualitative indication of the class of compound under investigation. With sufficient S/N ratios, unambiguous identification can result. While high resolution capillary GC/FTIR can provide excellent separations, co-elution of sample components may still occur. A sufficiently rapid data acquisition rate can aid in resolving co-eluting compounds by collecting several files across the peak(s) of interest. Though the analysis of aliphatic and aromatic hydrocarbons may not fully illustrate the advantages of GC/FTIR, important features of the capillary experiment can be evaluated. Certainly more polar compounds and stronger infrared absorbing functional groups (such as C=O, C-O) will benefit search routine efforts and, in many cases, reduce detection limits. The examples presented here have utilized an interferometer scanning

TABLE 1

SPECTRAL SEARCH RESULTS FOR

M-XYLENE COMPONENT

EPA Vapor Phase Library Number	Value of Hit	Compound
78	945	m-xylene
342	1601	Bitolyl, m,
2610	1716	Hexane, 1,3,5-Triphenyl-,
2476	1858	Benzene, 1-Ethyl-3-methyl-,
75	1919	Benzene, 1,3,4-Trimethyl-,
799	2004	Benzene, 1,3,5-Trimethyl-,
2498	2147	Benzene, 1,2,3,5-Tetramethyl

velocity close to the maximum of the instrument. Finally, the recognition and understanding of the parameters involved in the capillary GC/FTIR experiment should aid in making the analysis of complex samples successful and the identification of components unambiguous.

C. QUANTITATIVE GC-FTIR

The analytical technique GC/FTIR has made great progress in the past number of years. Improvements in lightpipe design, liquid nitrogen-cooled detectors, optics, and fast computers have made analysis of even very complex volatile samples possible. High efficiency, narrow bore capillary columns which provide the separating power needed for such complex samples have been interfaced successfully with FTIR spectrometers in several reports (7, 14-16). Such reports usually contain infrared spectra that have been collected on-line and spectra of one or two standards that have been run to show the sensitivity of the GC/FTIR method. These standards usually represent low nanogram quantities of compounds which often contain a strongly absorbing functionality. Compounds which have been used include isobutyl methylmethacrylate (17,19), ethyl acetate (16,20), anisole (5) and isobutyl acetate (2). These standard models may not represent the type of compounds found in "real world" samples and thus may not represent the actual GC/FTIR sensitivity.

For example, a standard mixture of priority pollutants has been analyzed by capillary GC/FTIR and identified by spectral search routines (10). The amount of each pollutant needed, however, for spectral search identification was not in the nanogram range but was on the order of eight micrograms. In other words, published detection limits do not reflect the amount of material required for a spectral search identification.

Several objectives of this phase of our work include determining (a) "detection limits" for a variety of compounds representing a variety of both polar and nonpolar functionalities; (b) the reliability (or ability at all) of the available spectral search routines to correctly match the known compound spectrum to a library file spectrum; and (c) whether linear absorbance/concentration plots can be constructed from infrared data collected on-the-fly.

The term "detection limits" is presented in quotation marks since the definition used here may not correspond to definitions more

frequently used. While many define the term as a recorded response
giving a signal twice or three times the background noise level, we
define the term in relation to the ultimate goal of our work which is
actual sample identity. This identity may come as a result of
spectral search routines and/or a visual "side-by-side" comparison of
sample and library infrared spectra.

The work to establish "detection (identification) limits":
was also performed keeping in mind the types of problems encountered
when attempting to analyze complex, unknown samples by capillary
GC/FTIR. First, samples such as aviation jet fuels and fractionated
coal liquefaction products can contain hundreds of components and
absolute identification can prove difficult. Since high resolution
capillary columns can often effectively separate these complex
samples, a significant amount of time could be spent identifying
individual components in even one sample. The use of computerized
infrared spectral search routines may help immensely. Their search
effectiveness, however, often relies on the amount of component
present (i.e. absorbance intensity) and/or the uniqueness of the
absorbance pattern of the unknown within the IR regions. Secondly,
the amount of component identifiable can be determined only if a
reliable absorbance vs concentration plot can be generated. Separate
plots may need to be constructed for different functional classes and
even for particular compounds of a single class. Finally, the
difficulties of establishing such "detection (identification) limits"
include the fundamental fact that FTIR data collection measures
transient occurrences within the lightpipe. The actual point where
the maximum absorbance occurs may be missed depending on the
frequency of these transient measurements. In addition, in order to
make identification limits truly meaningful, the same background
noise level should be reproduced, ideally, between actual sample and
standard compound in GC/FTIR determinations, i.e. the same number of
coadded FTIR data scans should be used for both analyses. Some
discretion is required. For example, while the co-addition of more
scans would decrease the overall noise level by $\sqrt{scans}$, the resulting
increase in the data collection time frame (sec/file) may result in

18

an apparent chromatographic co-elution of adjacent components. Our rule of thumb regarding an acceptable time frame is that several data files should define a chromatographic peak.

1. Spectral Search Routines

Several methods of computer searching were available (17,21). We chose to employ the method which uses any one of four search algorithms. The first algorithm involves computing the <u>Absolute</u> difference between the sample spectrum (S) and each member of the reference file (R)

$$\text{"match value"} = M_{AB} = \Sigma|S_i - R_i|$$

The second algorithm uses a least-squares approach

$$\text{"match value"} = M_{SQ} = \Sigma(S_i - R_i)^2$$

(This least-squares metric (algorithm) tends to weigh large differences in sample spectrum versus reference spectrum more than the absolute metric.) The third utilizes the first derivative spectra of sample and reference. For the absolute value using first derivative:

$$M_{AD} = \Sigma|\Delta S_i - \Delta R_i|$$

Finally, for least-squares method using the first derivative:

$$M_{SD} = \Sigma(\Delta S_i - \Delta R_i)^2$$

It has been stated that the derivative searches can minimize the effects of sloping base line and broad non-specific spectral features (such as wavelike baselines originating from interferometer instability and/or poor subtraction procedures). In practice, the AD and SD algorithms are of little additional advantage even for low S/N spectra. In most cases, the SQ algorithm was used more successfully.

The second parameter used quite frequently with the search routines allows certain areas of the infrared spectrum to be ignored. In most cases, the 400-700 cm^{-1} region corresponding to MCT-A detector cutoff was ignored. The third parameter allows the user to list up to 32 possible choices (hits) from the search routine. In most cases, 10 hits were listed and considered. The search data base used was compiled by the Environmental Protection Agency and contains

19

3300 spectra reduced to 16 cm^{-1} resolution. Several other model spectra were generated in-house and added to this library.

2. Chromatographic and FTIR Spectral Parameters

The actual sensitivity of FTIR cannot be discussed without recognizing several limiting factors regarding the FTIR signal. These factors include the general theory that the signal-to-noise ratio will improve by a factor equal to an increase in the square root of the number of coadded scans. The second factor involves the nonlinear response over the infrared region due to the infrared source, MCT detector, etc. These factors combine to influence the overall background noise which is present throughout an FTIR analysis.

The single beam spectrum shown in Figure 8 illustrates the nonlinear infrared response. The least throughput is seen near the area of C-H stretching frequencies (~3120); whereas, the best infrared throughput is seen at approximately 1270 cm^{-1}. The overall background noise versus wavenumber is represented in Figure 9. This infrared noise spectrum was generated with the same lightpipe temperature, mirror velocity and number of coadded scans as for the standard compounds tested, _vide infra_. Generally, a peak to peak noise level of less than 0.002 absorbance units can be expected over the entire working region of 4000-710 cm^{-1}.

Since the peak widths of components eluting from a high resolution GC column can be on the order of several seconds, a data acquisition rate consistent with the chromatography should be used. The data acquisition rate described previously (1.09 sec/file) represents a compromise between an acceptable S/N and a time frame fast enough to define an eluting component by several data files.

A useful tool in the GC/FTIR experiment is the on-line generation of a "Chemigram". The "Chemigram" consists of five user-defined infrared window regions which typically correspond to functional group vibrational frequencies. Such an on-the-fly output is shown in Figure 10. The sample analyzed was Standard Mixture D

20
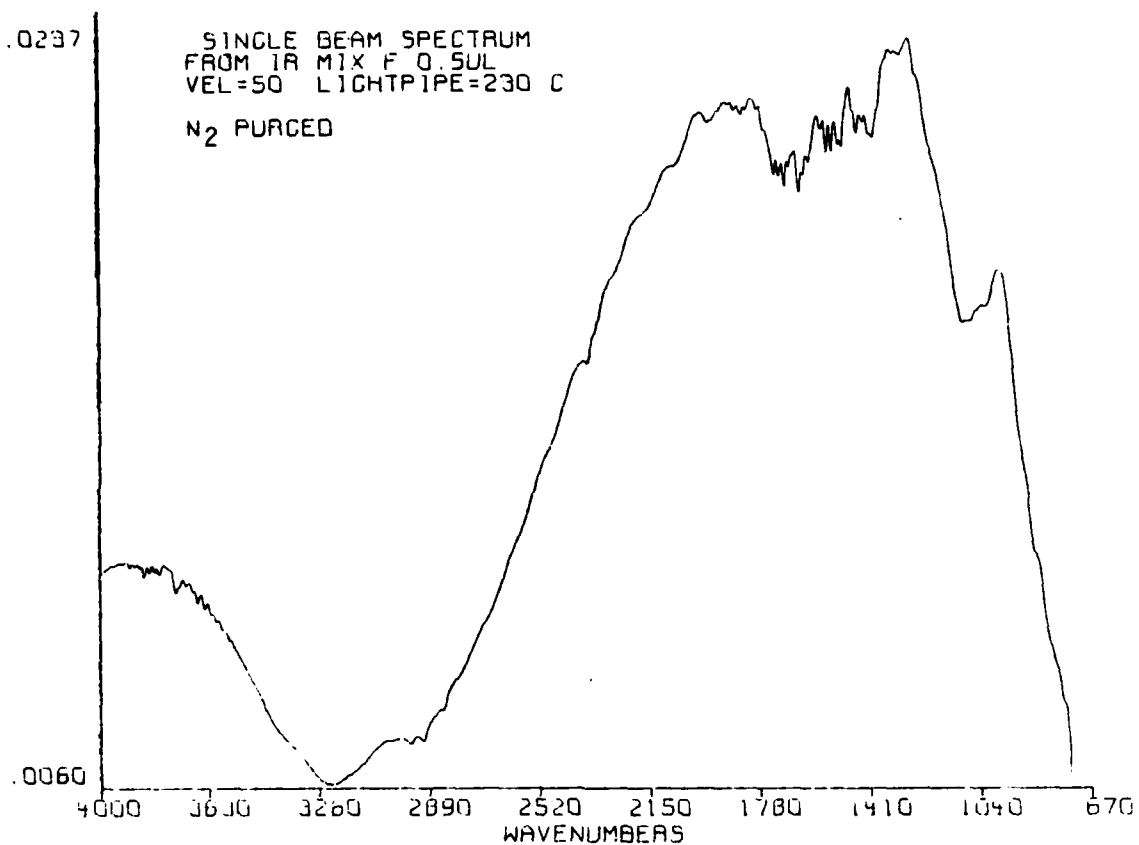
Figure 8. Single beam Fourier transform infrared spectrum of standard
           mixture F. Lightpipe temperature = 230°C, 0.5µL injected,
           N_2 purge.

21
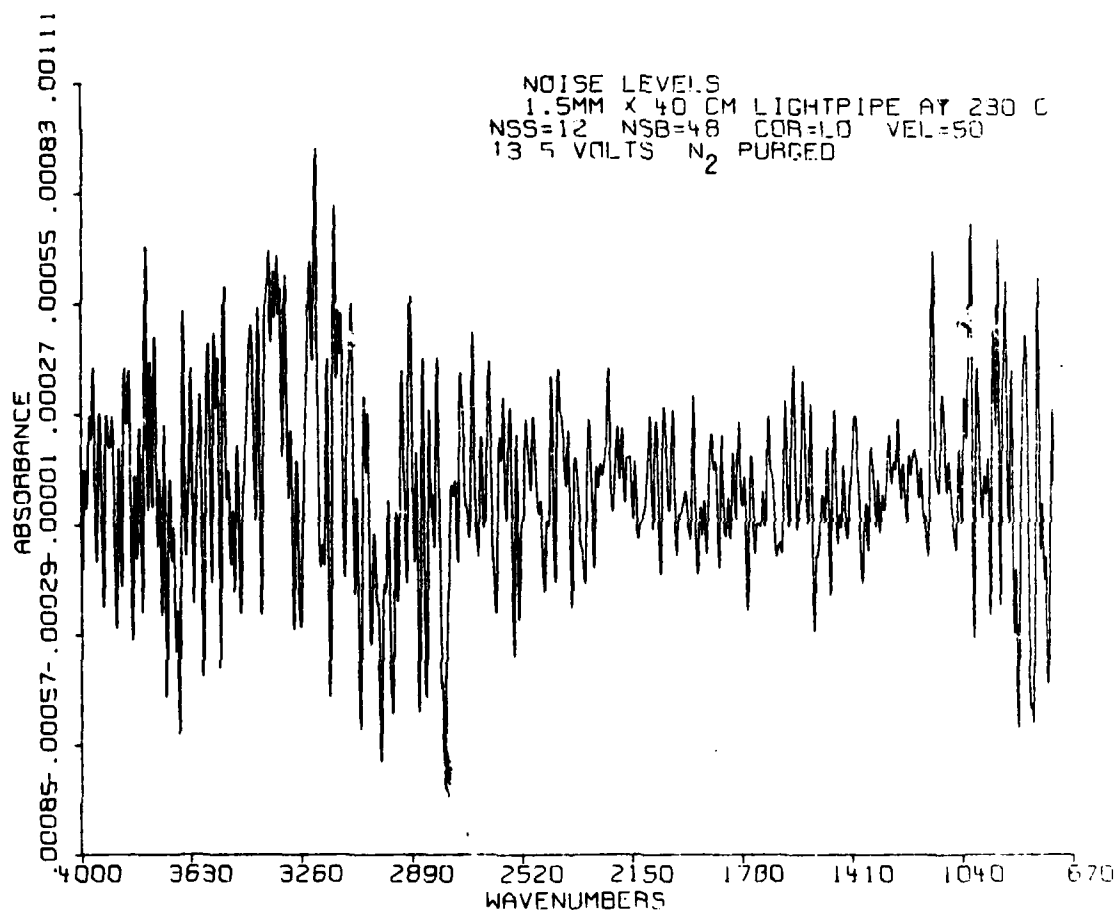
Figure 9. Background noise levels, lightpipe (1.5 mm x 40 cm) = 230°C, N$_2$ purge.

22

Absorbance Units

IR window (cm^{-1})

880   730

1280   1190

1660   1520

3050   2850

3550   3400

.015
.010
.006
.001
.003

.015
.010
.006
.001
.003

.015
.010
.006
.001
.003

.015
.010
.006
.001
.003

.015
.010
.006
.001
.003

.0   2.5   5.0   7.5   10.0   12.5   15.0   17.5   20.0   22.5   25.0
TIME MINUTES
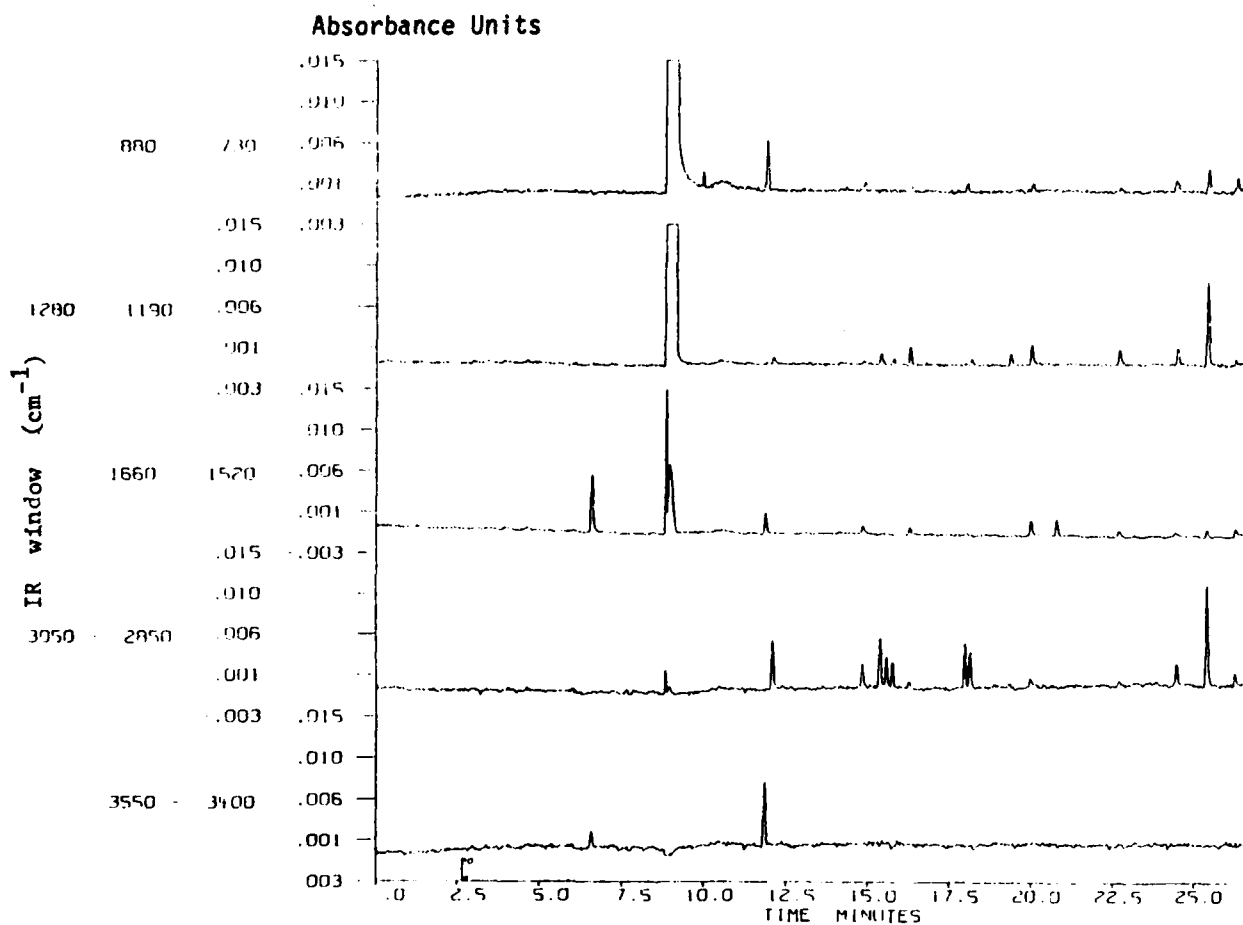
Figure 10.   Chemigrams generated for standard mixture D. See Table 3 for amount
injected and peak assignments. Temperature Program: 60°C for 3 min.,
7°C/min. to 210°C; 0.5 μl injection; Lightpipe temperature = 230°C;
Transfer Line Temperature = 200°C.

23

which contains eighteen components. The first peak from the left corresponds to water vapor from the 0.4-0.5 μL of air which is drawn up with the 0.5 μL of solution. The second peak corresponds to the chloroform solvent. The apparent double solvent peak (as evidenced in the center trace) is caused by a reduction in infrared sensitivity which is created when a 20 mL/min N_2 make-up purge is actuated. This temporary purge was needed to effectively flush the relatively large amount of vaporized solvent through the lightpipe. The original lightpipe gas flow of 8 mL/min was resumed after the solvent eluted. The "time into run", data file number and injected amount of each component in Standard Mixture D is listed in Table 2.

Another useful tool for component identification is the post-run generation of frequency-defined reconstructed chromatograms. Several reconstructed chromatograms are shown in Figure 11. Each one gives information concerning the presence of a functional group and the data file location for that particular functionality. The x-axis can be considered a time axis since the time between each data file is known. A further mode of data presentation is a Gram-Schmidt reconstruction which uses infrared absorbances from the entire working IR region. The Gram-Schmidt reconstruction can be considered a universal output similar to a flame ionization detector trace. We regret that a Gram-Schmidt reconstruction was not available to compare to the traces in Figure 11. The generation of such reconstructions (both from specific window regions and Gram-Schmidt) was not always possible because computer disc space had to be conserved. That is, instead of filling up the data disc with "empty files" corresponding to the time between eluting components, an on-off "trigger" was actuated corresponding to "save data"-"do not save data". These on-off intervals were possible by following a previously generated flame ionization detector trace or infrared Chemigram. Although reconstructions could have been generated, any relationship to actual relative retention times would have been misleading and confusing to the reader. Primarily, reconstructs were used by the analyst to locate the data files containing the actual component (infrared) information. Figure 11 reconstructions are

24

TABLE 2

Elution Order for Standard Mixture D

Compound	Data File #	Minutes Into Run	Amount Injected (ng)
pyrrole	22	11.86	1000
amyl alcohol	33	12.06	202
N,N-dimethyl formamide	65	12.64	28
3-picoline	185	14.82	333
cyclohexanol	215	15.38	192
n-nonane	225	15.56	86
cyclohexanone	235	15.74	188
anisole	263	16.25	74
o-ethyl toluene	356	17.94	326
2-octanol	366	18.13	163
cyclohexyl acetate	430	19.29	29
m-cresol	467	19.96	206
nitrobenzene	509	20.73	96
o-anisidine	614	22.64	98
quinoline	710	24.39	218
o-tert butyl phenol	714	24.47	250
2-tert-butyl-6 methyl phenol	764	25.37	1000
1,2,3,4,-tetrahydroquinoline	*	26.05	350

*Eluted after data disc was full.
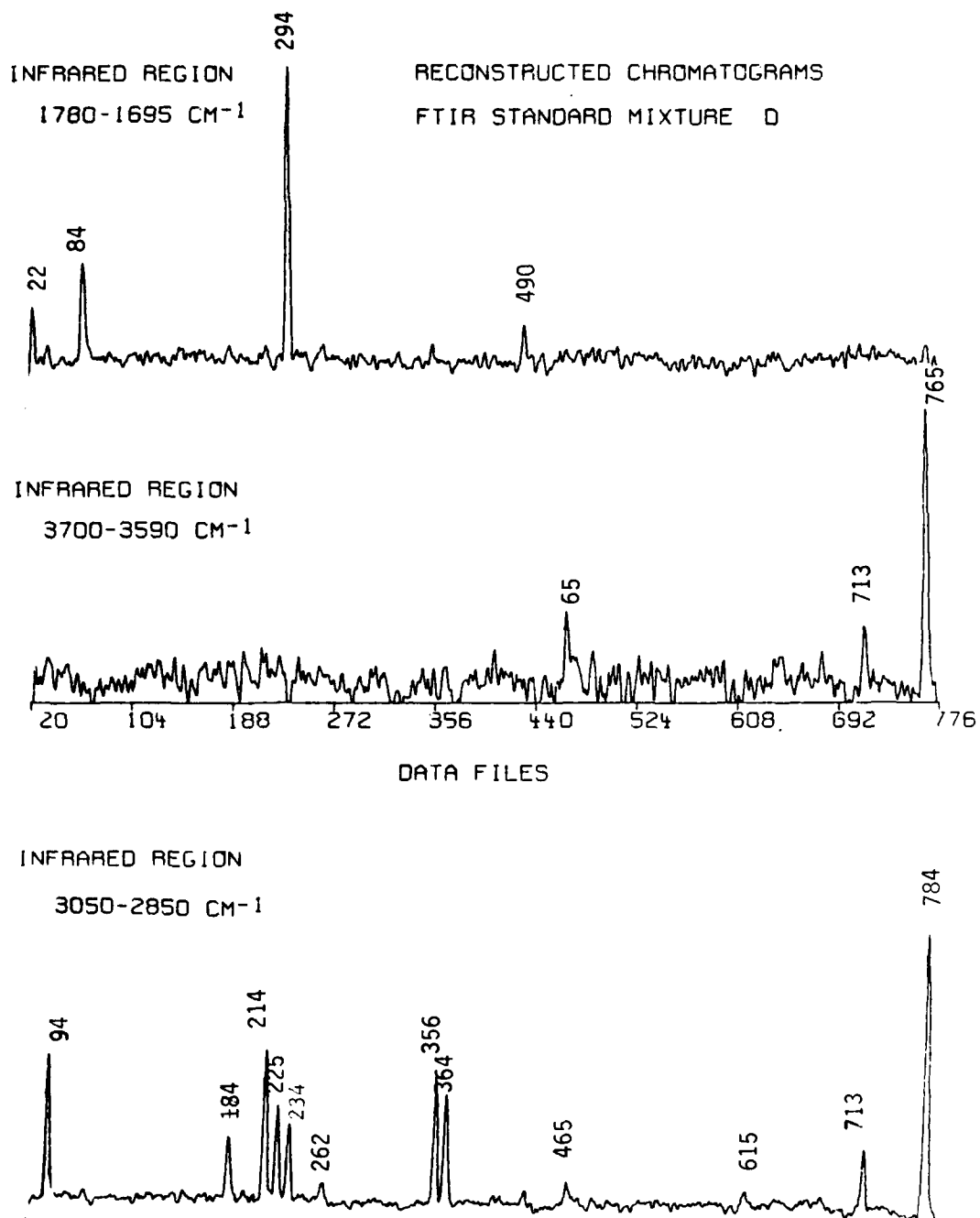
Figure 11. Frequency defined reconstructed chromatograms arising from the separation of standard Mixture D.

26

unique in that they were the only ones generated with the FTIR in a "save data" mode over the course of the chromatographic separation.

One advantage of using a rapid data acquisition rate can be realized in Figure 12. The infrared spectra shown in stack-plot format indicate the co-elution of quinoline and o-tert-butyl phenol. The elution of each compound can be followed easily even though the two most IR-intense data files are only 4.36 seconds apart. Note that the phenol OH stretching mode near 3600 cm^{-1} can be seen to appear (File 712) and disappear (File 716) even for rather low S/N spectra.

3. Establishment of Compound Identification Limits

As mentioned earlier, the term "detection limit" has been used in a broader sense in this report to indicate the point in concentration at which the actual identification of the compound (using infrared data) is no longer reliable. This approach is more desirable because infrared absorbance at two or three times the background noise level may indicate a functionality, but not necessarily an accurate compound identification. A computerized method based on spectral library search comparisons, was used in this work to produce a listing of the most probable compound identities. The search algorithms available are based on the differences in sample and reference spectra as calculated by using (1) a least squares matrix, (2) absolute difference, (3) a first derivative combined with least squares matrix, or (4) a first derivative combined with absolute difference. A more in-depth explanation of these algorithms has been given by Lowry and Huppler(17).

"Identification", therefore, for the 16 compounds that were examined has been defined as the ability of any one of these search routines to give the correct compound identification (i.e. compound listed first). The results for these 16 model compounds (which represent ketones, ethers, phenols, alkanes, etc.) are given in Table 3. The amount (ng) injected onto the capillary column by on-column
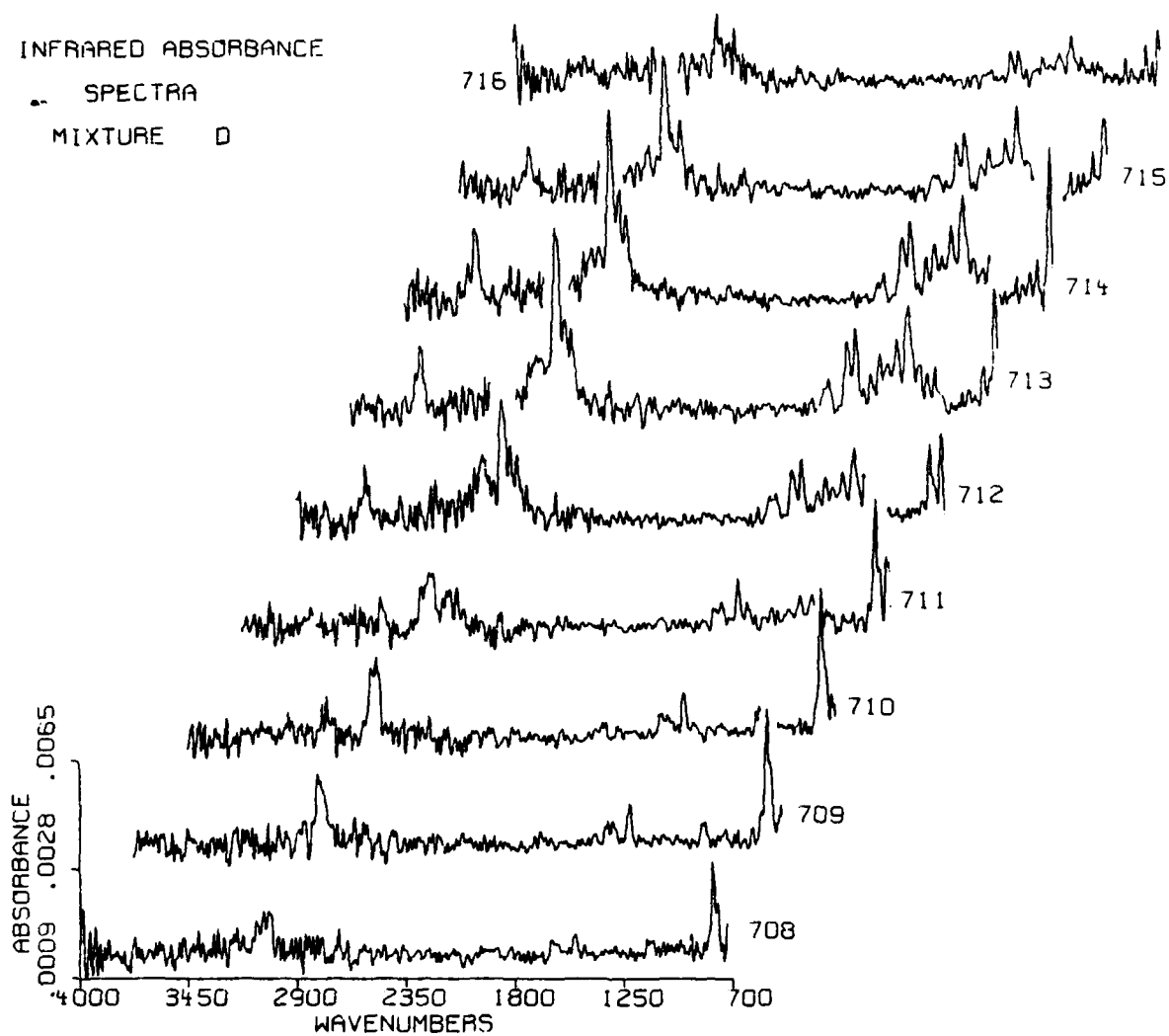
Figure 12. Fourier Transform infrared spectra as a function of retention time illustrating the co-elution of quinoline and O-tert-butyl phenol in standard mixture D.

TABLE 3

Spectral Search Results for each Standard Compound

Standard Mixture Compound	B *id?	B ng	C id?	C ng	D id?	D ng	E id?	E ng	F id?	F ng	G id?	G ng
pyrrole	N	240[d]	Y	480	N	28	Y	115	Y	192	Y	80
N,N-dimethyl formamide	Y	236	Y	57	N	202[b]	Y	66	N	18.8	N	250[b]
amyl alcohol							N	122	N	81	N	190
3-picoline	N	238			Y	333	N	285	Y	238	N	113
nonane	Y	178[c]	N	42[c]	N	86[c]			N	57[c]	Y	145
cyclohexanol					Y	192[d]	N	81	N	67[e]		
cyclohexanone					Y	188	Y	94[f]	N	66[g]	N	100
di-tert butyl ketone							Y	200	Y	263[h]		
o-ethyl toluene	N	220	Y	440	Y	326	N	105				
cyclohexyl acetate	Y	243	Y	68[i]	N	29	N	40	N	19.5	N	250
m-cresol			Y	180	N	206	N	103	N	154		
nitrobenzene	Y	300[a]	Y	100[k]	Y	96[j]	N	60	N	36[a]		
anisole	Y	248	Y	100[k]	N	74						
o-anisidine	Y	273	N	164[m]	N	98[a]	N	65[a]	N	142		
quinoline	Y	273	N	164	N	218	N	196				
2-tert butyl-6-methyl phenol	Y	250[p]	Y	500			N	150	N	100	N	200

a – second
b – OH listed first
c – alkane first
d – cyclohexanols first
e – eighth
f – sub. cyclohexanones first
g – fifth
h – sub. benz. first
i – acetates first
j – sub. nitro. benz. first
k – ethers first
m – oxyanilines first
n – anilines first
p – phenols first

*id? = Identified by Search

injection is given along with a "Y" for Yes or a "N" for No which indicates positive or negative "identification". The letter indicates the type of compound functionality present in the spectral search results listing. For example, "98[a] anilines", indicates that the results listed were various substituted anilines or aniline-type compounds. The second means that o-anisidine was listed as the second choice.

The success of the search routines to function properly was obviously dependent upon the amount of vaporized compound present in the IR flow cell. In addition, the uniqueness of the infrared absorbance pattern of the compound of interest over the entire spectral region may dictate how low "detection limits" can go. For example, eighty (80) nanograms of pyrrole can be identified unambiguously even though the apparent infrared information seems minimal (see Figure 13). The rather unique 718 cm^{-1} band and N-H stretching band may account for the low detection limit.

Other factors which affect the search result outcome include the final infrared S/N ratio and the infrared baseline stability. Because the infrared response curve is nonlinear over the range 4000-700 cm^{-1} (see Figure 8), the corresponding background noise levels are also not constant over that same region (see Figure 9). Due to the nonlinear response, (often) unique absorbances such as due to N-H stretching frequencies (3500-3400 cm^{-1}) may not always be utilized to advantage because of high background noise. An identification which was limited due to these factors is shown in Figure 23. The spectrum of m-cresol at 250 nanograms shows many infrared bands. S/N, however, above 2600 cm^{-1} is reduced considerably. Despite the high noise level around 3600 cm^{-1}, the -OH (phenol) frequency is still apparent. The search routines appear not to function, however, even though information is discernible.

Although the Michaelson interferometer can be described as relatively stable even at high mirror velocities (such as the velocity used for this work), anomalies in infrared spectra such as wave-like baselines can occur. Such wave-like baselines can be due to spectrometer instability. This instability is usually only seen

EPA VAPOR PHASE
3302   PYRROLE
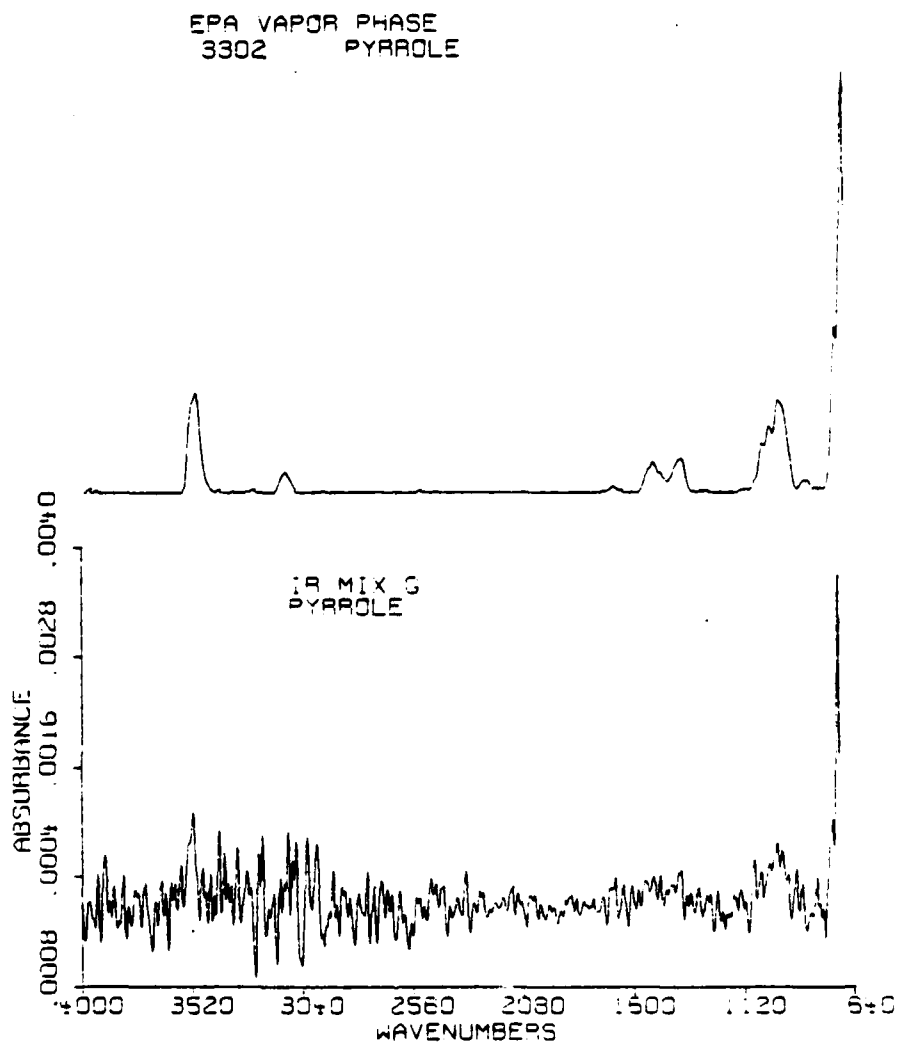
Figure 13. FTIR of peak file spectrum compared with EPA vapor phase
spectrum of pyrrole. Corresponds to the least amount of
compound identified (80 ng.) by the search routines
(Standard Mixture G). See tables 3 and 4.

31

when working at low concentrations in which low signal-to-noise ratio absorbance/frequency spectra result. The poorest stability usually is found for regions greater than 3000 cm-^{1}. Obtaining spectra with near flat baselines is desirable when search routines are to be incorporated. Improvement of very low S/N spectra can usually be accomplished by background subtraction. The use of subtraction procedures generally result in flattening of the infrared frequency baseline to make the spectra more amenable to reference spectra comparisons.

Although computerized spectral searching may be limited at times by the aforementioned properties, good detection limits are possible for many types of compounds. For example, the search routines do function for N,N-dimethyl formamide at 57 ng, anisole at 100 ng, cyclohexyl acetate at 68 ng and 2-tert-butyl-6 methyl phenol at 250 ng. Again, these data are compiled in Table 3.

One final feature of the search routine results can generally be recognized by merely scanning the compounds listed. Quite often, although positive identification may not have been achieved, the compound names listed can given an indication of the type of functional group(s) which may be present in the unknown spectra. For example, a substituted derivative of the compound type is listed first for cyclohexanol (192 ng), cyclohexanone (94 ng) and nitrobenzene (96 ng). Other functional group identification can be found for n-nonane and amyl alcohol in Table 3.

All infrared spectra, whose corresponding data appear in Table 3, were individually searched using the computerized Nicolet software. Where applicable, background noise subtractions were performed in an effort to improve the infrared (frequency) baseline. Infrared spectra for all entries in Table 3 are not included in this report. Instead, we have included spectra which represent the least amount of compound positively identified by search routine algorithms, and the greatest amount not identifiable by the library search algorithms. Pertinent infrared spectra and spectral search results are found in Figures 13-28 and Tables 4-17.

TABLE 4

Computer Search Routine Results for Injection of 80 ng of Pyrrole[a]

EPA Vapor Phase Library Number	Match Value	Compound[b],[c]
3302	567	pyrrole
371	1050	bromoform
3308	1059	3-phenyl pyridine
302	1094	1,1,1-Trichloroethane
3309	1218	4-azafluorene
832	1243	α-chlorotoluene
374	1248	1,2-dichloroethane
1892	1278	2-Iodothiophene
2625	1333	2-Thiophenecarbonitrile
128	1337	1,1-dichloroethane

[a]See Figure 14

[b]Squared algorithm used

[c]4000-3700 cm^{-1} and 715-400 cm^{-1} regions skipped

33

EPA VAPOR PHASE
517   FORMAMIDE, N,N-DIMETHYL-

FILE #69-65
N,N-DIMETHYL FORMAMIDE

WAVENUMBERS
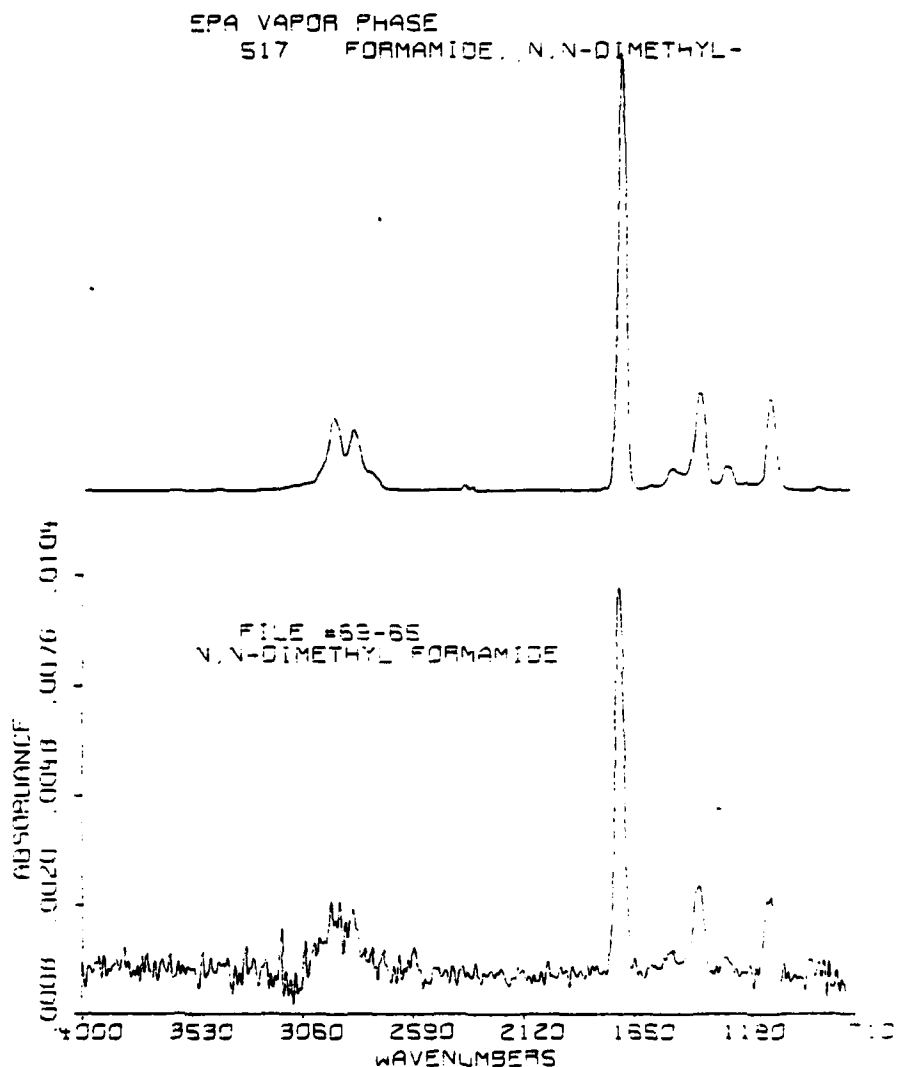
Figure 14A.   FTIR of peak file spectrum less background compared with
the EPA vapor phase spectrum of N,N-dimethylformamide.
Corresponds to (A) the least amount of compound positively
identified by the search routines (Standard Mixture C)....

34

FILE #65-61

N, N-DIMETHYL FORMAMIDE
NOT MATCHED
28 NG

Figure 14 B.   ....and (B) the greatest amount not identifiable by the
search routines (Standard Mixture D).   See Tables 3 and
5.

35

TABLE 5

Computer Search Routine Results for Injection of
57 ng of N,N-dimethyl formamide[a]

EPA Vapor Phase Library Number	Match Value	Compound[b,c]
517	213	N,N-dimethylformamide
2111	650	5-aminopentanoic Acid
1082	719	hexahydro-2-acepinone
300	766	2-cyclohexenone
596	771	N,N-diethylformamide
3255	780	2,5-dimethylbenzaldehyde
3005	943	2,3-dihydrophenalen-1-one
3192	1007	Thiazolo-5,4,3-quinolin-2-one
2509	1008	5-indancarboxaldehyde
3256	1016	2,4-dimethylbenzaldehyde

[a]See Figure 15

[b]squared algorithm used

[c]740-400 cm^{-1} region skipped

36

IR MIX G
AMYL ALCOHOL
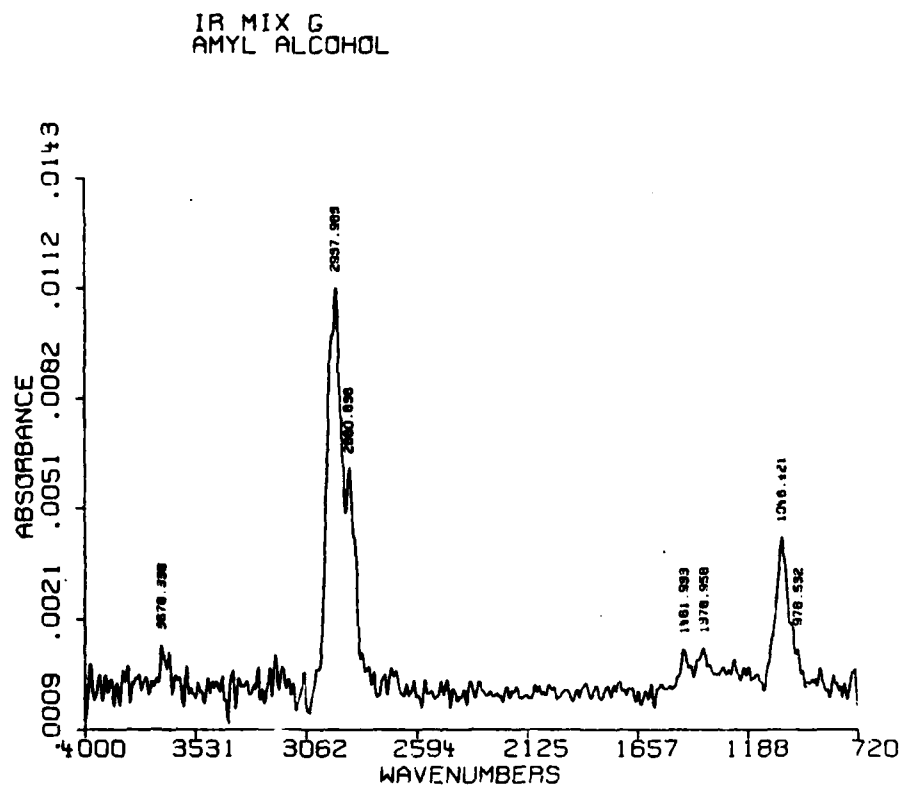
Figure 15. FTIR of peak file spectrum of material suspected to be
amyl alcohol. Corresponds to the greatest amount of
material injected (250 ng.) which was not identifiable by
the search routines (Standard Mixture G). See Table 3.

37

TABLE 6

Computer Search Routine Results for Injection
of 238 ng of 3-picoline[a]

EPA Vapor Phase Library Number	Match Value	Compound[b,c]
2236	1699	3-picoline
2481	2250	3-ethylpyridine
26	2465	methylbenzene
222	2571	3,5-lutidine
1591	2762	chloro-m-xylene
203	2876	2-chloroethylbenzene
808	3045	o-xylene
342	3096	bitolyl
2610	3107	1,3,5-triphenylhexane
172	3108	8-methylquinoline

[a]See Figure 16

[b]Squared algorithm used

[c]4000-3700 cm^{-1} and 740-400 cm^{-1} regions skipped

FILE #192-198
3-PICOLINE
IR MIX F

Figure 16A. FTIR of peak file spectrum less background file spectrum
compared with the EPA vapor phase spectrum of 3-picoline.
Corresponds to (A) the least amount of compound identified
by the search routines (Standard Mixture F)....

39

FILE #189-186

3-PICOLINE
NOT MATCHED
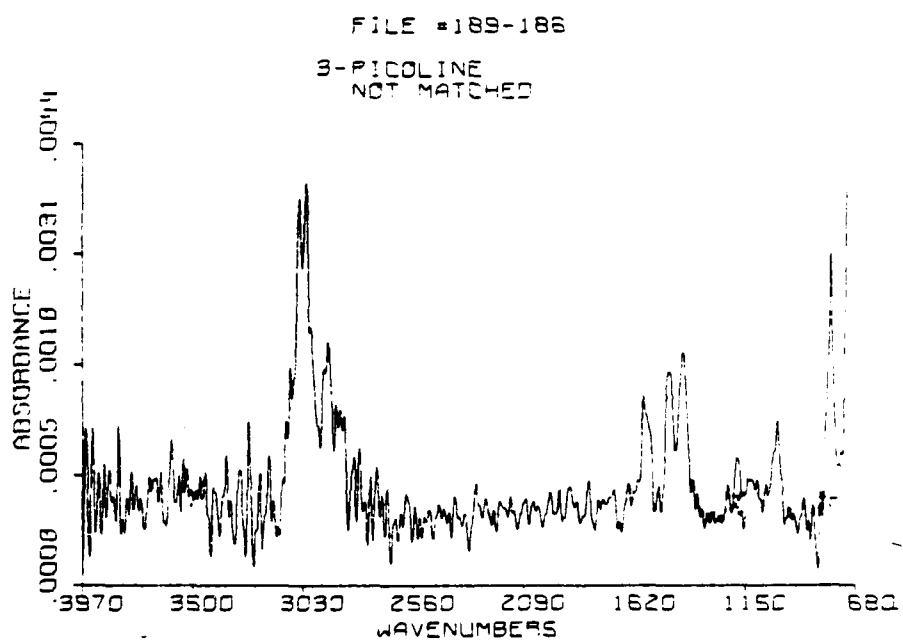
Figure 16B.   ....and (B) the greatest amount not identifiable by the
search routines (Standard Mixture E).   See Tables 3 and 6.

40

TABLE 7

Computer Search Routine Results for Injection of 42 ng of n-Nonane[a]

EPA Vapor Phase Library Number	Match Value	Compound[b,c]
887	65	n-Nonane
2553	70	6,9,12-Tripropylheptadecane
2554	70	6,12-diethyl-9-heptadecane
895	73	Octane
415	89	Decane
2555	103	6,11-dipentyl hexadecane
434	113	Hendecane
992	116	2,2-dimethyl-3-octanol
2155	117	Octyl disulfide
236	130	1-chloro octane

[a]See Figure 17

[b]Square algorithm used

[c]730-400 cm^{-1} region skipped

Figure 17 A. FTIR of peak file spectrum less background file spectrum
compared with EPA vapor phase spectrum of n-nonane. Corre-
sponds to (A) the least amount of compound positively
identified by the search routines (Standard Mixture B)....

42

FILE=232-237

NONANE
ALKANE MATCHES

Figure 17B.   ....and (B) the greatest amount not identifiable by the
              search routines (Standard Mixture F).   See Tables 3 and 7.

43

TABLE 8

Computer Search Routine Results for Injection of 145 ng
of Cyclohexanol[a]

EPA Vapor Phase Library Number	Match Value	Compound[b,c]
378	186	Cyclohexanol
1712	256	2-cyclohexyl-cyclohexanol
1564	266	2-butyl-cyclohexanol
780	287	α-propyl-cyclohexane methanol
320	296	α-methyl-cyclohexane methanol
1225	298	1-butyl cyclohexanol
1581	301	cyclohexane propanol
798	307	1,10-decane dithiol
2225	311	2-cyclohexylamino ethanol
7	314	cyclohexane

[a]See Figure 18

[b]Square algorithm used

[c]4000-3700 cm^{-1} and 720-400 cm^{-1} regions skipped

Figure 18A. FTIR of peak file spectrum less background file spectrum compared with EPA vapor phase spectrum of cyclohexanol. Corresponds to (A) the least amount of compound positively identified by the search routines (Standard Mixture G)....

45

FILE #219-216

CYCLOHEXANOL

Figure 18B.   ....and (B) the greatest amount not identifiable by the
search routines (Standard Mixture E).   See Tables 3 and 8.

46

TABLE 9

Computer Search Routine Results for Injection of
94 ng Cyclohexanone[a]

EPA Vapor Phase Library Number	Match Value	Compound[b,c]
518	230	Cyclohexanone
1592	443	3-methyl cyclohexanone
495	471	4-methyl cyclohexanone
3246	613	4-ethyl cyclohexanone
679	732	2-propyl cyclohexanone
1211	830	2-butyl cyclohexanone
233	998	Cycloheptanone
3101	1050	pipecolamide
2661	1180	1-butyl-2-pyrrolidinone
2521	1218	3-t-butyl cyclohexanone

[a]See Figure 19.

[b]Square algorithm used

[c]730-400 cm^{-1} region skipped

Figure 19A. FTIR of peak file spectrum less background file spectrum compared with the EPA vapor phase spectrum of cyclohexanone. Corresponds to (A) the least amount of compound positively identified by the search routines (Standard Mixture E)....

48

FILE #240-235

CYCLOHEXANONE

Figure 19B.   ....and (B) the greatest amount not identifiable by the
              search routines (Standard Mixture F).   See Tables 3 and 9.

49

TABLE 10

Computer Search Routine Results for Injection of 200 ng of di-tert-Butyl Ketone[a]

EPA Vapor Phase Library Number	Match Value	Compound[b,c]
3301	284	di-tert-butyl ketone
254	1248	Trans-3-hexene
1863	1512	4-methyl-2-pentene
1891	1521	amino phosphonic diamide
784	1599	2-methyl-3-pentanol
888	162-	2-pentene
1228	1661	2,2,4-trimethyl-3-pentanol
117	1684	2-chloro butane
201	1685	2,3-dimethyl-3-pentanol
2927	1723	propane

[a]See Figure 20

[b]Square algorithm used

[c]730-400 cm^{-1} region skipped

Figure 20A.   FTIR of peak file spectrum less background file spectrum
compared with the EPA vapor phase spectrum of di-tert-
butyl ketone. Corresponds to (A) the least amount of
compound positively identified by the search routines
(Standard Mixture E)....

51

IR MIX G
DI-TERT BUTYL KETONE
NOT MATCHED

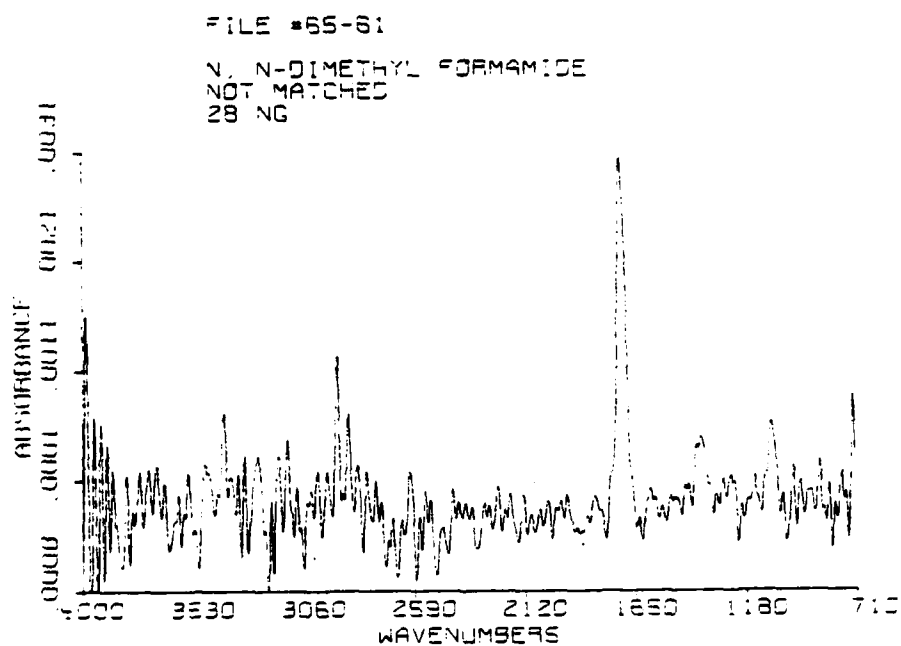Figure 20B.   ....and (B) the greatest amount not identifiable by
the search routines (Standard Mixture G). See Tables
3 and 10.

52

TABLE 11

Computer Search Routine Results for Injection of 263 ng of
o-Ethyl Toluene[a]

EPA Vapor Phase Library Number	Match Value	Compound[b,c]
2489	393	o-ethyl toluene
538	638	ethyl benzene
2486	957	propyl benzene
2649	973	3,6-dimethyl-3,6-diphenyl octane
2476	1033	1-methyl-3-methyl benzene
2492	1058	o-diethyl benzene
539	1144	sec-butyl benzene
806	1160	o-xylene
1840	1216	β-ethyl-β-hydrocinnamonitrile
90	1274	m-diethyl benzene

[a]See Figure 21

[b]Square algorithm used

[c]$4000\text{-}3700$ cm^{-1} and $740\text{-}400$ cm^{-1} regions skipped

EPA VAPOR PHASE
2489 TOLUENE. O-ETHYL-.

FILE #349-353
O-ETHYL TOLUENE

Figure 21A. FTIR of peak file spectrum less background file spectrum compared with the EPA vapor phase spectrum of o-ethyl toluene. Corresponds to (A) the least amount of compound positively identified by the search (Standard Mixture F)...

54

FILE =343-339
NOT MATCHED
O-ETHYL TOLUENE
APPROX. 250 NG

Figure 21B.   ....and (B) the greatest amount not identifiable by the
search routines (Standard Mixture B). See Tables 3 and
11.

55

TABLE 12

Computer Search Routine Results for Injection of 68 ng of
Cyclohexyl Acetate[a]

EPA Vapor Phase Library Number	Match Value	Compound[b,c]
1043	530	cyclohexyl acetate
574	624	pentyl acetate
592	694	hexyl acetate
1793	736	heptyl acetate
76	744	butyl acetate
516	762	2-pentanol-4-methyl acetate
523	765	Isobornyl acetate
571	772	propyl acetate
498	821	2-ethylbutyl acetate
2002	833	6-methyl-3-cyclohexene-1-methanol

[a]See Figure 22

[b]Square algorithm used

[c]740-400 cm^{-1} region skipped

56

EPA VAPOR PHASE
1043 ACETIC ACID CYCLOHEXYL ESTER
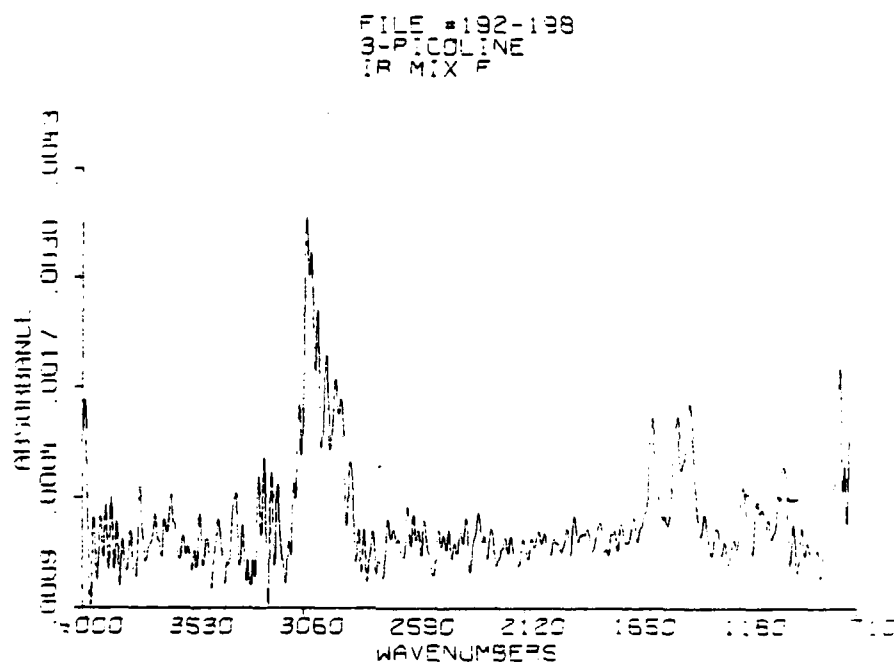
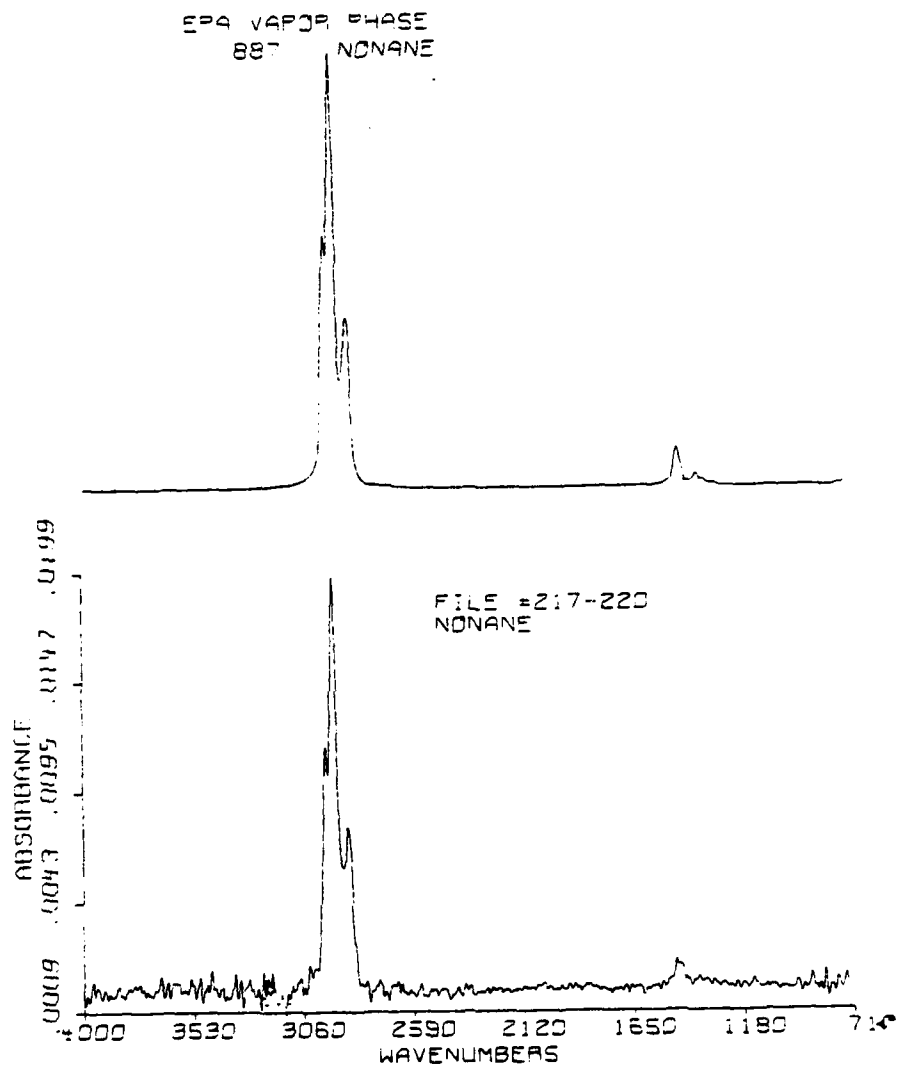FILE #420-416
CYCLOHEXYL ACETATE

Figure 22A. FTIR of peak file spectrum less background file spectrum compared with the EPA vapor phase spectrum of cyclohexyl acetate. Corresponds to (A) the least amount of compound positively iden.ified by the search (Standard Mixture C)....
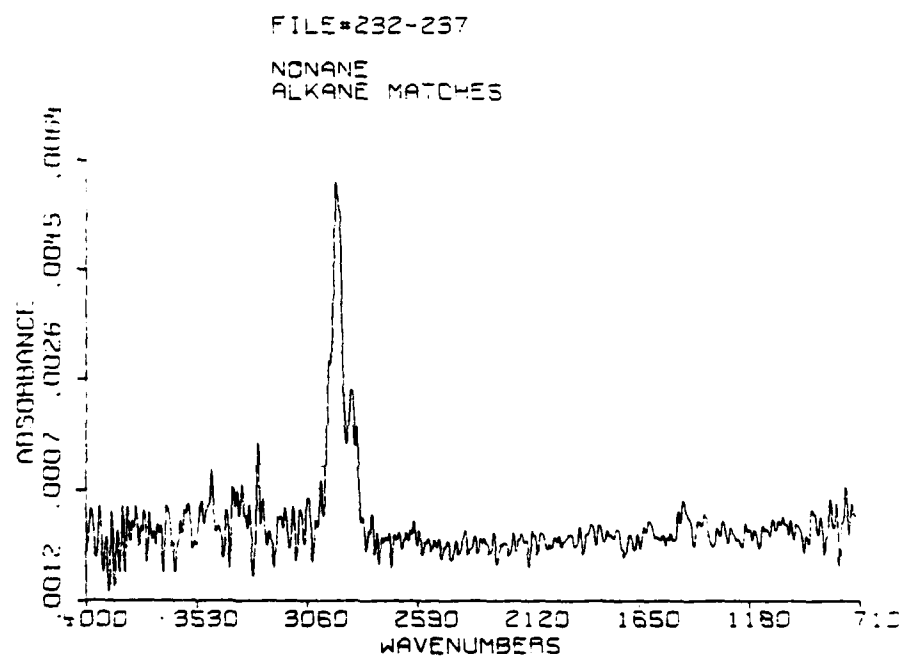
57

FILE #437-;5:

40 NG
CYCLOHEXYL ACETATE

Figure 22B.   ....and (B) the greatest amount not identifiable by the
search routines (Standard Mixture E). See Tables 3 and
12.

58

EPA VAPOR PHASE
872   M-CRESOL

IR MIX G
M-CRESOL
NOT MATCHED
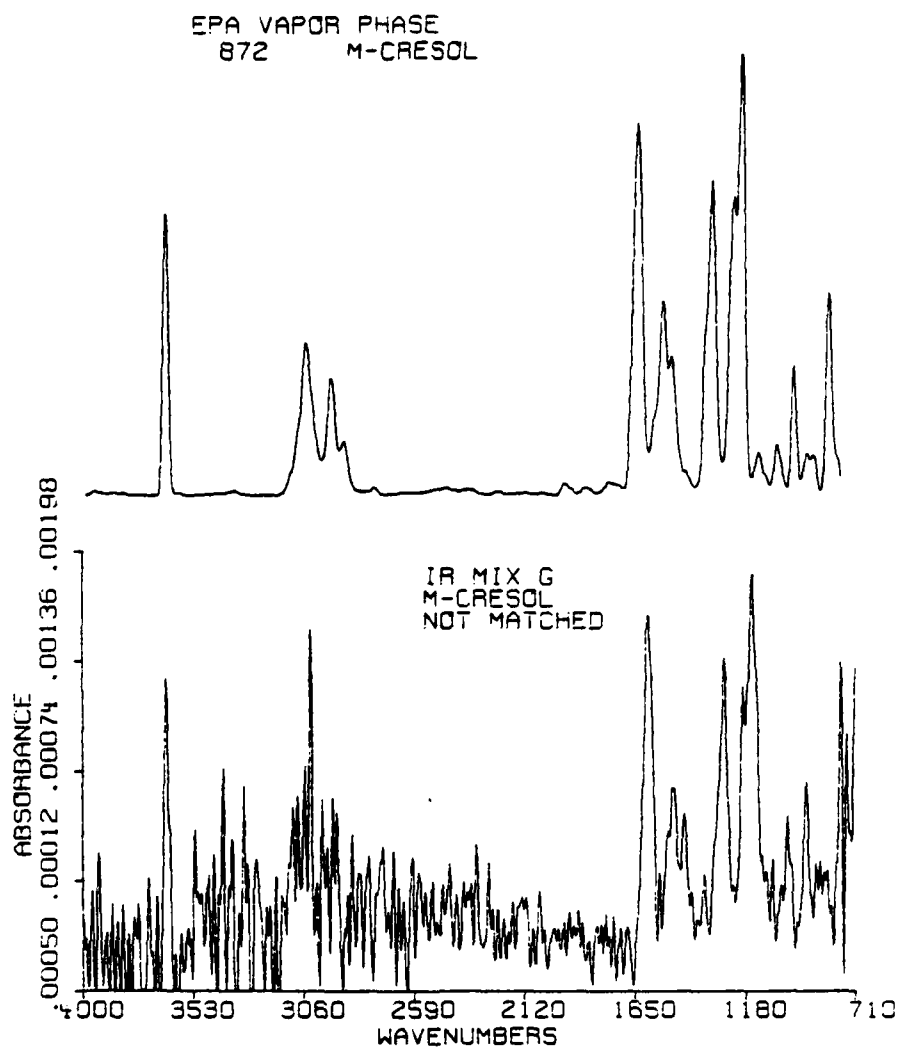
Figure 23.   FTIR of peak file spectrum compared with the EPA vapor
             phase spectrum of m-cresol. Corresponds to the greatest
             amount of material injected (250 ng.) which was not
             identifiable by the search routines (Standard Mixture G).
             See Table 3.

59

TABLE 13

Computer Search Routine Results for Injection of 96 ng of
Nitrobenzene[a]

EPA Vapor Phase Library Number	Match Value	Compound[b,c]
493	219	nitrobenzene
2878	231	2,4-dinitromesitylene
1204	240	2,6-dinitrotoluene
1315	248	1-chloro-3-nitrobenzene
2429	249	2,3-dinitrotoluene
2432	254	3-nitrobiphenyl
3097	262	3,5-dichloronitrobenzene
1470	265	2-chloro-1,3-dintrobenzene
1405	266	2-nitro-1,3,5-trichlorobenzene
2295	268	α-bromo-m-nitrotoluene

[a]See Figure 24

[b]Square algorithm used

[c]4000-3700 cm^{-1} and 730-400 cm^{-1} regions skipped

60

EPA VAPOR PHASE
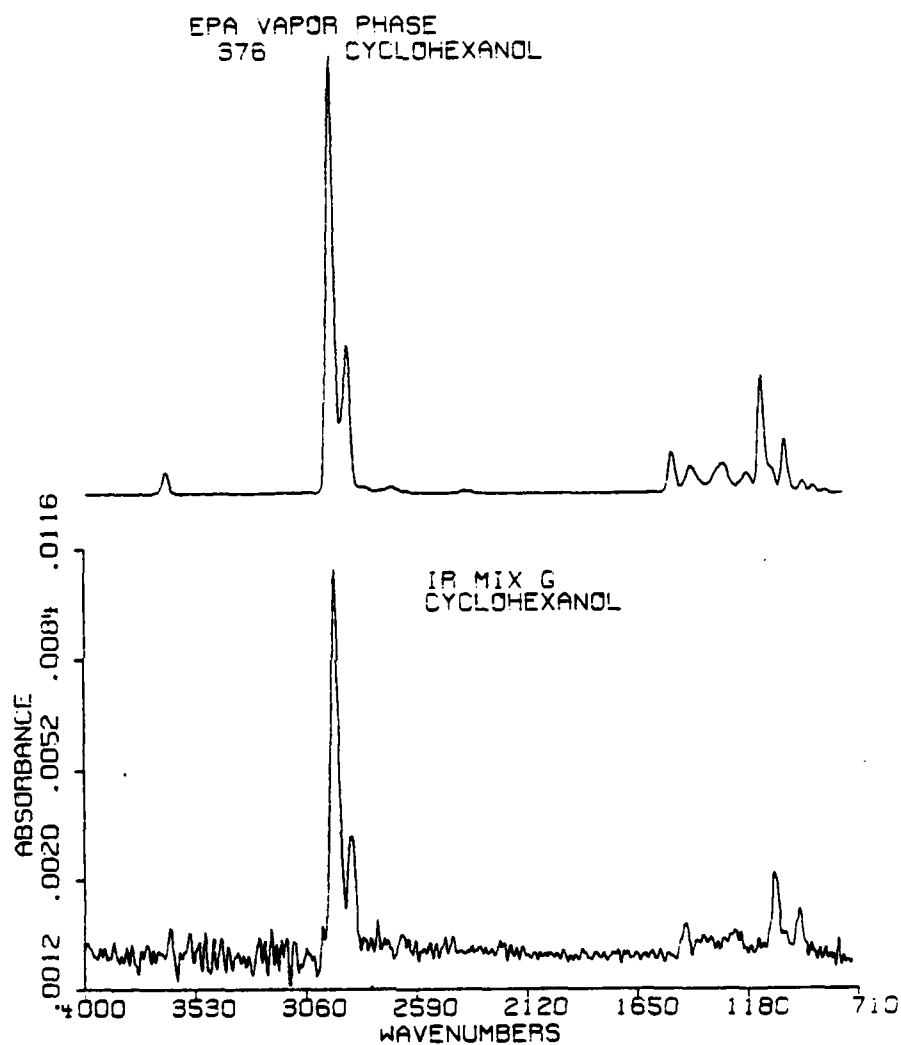#93   BENZENE, NITRO-

FILE #509-50%
NITROBENZENE
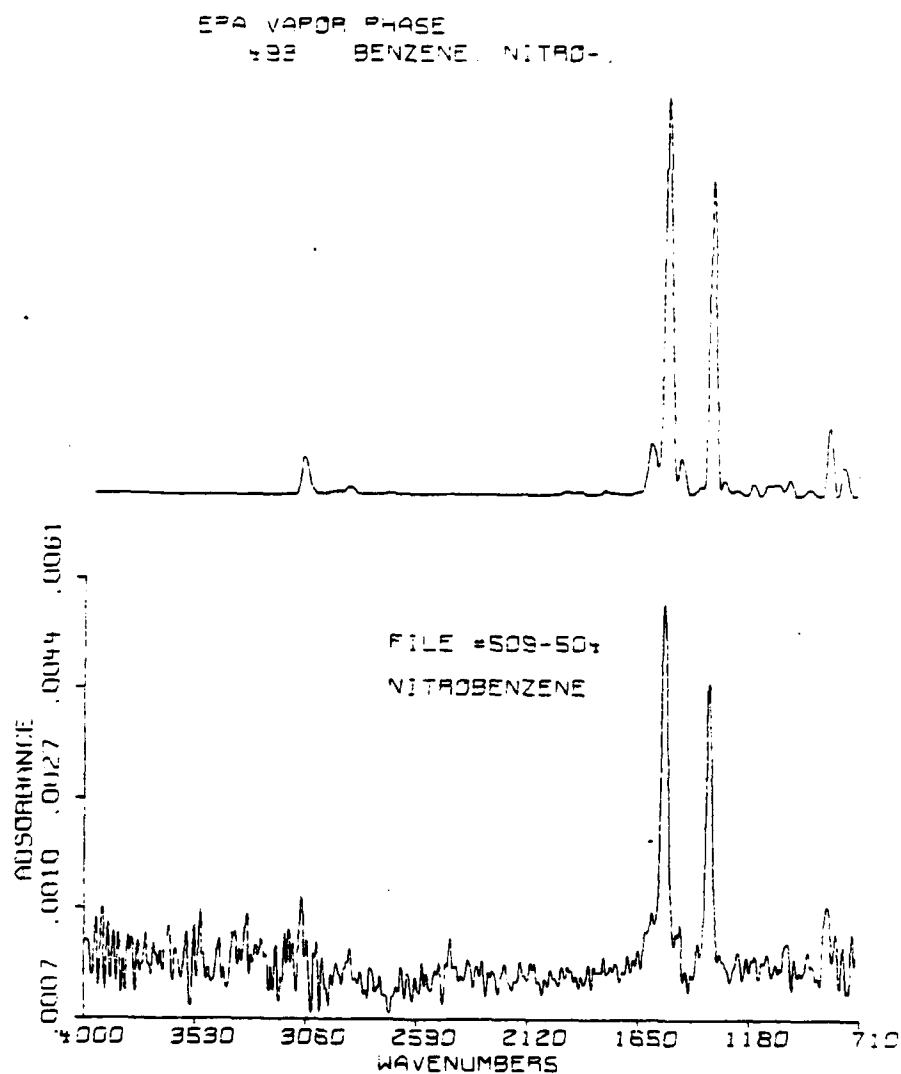
Figure 24A.   FTIR of peak file spectrum less background file spectrum
compared with the EPA vapor phase spectrum of nitro-
benzene. Corresponds to (A) the least amount of compound
positively identified by the search routines (Standard
Mixture D)....

61

FILE #515-520
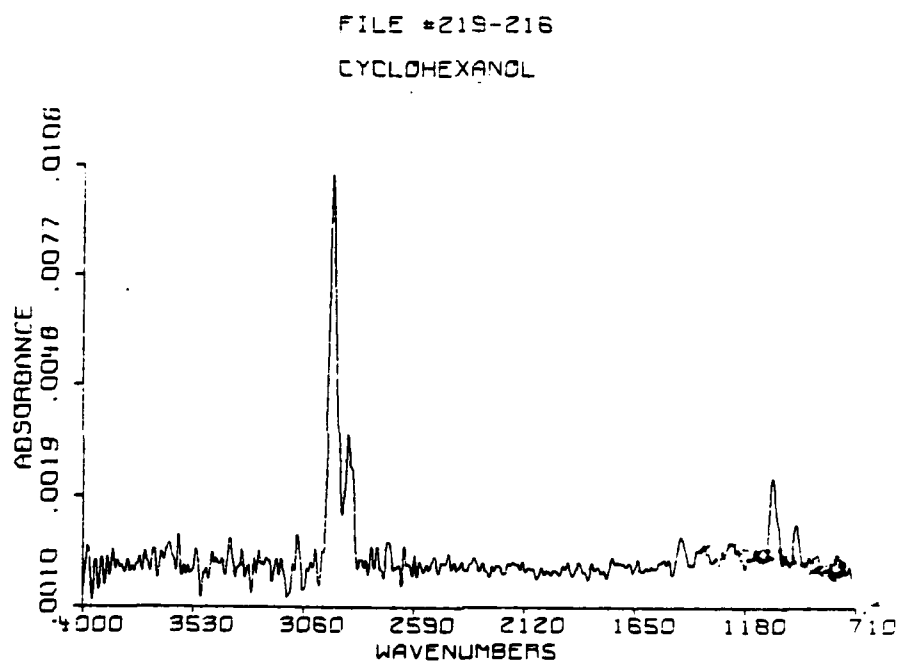NITROBENZENE

Figure 24B.   ....and (B) the greatest amount not identified by the
              search routines (Standard Mixture E). See Tables 3
              and 13.

62

TABLE 14

Computer Search Routine Results for Injection of
100 ng of Anisole[a]

EPA Vapor Phase Library Number	Match Value	Compound[b,c]
881	620	anisole
11	768	ethoxybenzene
946	940	phenylether
1708	997	o-methylphenetole ether
1732	1056	2-chloroethylphenyl
1706	1088	butylphenyl ether
1469	1150	4-phenoxybiphenyl
2771	1154	o-methoxyphenyl acetonitrile
1210	1163	4-chlorobutyl-o-tolyl ether
2524	1178	phenylpropyl ether

[a]See Figure 25

[b]Squared algorithm used

[c]725-400 cm^{-1} region skipped
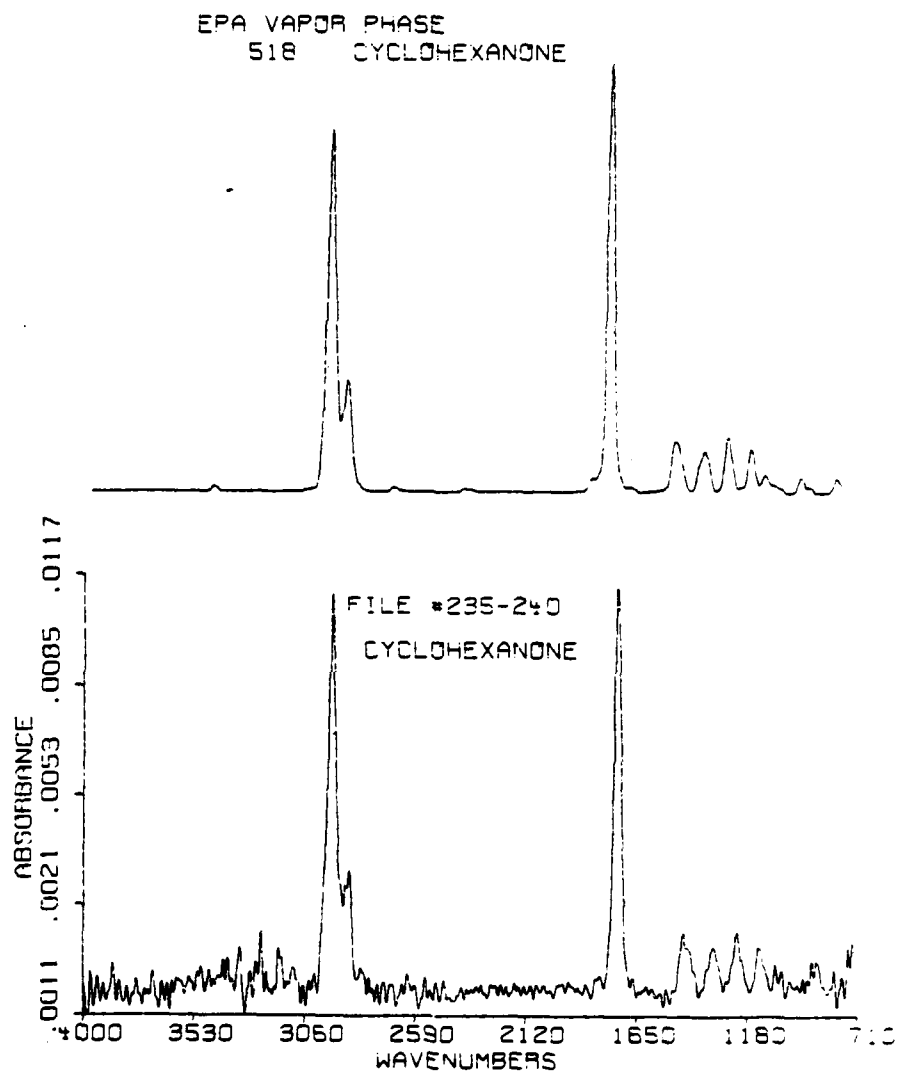
EPA VAPOR PHASE
88:    ANISOLE

FILE #257-252
ANISOLE
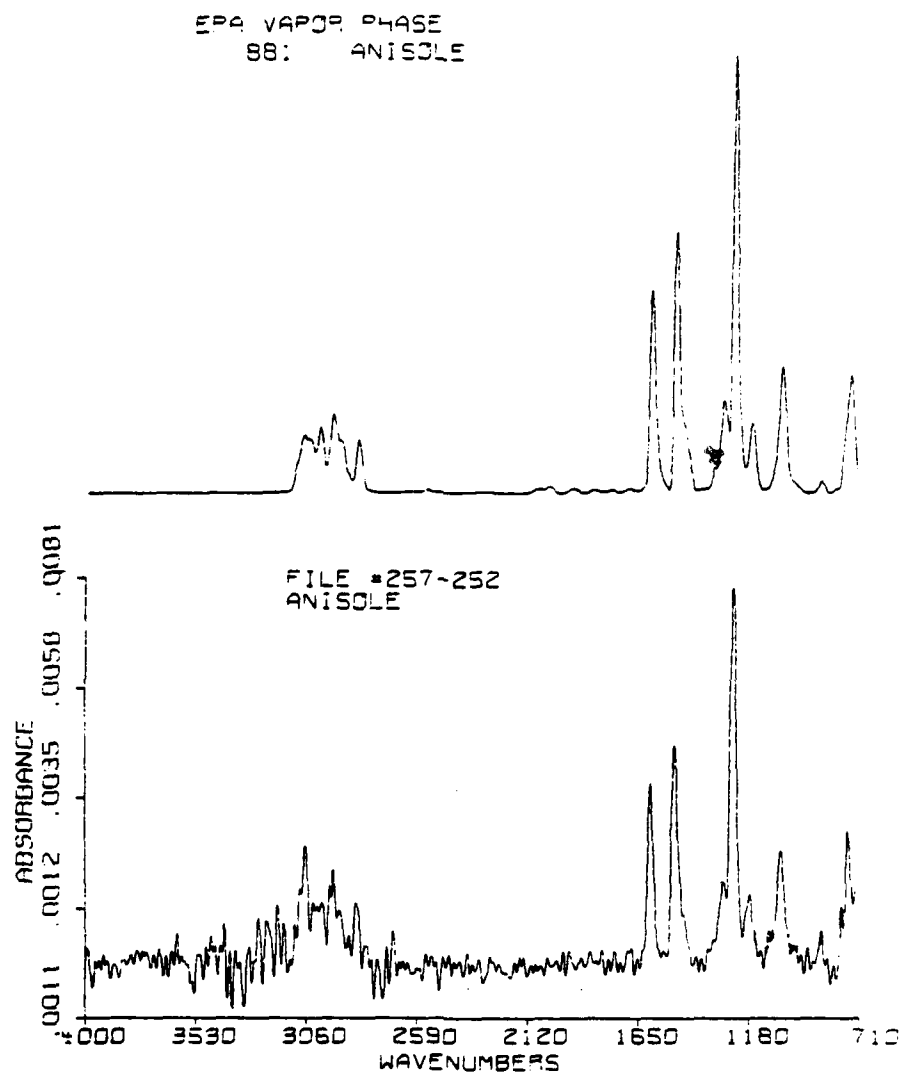
Figure 25A.   FTIR of peak file spectrum less background file spectrum
compared with the EPA vapor phase spectrum of anisole.
Corresponds to (A) the least amount of compound identi-
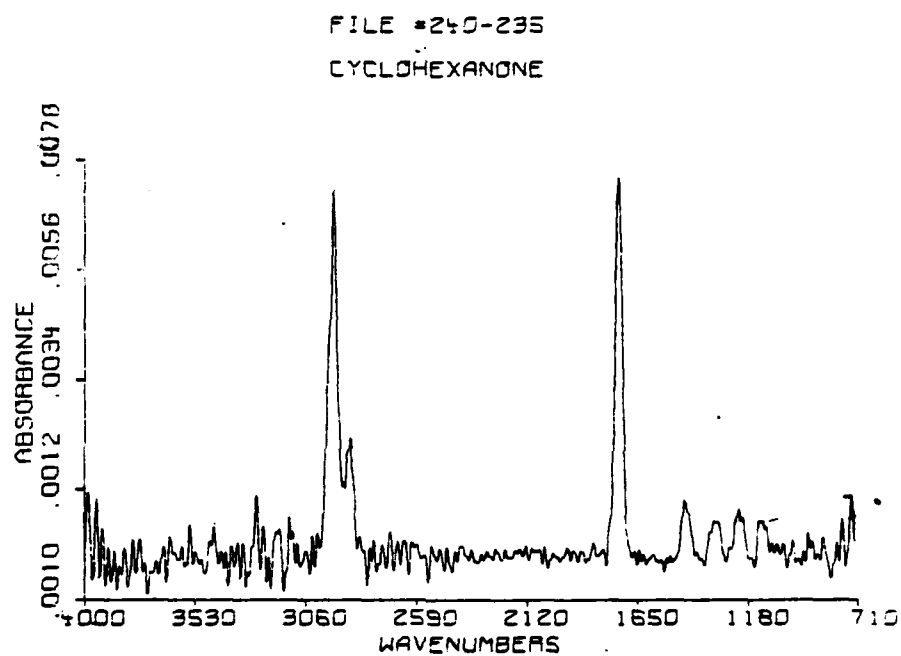fied by the search routines (Standard Mixture C)....

64
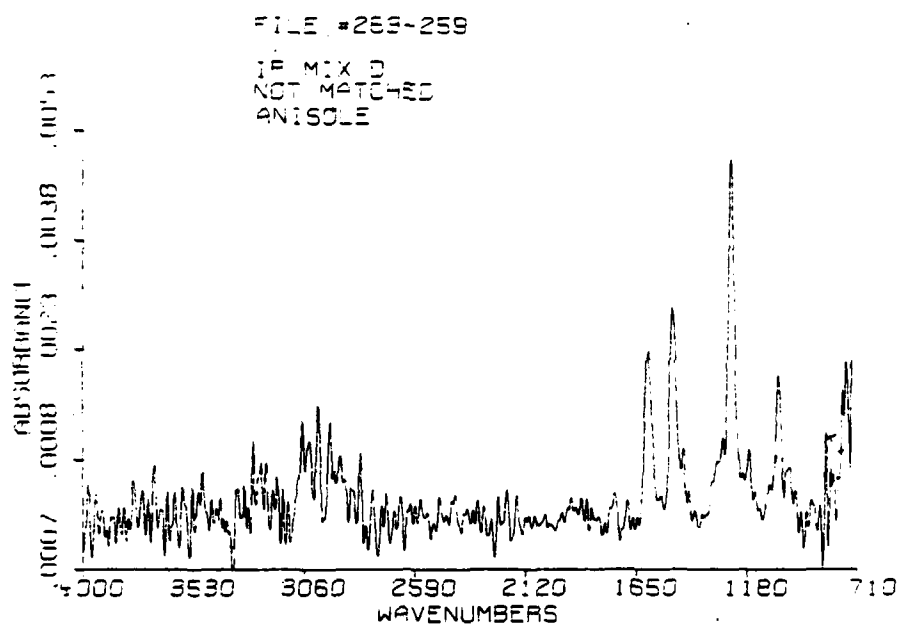
Figure 25B.   ....and (B) the greatest amount not identifiable by the
search routines (Standard Mixture D).   See Tables 3 and
14.

65

TABLE 15

Computer Search Routine Results for Injection of
273 ng of o-Anisidine[a]

EPA Vapor Phase Library Number	Match Value	Compound[b,c]
886	306	o-anisidine
1780	930	o-ethoxy aniline
2019	1442	o-butoxy aniline
1945	1601	o-tolyloxy aniline
2175	1676	5-tert-pentyl-2-phenoxy aniline
507	1866	quaiacol
331	2197	1,2,4-trimethoxy benzene
102	2371	o-ethoxy phenol
694	2407	2-chloro-1,4-dimethoxy benzene
2856	2408	2,3-epoxy propoxy anisole

[a]See Figure 26

[b]Square algorithm used

[c]720-400 cm^{-1} region skipped
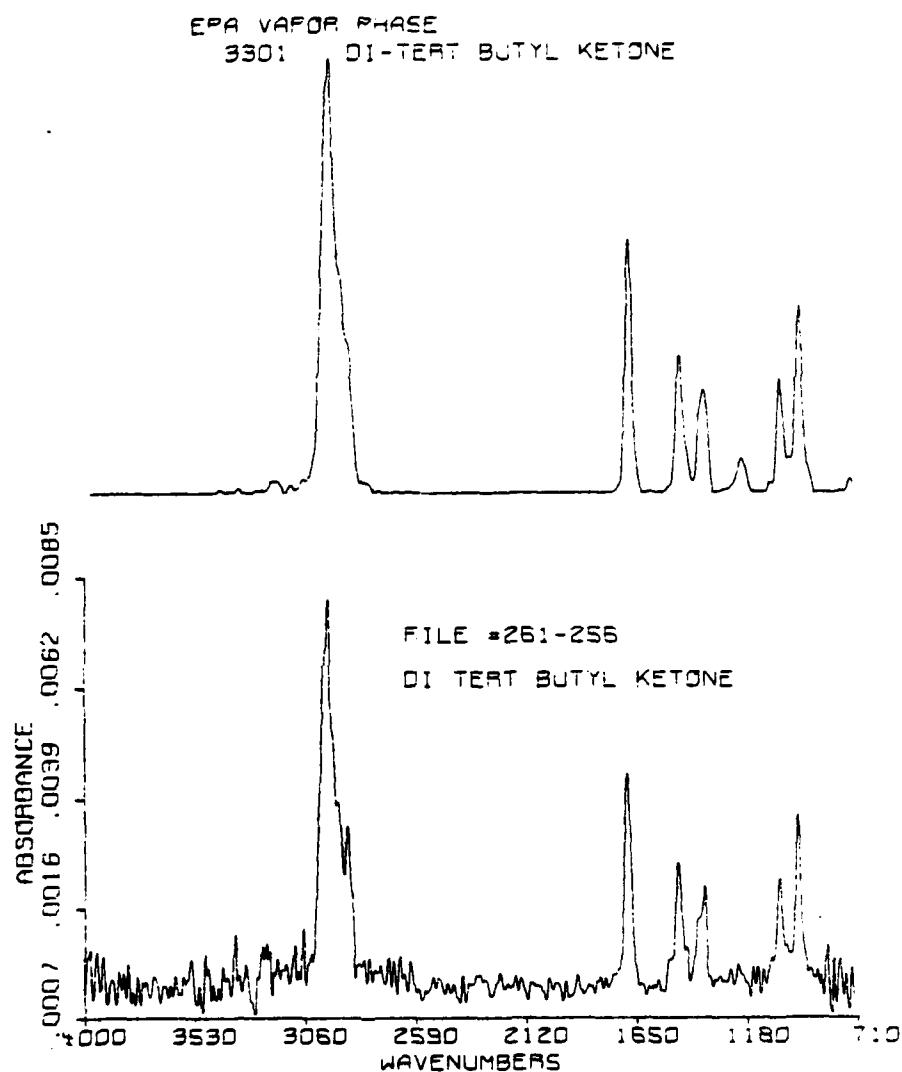
66

EPA VAPOR PHASE
886   O-ANISIDINE

FILE #601-607
O-ANISIDINE
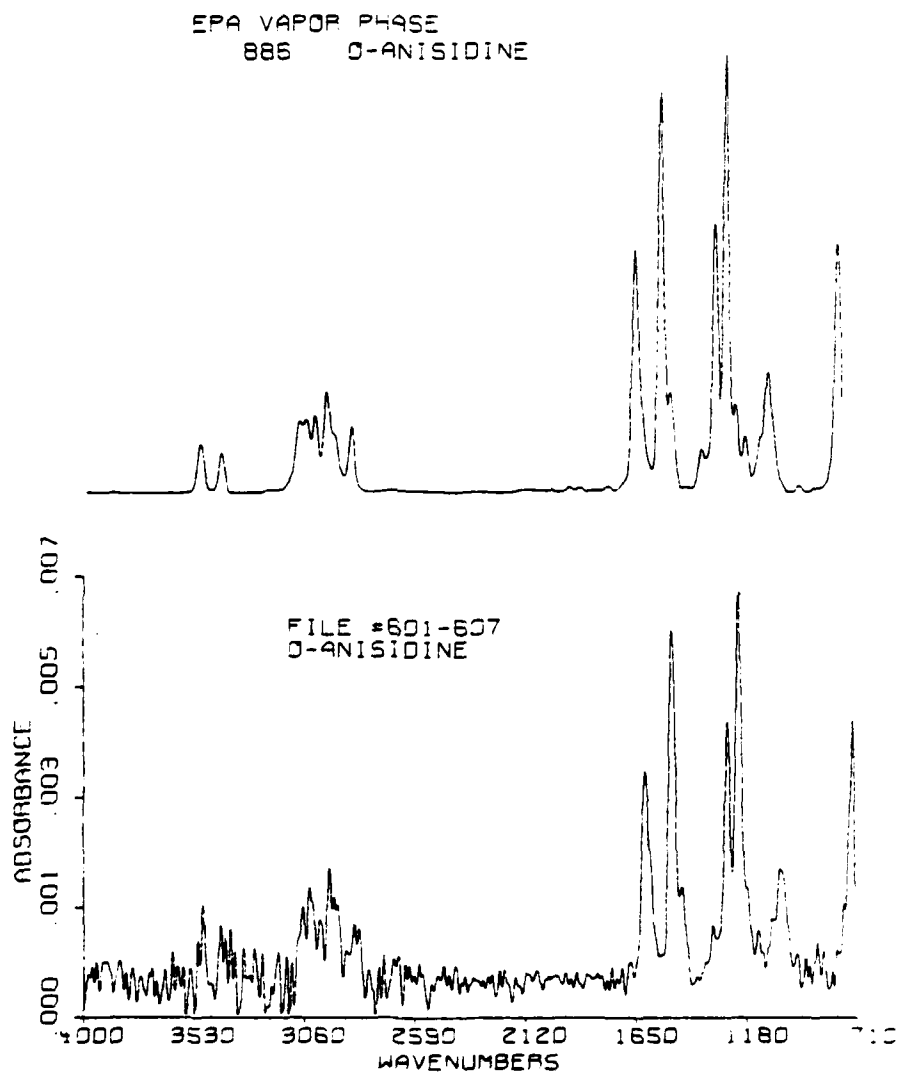
Figure 26A. FTIR of peak file spectrum less background file spectrum
compared with the EPA vapor phase spectrum of o-anisidine.
Corresponds to (A) the least amount of compound posi-
tively identified by the search routines (Standard
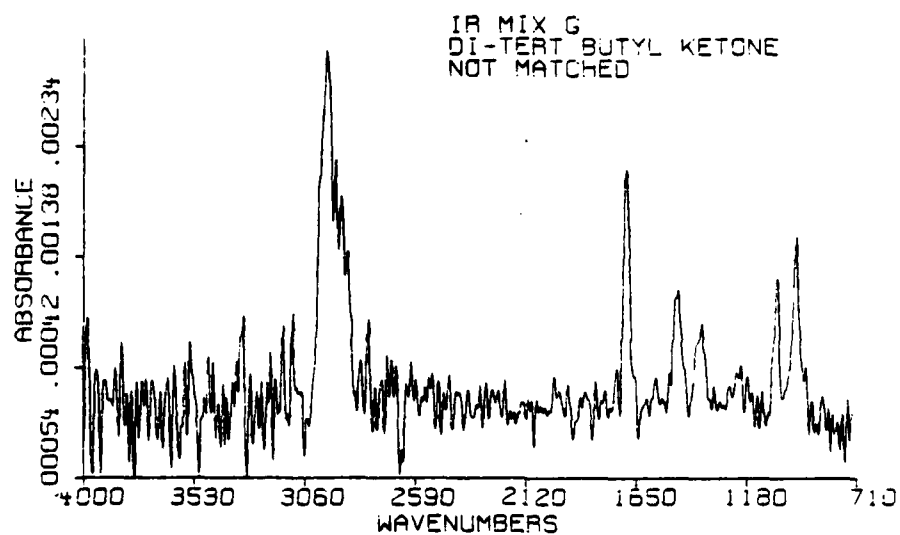Mixture B)....

67
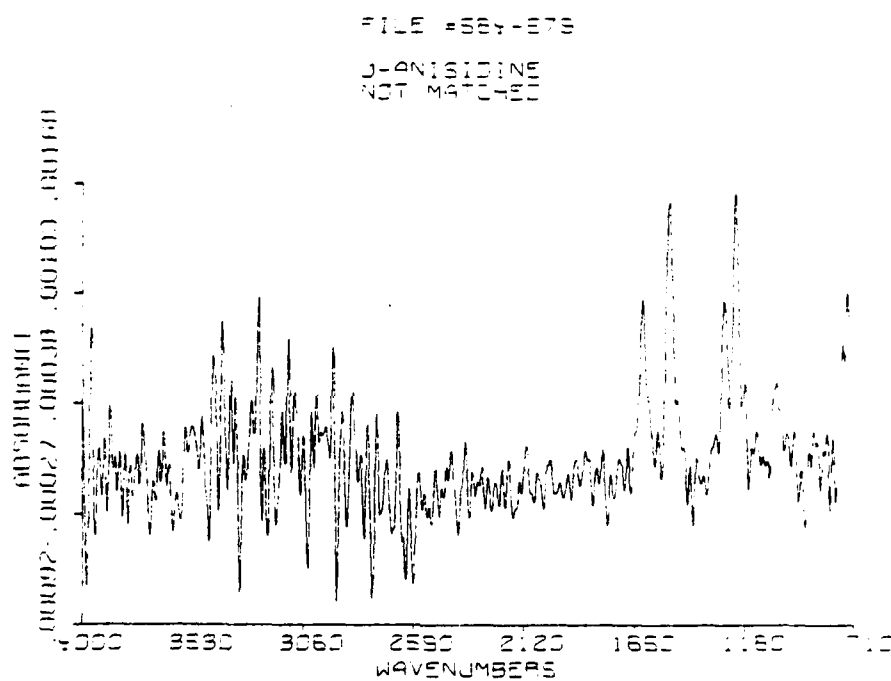
Figure 26B. ....and (B) the greatest amount not identified by the search routines (Standard Mixture C). See Tables 3 and 15.

TABLE 16

Computer Search Routine Results for Injection of
273 ng of Quinoline[a]

EPA Vapor Phase Library Number	Match Value	Compound[b,c]
855	847	quinoline
804	1397	α,α,α-trichloro toluene
1101	1441	phenanthrene
832	1730	α-chloro toluene
840	1855	carbon tetrachloride
1357	1857	naphthalene
1917	1880	chlorodiphenyl methane
934	1908	α,α2,6-tetrachloro toluene
2518	1924	1-naphth ene carbonitrile
1244	1933	o-α,α,α-tetrachlorotoluene

[a]See Figure 27

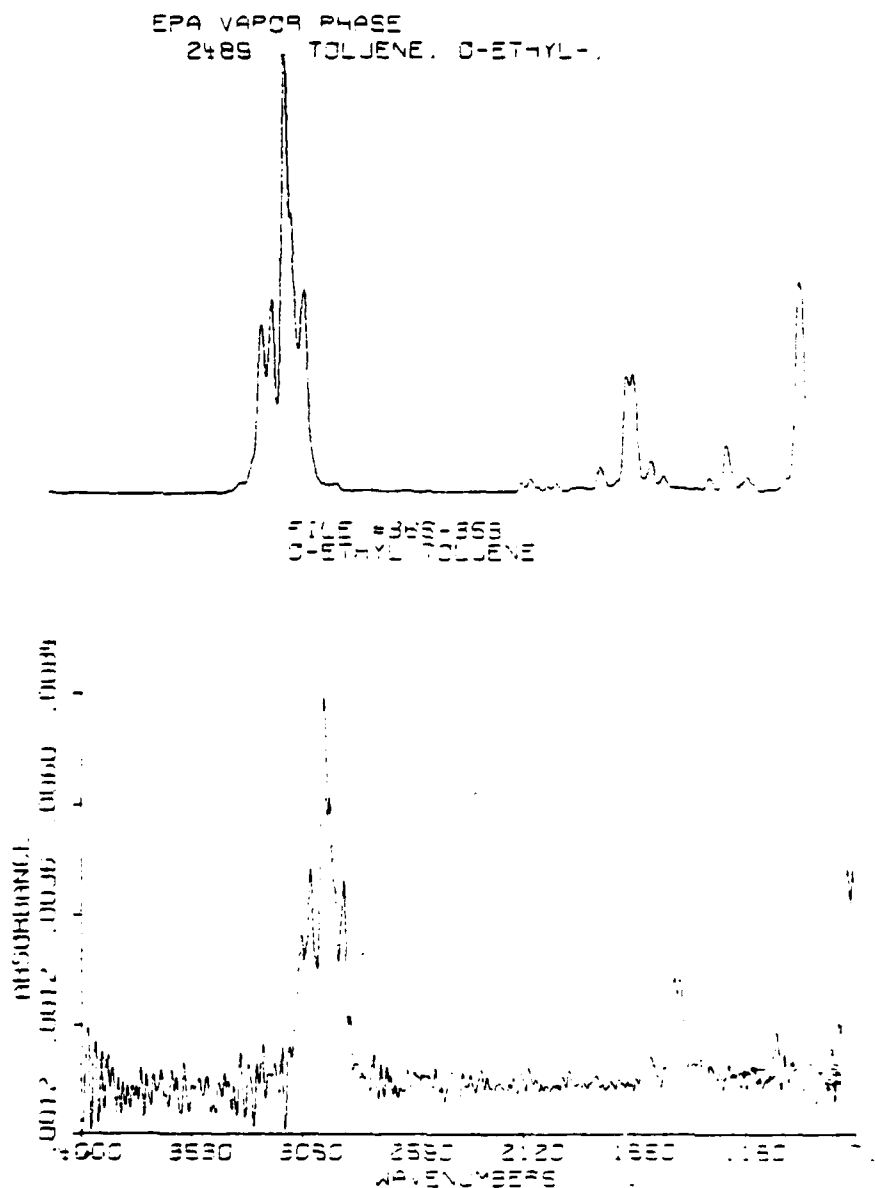[b]Squared algorithm used

[c]740-40C cm^{-1} region skipped

69
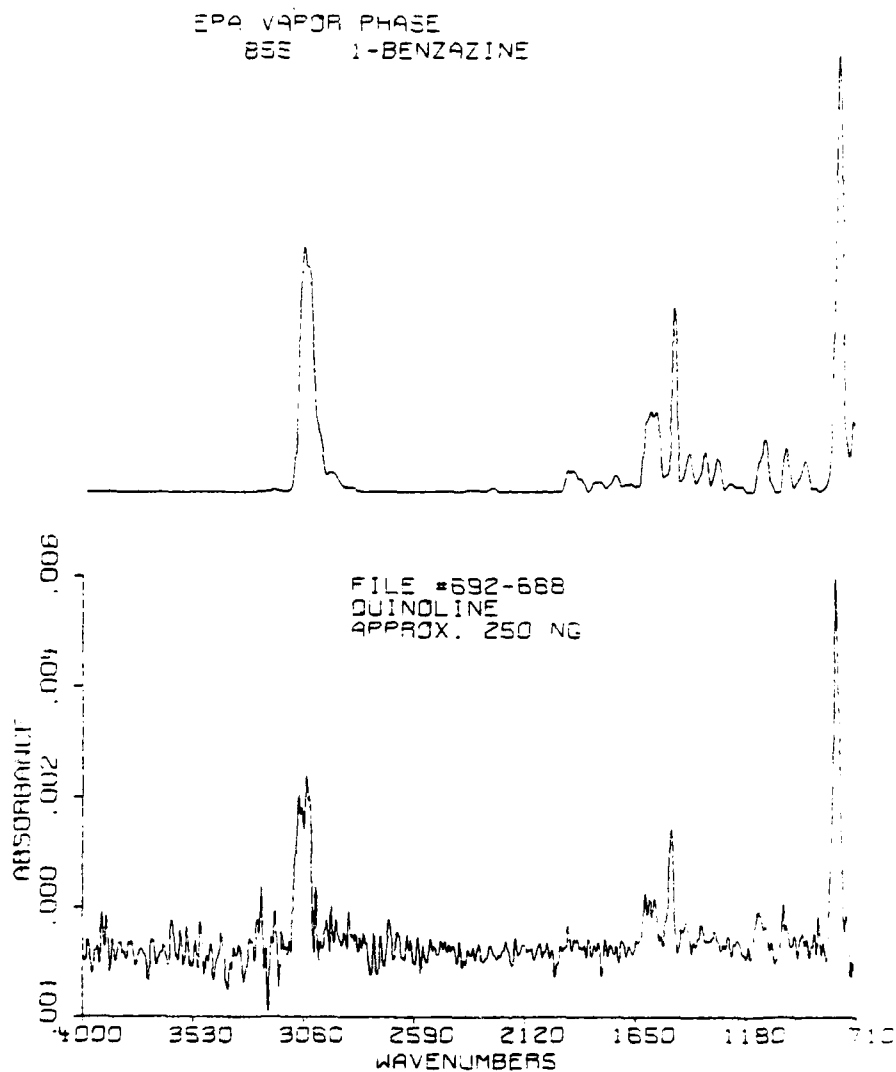
Figure 27A. FTIR of peak file spectrum less background file
spectrum compared with the EPA vapor phase spectrum of
quinoline. Corresponds to (A) the least amount of
compound positively identified by the search routines
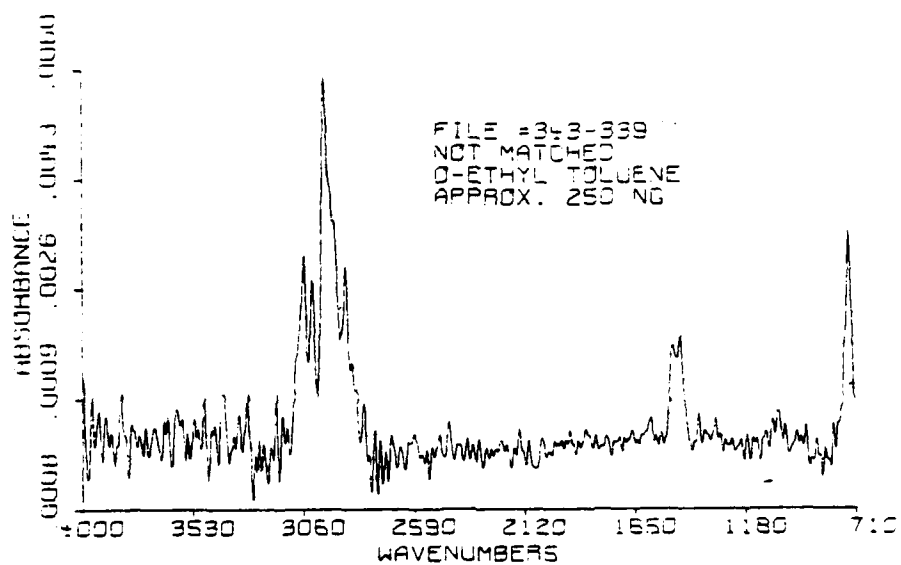(Standard Mixture B).

70

FILE #710-704

QUINOLINE
NOT MATCHED
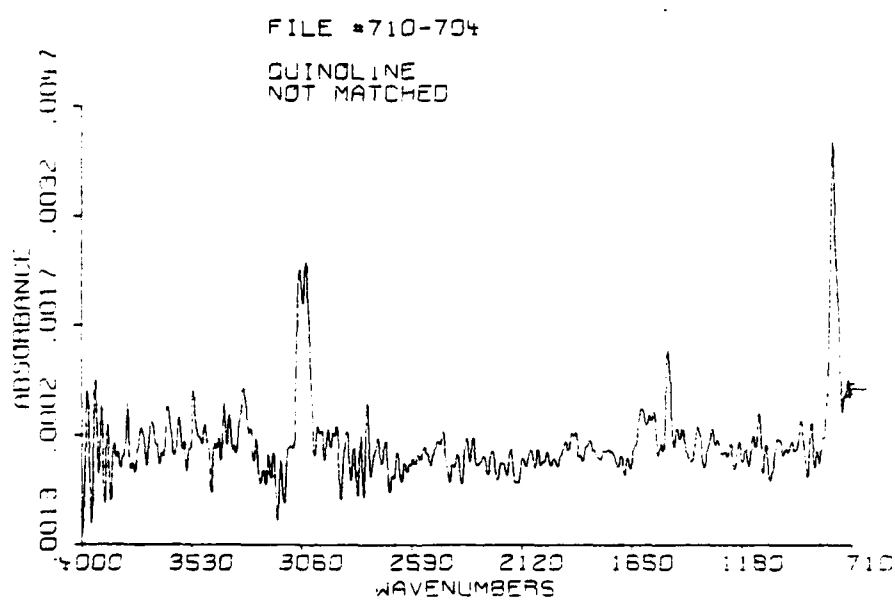
Figure 27B.   ....and (B) the greatest amount not identified by the
search routines (Standard Mixture D). See Tables 3
and 16.

71

TABLE 17

Computer Search Routine Results for Injection of
250 ng of 2-tert-Butyl Phenol[a]

EPA Vapor Phase Library Number	Possible Hits	Compound[b,c]
3303	263	2-tert-butyl phenol
114	402	6-tert-butyl o-cresol
231	964	2,6-diisopropyl phenol
3264	1072	2,6-disec-butyl phenol
1083	1145	2,6-di-tert-butyl p-cresol
1414	1283	2,6-di-tert-butyl 4-phenol
1345	1342	3,5-di-tert-butyl benzyl alcohol
63	1422	6-tert-butyl 2,4-xylenol
2102	1438	o-sec-pentyl phenol
3209	1444	3,5-di-tert-butyl 4-benzonitrile

[a]See Figure 28

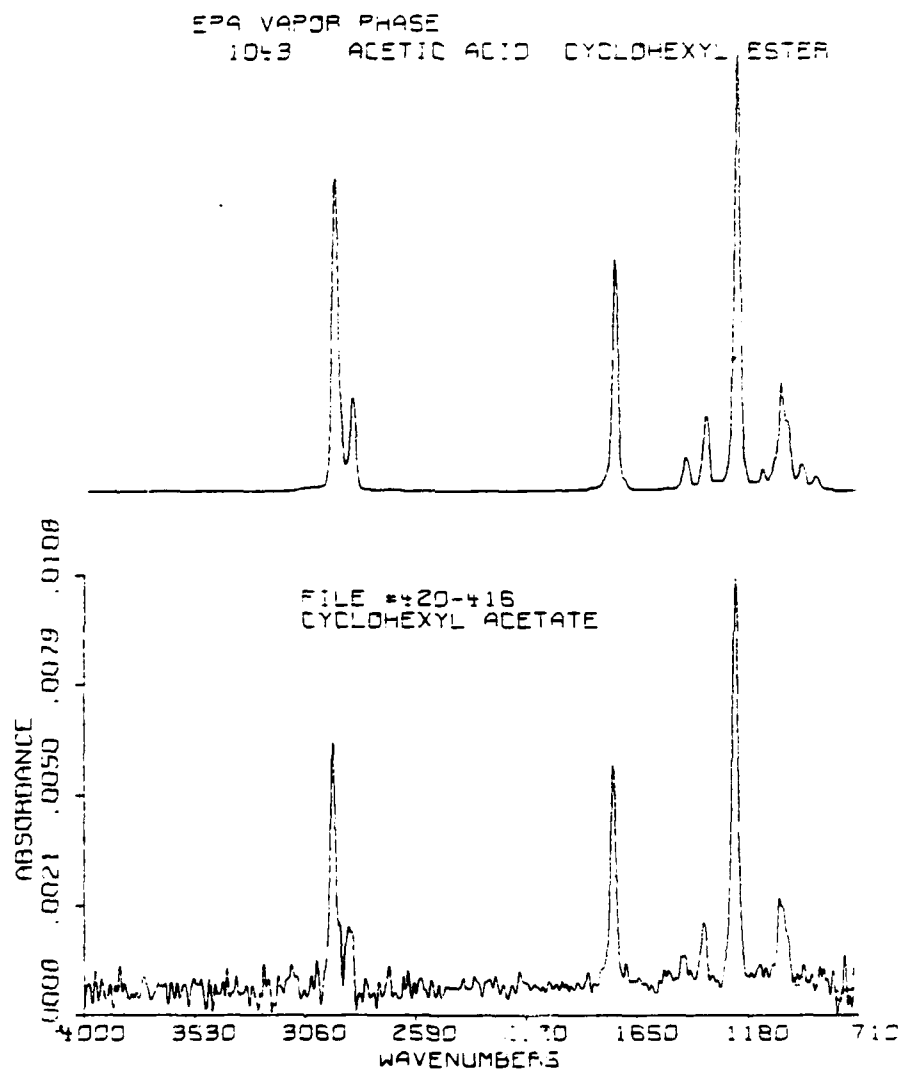[b]Square algorithm used

[c]730-400 cm^{-1} region skipped
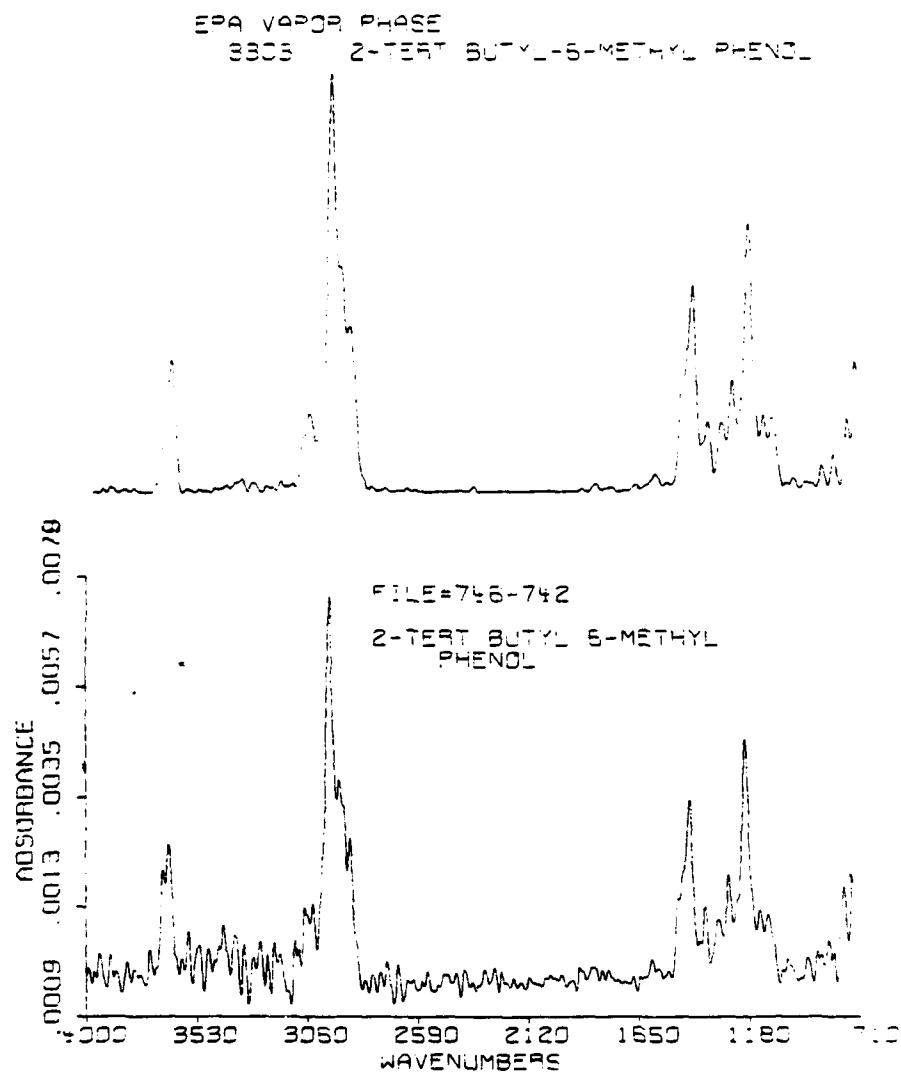
Figure 28A.   FTIR of peak file spectrum less background file
               spectrum compared with the EPA vapor phase spectrum of
               2-tert-butyl 6-methyl phenol. Corresponds to (A) the
               least amount of compound positively identified by the
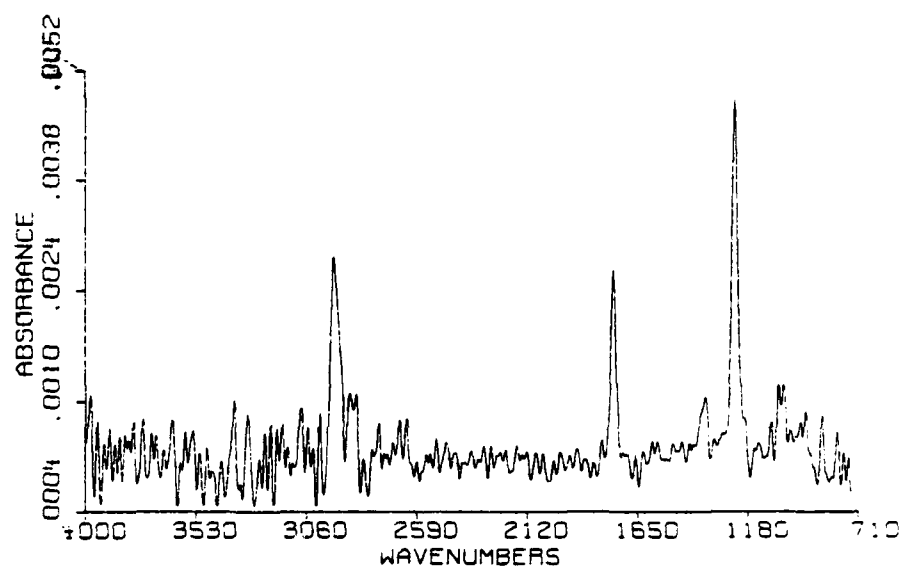   search routines (Standard Mixture B).

73
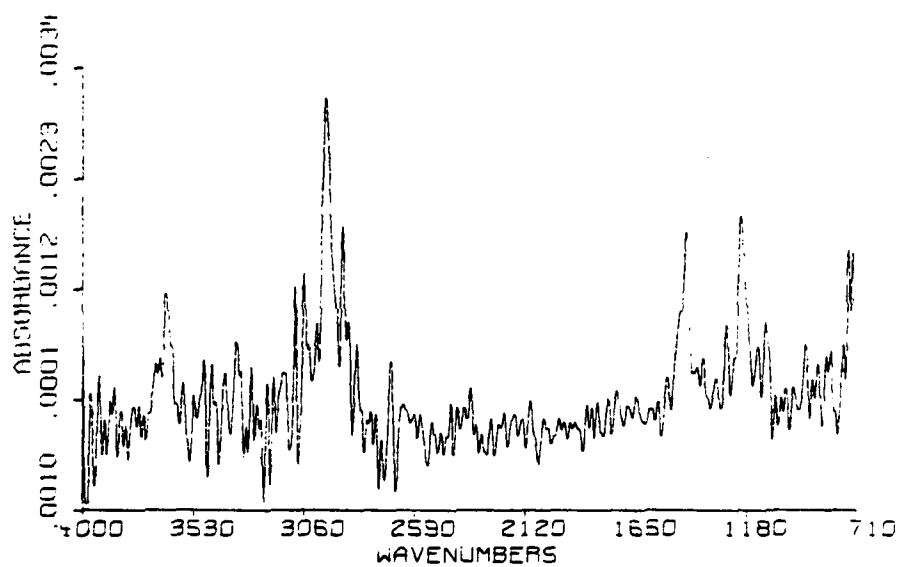
Figure 28B.   ....and (B) the greatest amount not identified by the search routines (Standard Mixture G). See Tables 3 and 17.

4. Absorbance Versus Concentration

Another objective of this work was to determine whether an absorbance/concentration relationship could be generated from IR data collected on-the-fly. A linear Beer-Lambert relationship was envisioned where absorbance/concentration plots could be used for determining the concentration of functionally similar compounds. Tables 18 and 19 list the absorbance intensity (peak height) for certain infrared bands at different concentrations. In one case the most intense peak absorbance was chosen, although the choice may not have represented the compound's more unique functionality. In the other case the peak absorbance chosen represented the one most characteristic of the compound in question. For many compounds, the "most characteristic" peak absorbance was by far not the most intense peak.

By applying a linear regression calculation the slope, y-intercept and linear correlation (squared) were generated using the absorbance/concentration data from Tables 18 and 19. The results are shown in Tables 20 and 21 for the specified wavenumber absorbance intensity. Multiple calculations are given for several individual compounds due to questionable data scatter.

The results of these calculations are presented in Figures 29-31 along with the structure of each compound. One can easily correlate the amount of material injected with the infrared absorbance intensity of the most intense peak. Only cyclohexanol gave a relatively poor correlation. For the most characteristic peak of cyclohexanol the correlation factor was appreciably lower. Two other compounds each containing an hydroxyl functionality (2-tert-butyl-6-methyl phenol and amyl alcohol) gave correlation factors less than 90% when the most characteristic peak absorbance (-OH) was used. The slopes of several lines, however confirm that the C=O stretching mode (1715 cm^{-1}) in amides, the C-H stretching vibration (2940 cm^{-1}) of alkane species and the C-O stretch (1240 cm^{-1}) in esters are three of the strongest absorbing functionalities measured. Not surprisingly, the majority of the y-intercepts give

75

TABLE 18

Absorbance - Concentration Data For Most Intense Peak

Standard Mixture Compound	cm⁻¹	B ng	B abs	C ng	C abs	D ng	D abs	E ng	E abs	F ng	F abs	G ng	G abs
pyrrole	718	240	.0095	480	.0225	--	--	115	.0035	192	.0072	80	.0037
N,N-dimethylformamide	1715	236	0.043	57	.0102	28	.0030	66	.0092	18.8	.00145	--	--
amyl alcohol	2938	--	--	--	--	202	.0123	122	.0059	81	.0045	250	.0143
3-picoline	3040	238	.0041	--	--	333	.0055	285	.0039	238	.0037	190	.0020
n-nonane	2930	178	.0195	42	.0050	86	.0094	--	--	57	.0060	113	.0112
cyclohexanol	2940	--	--	--	--	192	.0238	81	.0103	67	.0071	145	.0112
cyclohexanone	1730	--	--	--	--	188	.0113	94	.0073	66	.0045	--	--
di-tert-butyl-ketone	2940	--	--	--	--	--	--	200	.0080	--	--	100	.0032
o-ethyl toluene	2970	220	.0060	440	.015	326	.0104	105	.0031	263	.0084	--	--
cyclohexyl acetate	1240	243	.0321	68	.0108	29	.0039	40	.0048	19.5	.0019	--	--
m-cresol	1150	--	--	--	--	206	.0055	103	.0022	154	.0032	250	.0019
nitrobenzene	1540	300	.0158	188	.0129	96	.0057	60	.0039	36	.0022	--	--
anisole	1245	248	.0175	100	.0081	74	.0049	--	--	--	--	--	--
o-anisidine	1225	273	.0125	164	.0065	98	.0031	65	.0016	142	.0044	--	--
quinoline	7957	273	.0063	164	.0034	218	.0043	196	.0039	--	--	--	--
2-tert-butyl 6methyl phenol	2966	250	.0075	500	.0165	--	--	150	.0049	100	.0031	200	.0041

76

TABLE 19

Absorbance-Concentration Data for Characteristic Peak

Standard Mixture		B		C		D		E		F		G	
Compound	cm^{-1}	ng	abs	ng	abs	ng	abs	ng	abs	ng	abs	ng	abs
pyrrole	3520	240	.0053	480	.0124	--	--	115	.0021	192	.0046	80	.0011
cyclohexylacetate	1755	243	.0165	68	.0057	29	.0019	40	.0026	19.5	.0007	--	--
m-cresol	3650	--	--	--	-	206	.0036	103	.0015	154	.0020	250	.0008
o-ethyl toluene	745	220	.0035	440	.0085	326	.0057	105	.0014	263	.0045	--	--
nitrobenzene	1350	300	.0133	180	.0110	96	.0045	60	.0027	36	.0018	--	--
2-tert-butyl-6-methyl phenol	3640	250	.0026	500	.0054	--	--	150	.019	100	.0011	200	.0008
amyl alcohol	1045	--	--	--	--	202	.0048	122	.0021	81	.0014	250	.0043
di-tert-butyl ketone	1695	--	--	--	--	--	--	200	.0045	--	--	100	.0022
cyclohexanol	1070	--	--	--	--	192	.0052	81	.0025	67	.0017	145	.0022
3-picoline	780	--	.0024	--	--	--	.0038	--	.0031	--	.0019	--	.0016

77

TABLE 20

Beer-Lambert Results from Infrared Absorbance-Concentration Study
Most Intense Peak

Compound	Pts used	Pts avail	Slope	y-Intercept	$(corr)^2$	peak cm^{-1}
pyrrole	5	5	4.92×10^{-5}	$-.0016$	0.9864	718
pyrrole	4	5	5.24×10^{-5}	$-.0027$	0.9991	718
N,N-dimethyl formamide	5	5	1.91×10^{-4}	$-.0021$	0.9967	1715
amyl alcohol	4	4	6.2×10^{-5}	-9.08×10^{-4}	0.9814	2938
3-picoline	4	5	2.25×10^{-5}	$-.0021$	0.9333	3040
n-nonane	5	5	1.07×10^{-4}	6.02×10^{-5}	0.9902	2930
cyclohexanol	4	4	1.13×10^{-4}	-6.62×10^{-4}	0.8061	2940
cyclohexanone	3	3	5.24×10^{-5}	1.62×10^{-3}	0.9601	1730
di-tert butyl ketone	2	2	4.82×10^{-5}	$-.0016$	1	2970
o-ethyl toluene	5	5	3.60×10^{-5}	-1.18×10^{-3}	0.9883	2970
cyclohexyl acetate	5	5	1.33×10^{-4}	7.8×10^{-5}	0.9938	1240
m-cresol	3	4	3.17×10^{-5}	-1.24×10^{-3}	0.9491	1150
nitrobenzene	5	5	5.36×10^{-5}	9.02×10^{-4}	0.9468	1540
nitrobenzene	4	5	7.41×10^{-5}	-7.14×10^{-4}	0.9898	1540
anisole	3	3	6.94×10^{-5}	4.08×10^{-4}	0.9884	1245
o-anisidine	5	5	5.29×10^{-5}	-2.24×10^{-3}	0.9856	1225
quinoline	4	4	2.71×10^{-5}	-1.29×10^{-3}	0.9561	795
2-tert-butyl 6 methyl phenol	5	5	3.43×10^{-5}	-1.01×10^{-3}	0.9641	2966
2-tert-butyl 6 methyl phenol	4	5	3.35×10^{-5}	-3.42×10^{-4}	0.9967	2966

TABLE 21

Beer-Lambert Results From Infrared Absorbance/Concentration Study
Most Characteristic Peak

Compound	Pts used	Pts avail	Slope	y-Inter	$(corr)^2$	Peak cm^{-1}
pyrrole	5	5	2.81×10^{-5}	-1.16×10^{-3}	0.9973	3520
cyclohexyl acetate	5	5	6.88×10^{-5}	-1.47×10^{-5}	0.9909	1755
m-cresol	3	4	2.06×10^{-5}	-8.09×10^{-4}	0.9180	3650
o-ethyl toluene	5	5	2.12×10^{-5}	-1.03×10^{-3}	0.9942	745
nitrobenzene	5	5	4.66×10^{-5}	3.81×10^{-4}	0.9409	1350
2-tert-butyl-6 methyl phenol	5	5	1.11×10^{-5}	-3.06×10^{-4}	0.8805	3640
2-tert-butyl-6 methyl phenol	4	5	1.05×10^{-5}	1.18×10^{-4}	0.9960	3640
amyl alcohol	4	4	2.0×10^{-5}	-1.2×10^{-4}	0.8713	1045
amyl alcohol	3	4	2.84×10^{-5}	-1.06×10^{-3}	0.9837	1045
di-tert butyl ketone	2	2	2.31×10^{-5}	-1.5×10^{-4}	1	1695
cyclohexanol	4	4	2.29×10^{-5}	9.85×10^{-5}	0.7044	1070
cyclohexanone	3	4	2.70×10^{-5}	4.3×10^{-5}	0.9873	1070
3-picoline	4	5	1.64×10^{-5}	-1.67×10^{-3}	0.9633	780
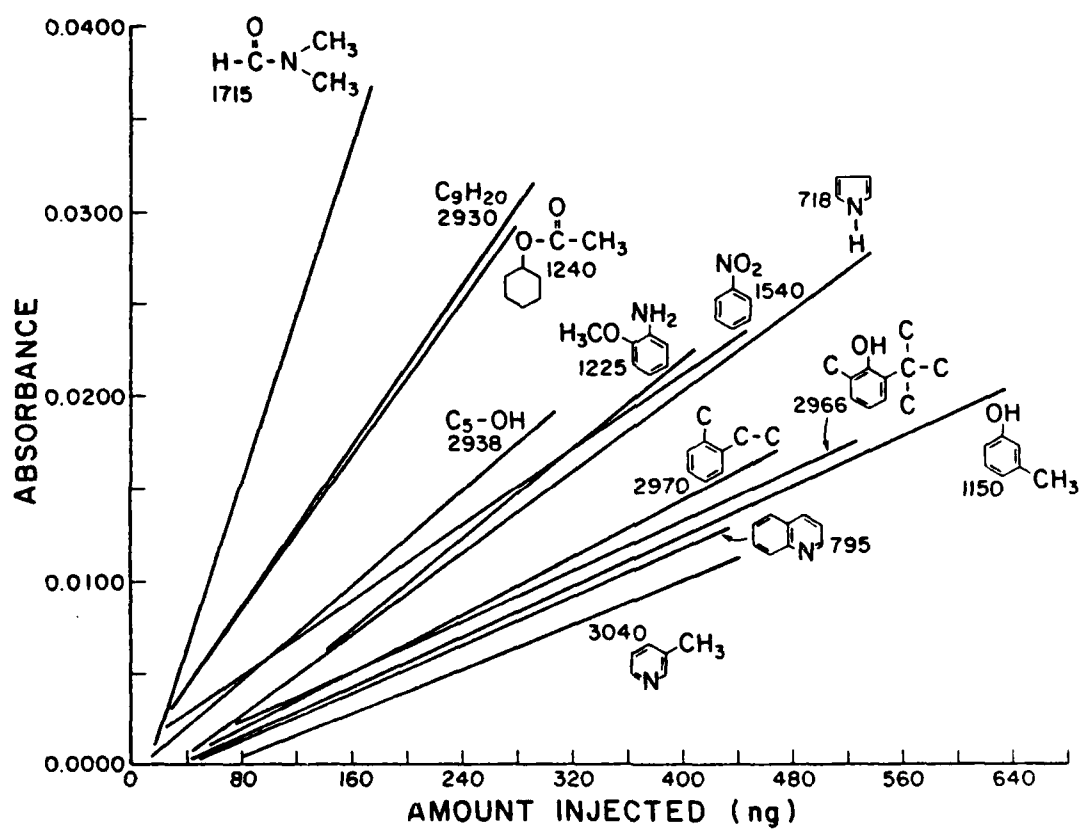
Figure 29.   Plot of absorbance of indicated wavenumber band
versus amount injected onto GC column.
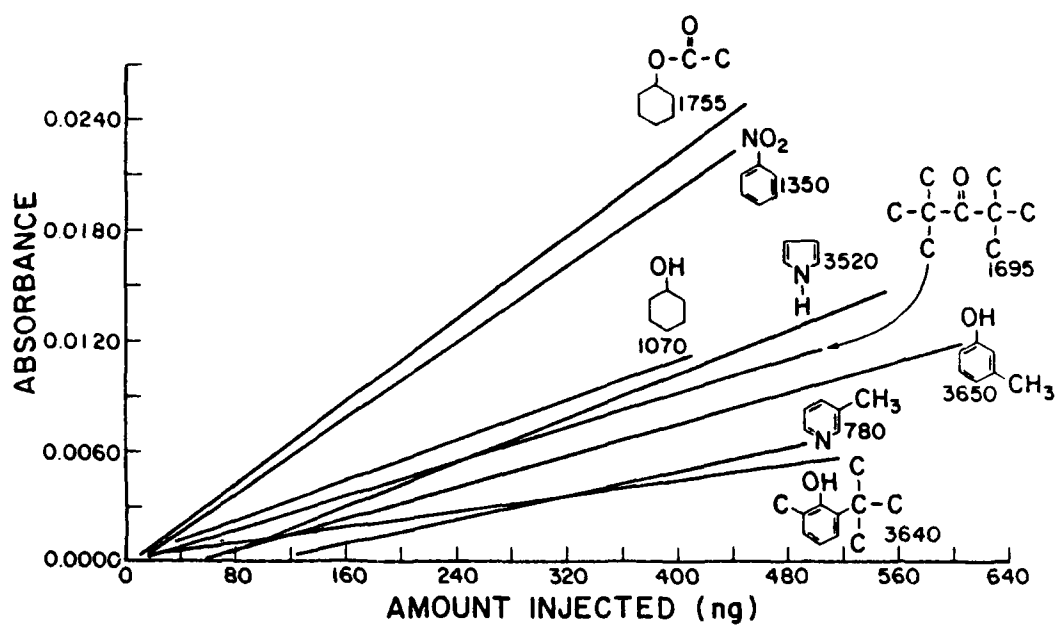
Figure 30. Plot of absorbance of indicated wavenumber band versus amount injected onto GC column.
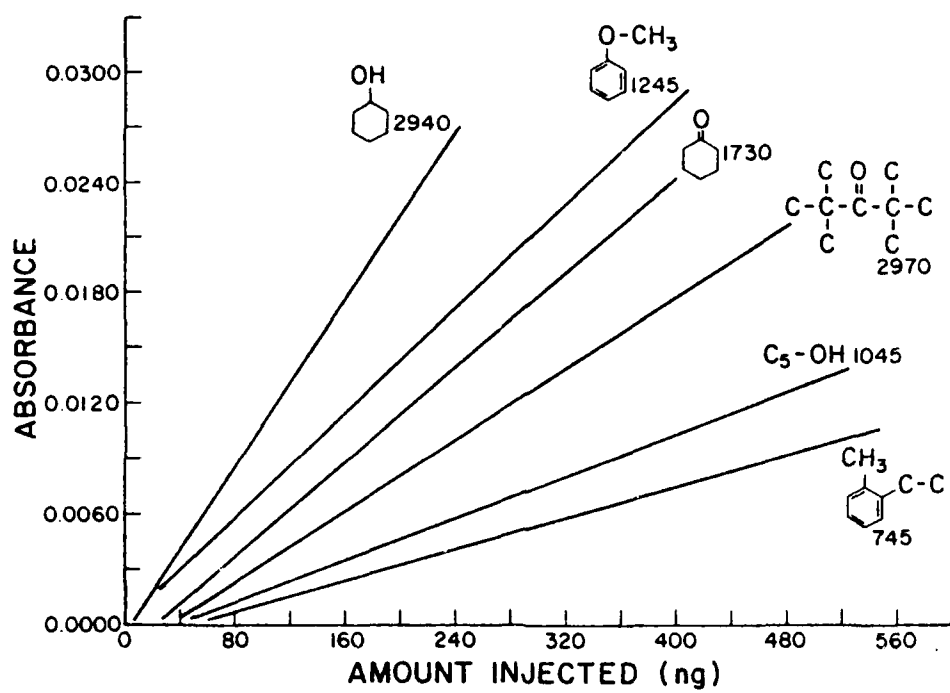
Figure 31.   Plot of absorbance of injected wavenumber band
versus amount injected onto GC column.

82

negative values, indicating that for certain very low injected
amounts, any absorbance intensity will be lost in the infrared
background noise.

In summary, the measurement of transient occurrences such
as are found in the GC/FTIR experiment create certain difficulties as
related to the construction of calibration curves or plots. The
possibility of not recording the actual maximum absorbance can always
exist despite relatively rapid data acquisition rates. Also, the
specification of which vibrational frequency to use may determine the
linearity of the data points. For weakly absorbing functional
groups, background noise may become increasingly significant at lower
concentrations. For multi-functional compounds, unique combinations
of absorbance patterns should aid computerized spectral search
routines in unambiguous identifications.

D. ANALYSES OF FUEL SAMPLES

Data previously generated by capillary GC/FTIR analysis of
"real world" samples have demonstrated the usefulness of the method.
Wide bore glass columns have been used to separate diesel fuel(11)
and a wastewater sample(9) with FTIR as detector. More narrow fused
silica columns have been used for separation of an ink industry
sample(6), a lacquer thinner(7), a petroleum distillate cut(16), and
coriander oil(20).

The work reported here is concerned with the analysis of
jet fuel products by capillary GC/FTIR. The overall objective was
the identification (via infrared spectral library search routines
and/or visual interpretation) of polar components separated by high
resolution fused silica capillary chromatography. While capillary
GC/FTIR can be a very useful technique for unambiguous identification
of compounds, the performance of the method may be limited by (1)
sample loading, (2) vibrational frequency characteristics of certain
functional groups or molecular species, (3) the complexity of the
sample (wherein coelution may still occur), and (4) interferometer

83

END

FILMED

DTIC
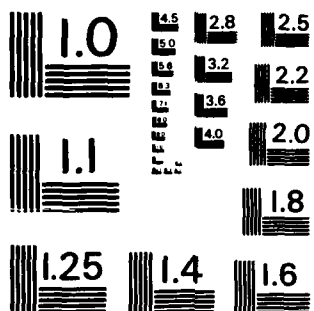
MICROCOPY RESOLUTION TEST CHART

NATIONAL BUREAU OF STANDARDS-1963-A

stability at high scanning velocities (which would be needed for complex samples). Nonetheless, several advantages of FTIR as a detector include isomer differentiation due to unique infrared absorbance patterns and qualitative functional group identification by monitoring specific wavenumber regions. One further concern with the GC/FTIR method is the amount of computer storage which may be required for samples which contain components of a wide vaporization range. Gas chromatographic separations of forty minutes to an hour are common for highly complex mixtures.

1.   Samples

Samples of jet fuel products were provided by the Monsanto Research Corporation, Dayton Laboratory, Dayton, Ohio. Four of the samples received had been fractionated previously using chloroform and ethanol to strip polar components from a silica gel column. A volume of 100 ml of each fuel was processed. The final volume of each chloroform fraction was 50 ml, giving an effective two-fold enrichment of polar components in the fraction as compared to the original fuel. A volume of 5 ml of ethanol was required for the final rinse in order to remove any material which remained on the column after chloroform elution. Eight fractions were thus generated (4 chloroform, 4 ethanol) and provided by Monsanto Research Corp. Approximately 50 ml of 0321-Chloro was supplied; while, only about 7 mL of samples 005-Chloro, 0511-Chloro and 0986-Chloro were available to us. Ethanol fractions were supplied in 5 ml quantities. The sample vials were sealed using silicon rubber septa.

Total description of the four samples was

Vial Number	Comment
81-D-POSF-005	Shale JP-4
82-POSF-0511	Syncrude JP-4
83-POSF-0986	Undesignated
82-POSF-0321	Oxy light shale oil

84

The fractionated samples provided were further concentrated in our laboratory using dry nitrogen as follows:

Sample	Approximate Final Volume	Color
0321-Chloro	20 mL	Dark Black
005-Chloro	0.02 mL	Dark Brown
0986-Chloro	< 0.02 mL	Dark Brown
0511-Chloro	0.2 mL	Dark Brown
0321-Ethano	1.1 mL	Dark Brown
005-Eth	0.8 mL	Brown
0986-Eth*	0.05 mL	Yellow
0511-Eth*	0.12 mL	Brown

*Volume reduction resulted in precipitation of oily substance; final volume indicates added chloroform.

Secondary volume reductions were performed in tapered 2 mL vials.

2. Spectrometer

All GC/FTIR spectra were generated using a Nicolet 6000 FTIR. The IR beam from the 6000 was brought out to a Nicolet 7000 lightpipe/detector bench. The entire system was enclosed and purged with dry nitrogen gas. A liquid nitrogen cooled mercury-cadmium-telluride (MCT) detector with an infrared spectral window of 5000-710 cm^{-1} (narrow range) was employed. The lightpipe used in these experiments had a 1.5 mm i.d. x 40 cm gold coated bore with KBr windows at each end. The lightpipe temperature was 250°C; except for the examination of 005-Chloro and 0986-Chloro samples in which case 260°C was used. For samples run with FTIR detection, total make-up gas flow through the lightpipe was 8 mL/min via dry nitrogen gas.

Interferograms involving 2048 points were collected and coadded per data file. Infrared spectra of 8 cm^{-1} resolution resulted after Fourier transformation to the absorbance/frequency

85

domain. Fourteen interferometric data scans were coadded on-the-fly giving a data acquisition time frame of 1.27 sec/file. For sample fractions 0511-Eth and 0321-Eth, 16 data scans were collected and coadded on-the-fly to give a data acquisition rate of 1.44 sec/file. The Michelson interferometer mirror velocity was 2.22 cm/sec.

3. Gas Chromatographic Parameters

All fractions were separated on a 60 m x 0.33 mm i.d. DB-5 (equivalent to SE-54) fused silica column capable of 3010 plates per meter for C_{13} at k'=5.1 (helium flow rate ~2.5 mL/min or 33 cm/sec). The liquid phase film thickness was 1 micron. On-column injection was used exclusively for the fuel samples. A syringe with a 0.17 mm o.d. fused silica needle facilitated injection within the DB-5 column. The temperature program consisted of an initial temperature of 60°C for 5 minutes with heating rates of 3-5°C/min. The final temperature was 250°C except for 0321-Chloro which was 220°C.

A Varian 3700 GC was interfaced to the Nicolet 7000 lightpipe/ detector bench via ~1 mm i.d. stainless steel tubing. The DB-5 column was threaded through the transfer line up to the entrance of the infrared lightpipe. The transfer line temperature varied between 245 and 260°C (controlled by variac). A return transfer line to the GC from the lightpipe was introduced using 0.7 mm i.d. glass lined stainless steel tubing which was allowed to pass adjacent to the aforementioned heated line. The return line terminated at a catalytic flame ionization detector (Detector Engineering Technology, CA).

Preliminary FID traces of each fraction were generated before FTIR analysis by using the above temperature program and a make-up dry-nitrogen gas flow of 20 ml/min through the transfer line system. These FID traces were subsequently used to estimate needed FTIR sample loadings.

4. Data Collection and Search Routines

As mentioned earlier, the FTIR data storage needed for each separated fraction was generally greater than that available. The 10 megabyte hard disk cartridges used with the data system only contain 770 files at 8 cm^{-1} resolution. With the two data acquisition rates described previously, only 16.3 or 18.48 minutes worth of data can be generated while collecting continuously. The preliminary FID traces served a dual purpose. The traces provided information on the complexity and concentration dynamic range of the sample. In addition, the FID provided a sort of road map for the eventual FTIR data collection which was manipulated so that data was only saved when component peaks were present at the lightpipe as predicted by the FID trace. A maximum amount of FTIR information per sample was therefore generated in this way and no data space was wasted on "empty files" between eluting components.

Two spectral search methods were available for analysis of infrared data(17,21). One method identifies a component by selective infrared absorbance "peak" specification. It, however, does not appear to have significant advantages over the other method for low signal-to-noise spectra and it is more time intensive. The other method uses any one of four mathematical algorithms to match an unknown spectrum to a library spectrum. The search results consist of a listing of compounds with the most probable match first followed by a succession of less probable matches. A "perfect" match gives a value of zero. Typical match values range from 50 to 2000, depending on the signal-to-noise ratio. The library data base which consists of 3300 infrared spectra reduced to 16 cm^{-1} resolution was compiled by the Environmental Protection Agency. Several other model spectra were generated in-house and added to this library.

5. GC-FTIR Spectra of Jet Fuel Samples

As mentioned earlier, due to a somewhat limited amount of data space available, an on/off mode of data collection had to be

used for the fractionated samples. Again, for 14 FTIR scans coadded, only 16.3 minutes of data could be stored continuously and for 16 scans coadded only 18.48 minutes of data could be stored. An effort was made during the running of each sample to maximize the amount of information possible over one chromatographic run. Due to the "on/off" method of data collection, however, the usefulness of the frequency-specified reconstructed chromatograms was limited. Specifically, since the format of the reconstructed chromatogram has the x-axis in units of data files and since certain periods of the sample elution were not recorded, the reconstruction cannot be easily correlated with elution time. Their use was, therefore, primarily confined to component (file) location on the computer data disk. As an indication of the boiling range and complexity of each fraction, we have included a CFID trace (Figures 32-39). The 0986 sample appears quite simple. The low boiling 005 material concentrates in the ethanol fraction; whereas, the higher boiling but less abundant components occur in the chloroform fraction. The opposite situation seems to hold for sample 0321 (i.e. the chloroform fraction contains most of the sample). Both the chloroform and ethanol fractions of sample 0511 appear similar.

An interesting type of compound was found in the majority of the eight fractions supplied by Monsanto. This compound has infrared spectra very similar to octamethyl cyclotetrasiloxane and was found in highest abundance in the fractions that had been eluted with ethanol. Siloxane-type compounds were also found in three of the four chloroform fractions. Since no septa were used for the GC analysis (i.e. on-column injection was employed), the compounds may have originated during sample preparation at Monsanto. The whole samples were shipped in glass vials with silicone rubber septa and this may be the origin of such compounds. The chloroform and ethanol fractions were, however, packaged using different types of septa. The 0321-Chloro fraction for example was shipped using a black colored septum. Although the 2 ml tapered vials used for the final concentration under dry nitrogen used silicone rubber cap liners, contamination is unlikely from this source since the vials were

Figure 32.   CFID trace of 005-Chloro fraction

Figure 33.   CFID trace of 005-Eth fraction

90
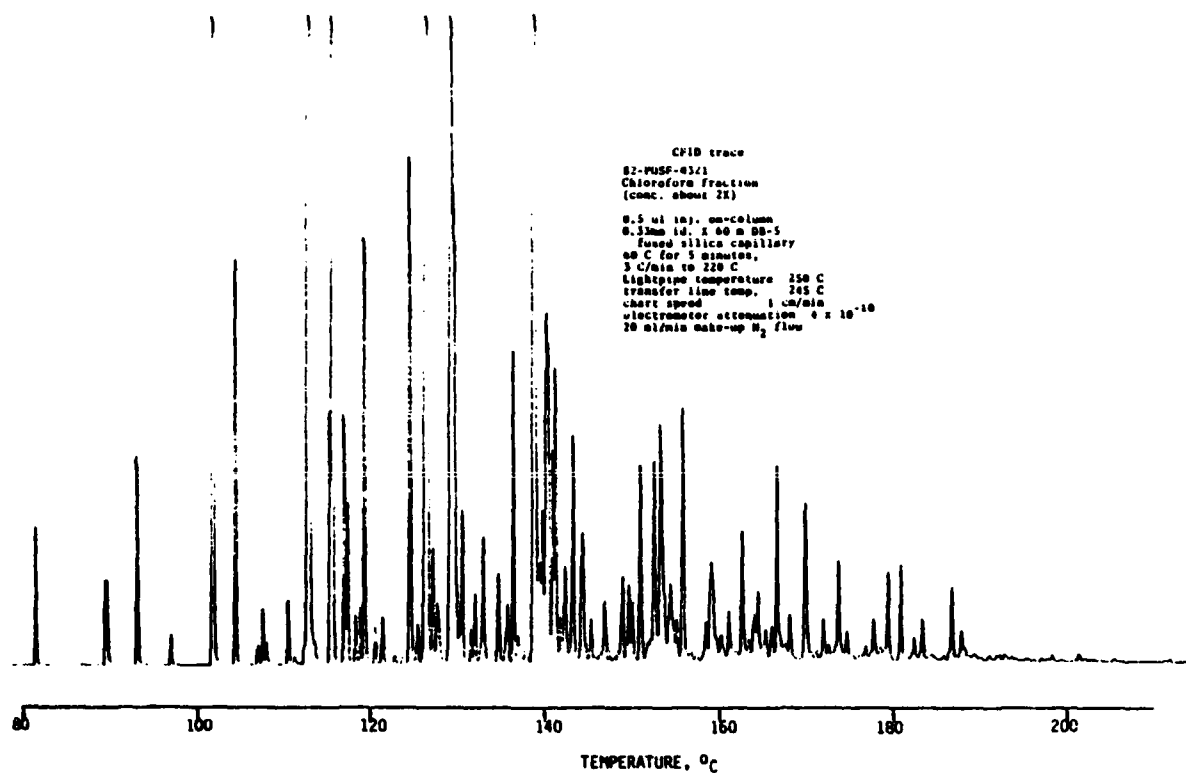
Figure 34.   CFID trace of 0321-Chloro fraction

CFID trace
82-POSF-0321
ethanol fraction
(conc. under nitrogen)

0.5 ul inj. on-column
0.33mm id. X 60 m DB-5
  fused silica capillary
60 C for 5 minutes,
5 C/min to 250 C
Lightpipe temperature 250 C
transfer line temp.   245 C
chart speed   1 cm/min
electrometer attenuation 4 x 10^{-10}
20 ml/min make-up N₂ flow

TEMPERATURE, °C

80   104   128   152   176   200   224   248

Figure 35.   CFID trace of 0321-Eth fraction

CFID trace

02-POSF-0511
Chloroform fraction
(conc. under nitrogen)

0.5 ul inj. on-column
0.25mm id. X 60 m DB-5
  fused silica capillary
60 C for 5 minutes,
4 C/min to 250 C
Lightpipe temperature 250 C
transfer line temp.   245 C
chart speed   1 cm/min
electrometer attenuation   4 x 10⁻¹⁰
20 ml/min make-up N₂ flow
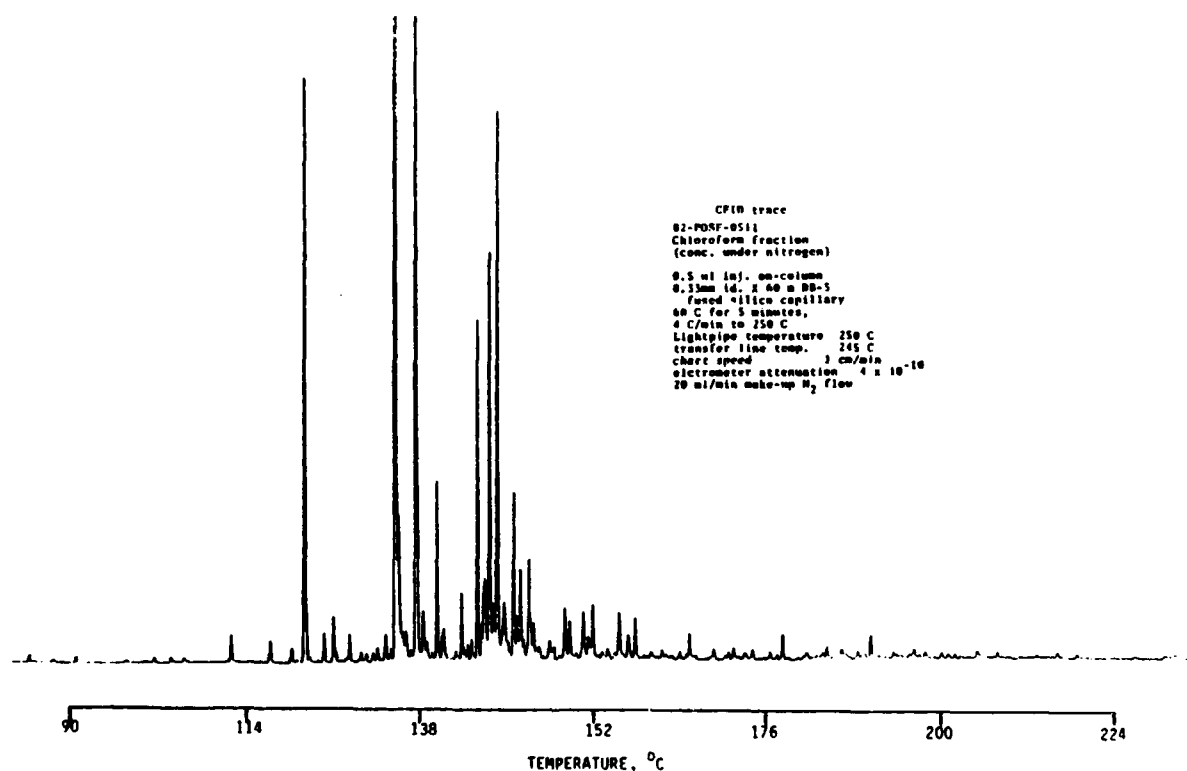
Figure 36.   CFID trace of 0511-Chloro fraction

CFID trace
82-POSF-0511
ethanol fraction
(conc. under nitrogen
diluted in CHCl₃)

60 C for 5 minutes.
4 C/min to 250 C
0.5 ul inj. on-column
0.33mm i.d. X 60 m DB-5
fused silica capillary
Lightpipe temperature   250 C
transfer line temp.   250 C
chart speed   1 cm/min
20 ml/min make-up N₂ flow

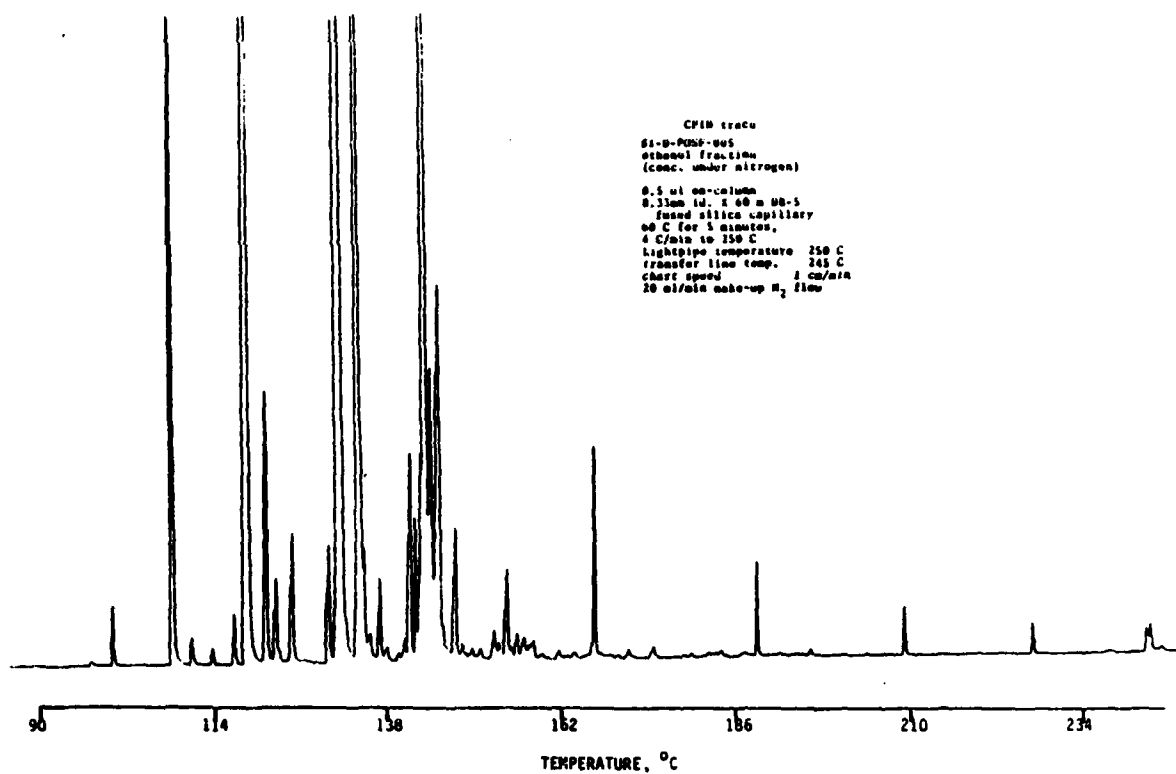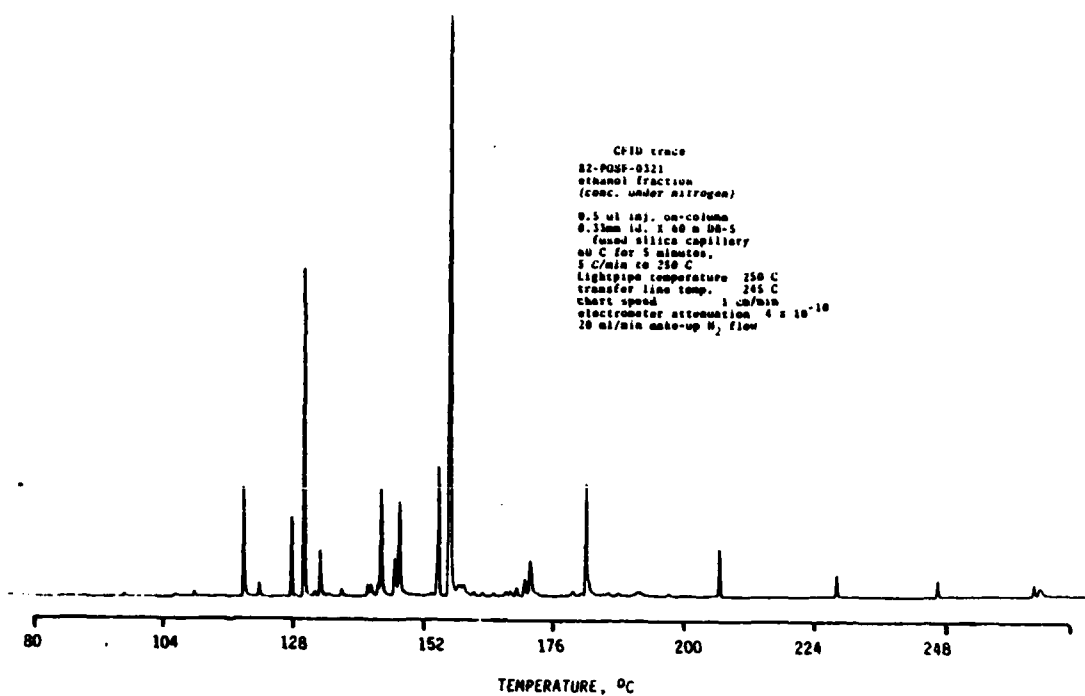| 90 | 108 | 136 | 164 | 192 | 220 | 248 |

TEMPERATURE, °C

Figure 37.   CFID trace of 0511-Eth fraction

94

Figure 38.   CFID trace of 0986-Chloro fraction

95

Figure 39.   CFID trace of 0986 Eth fraction
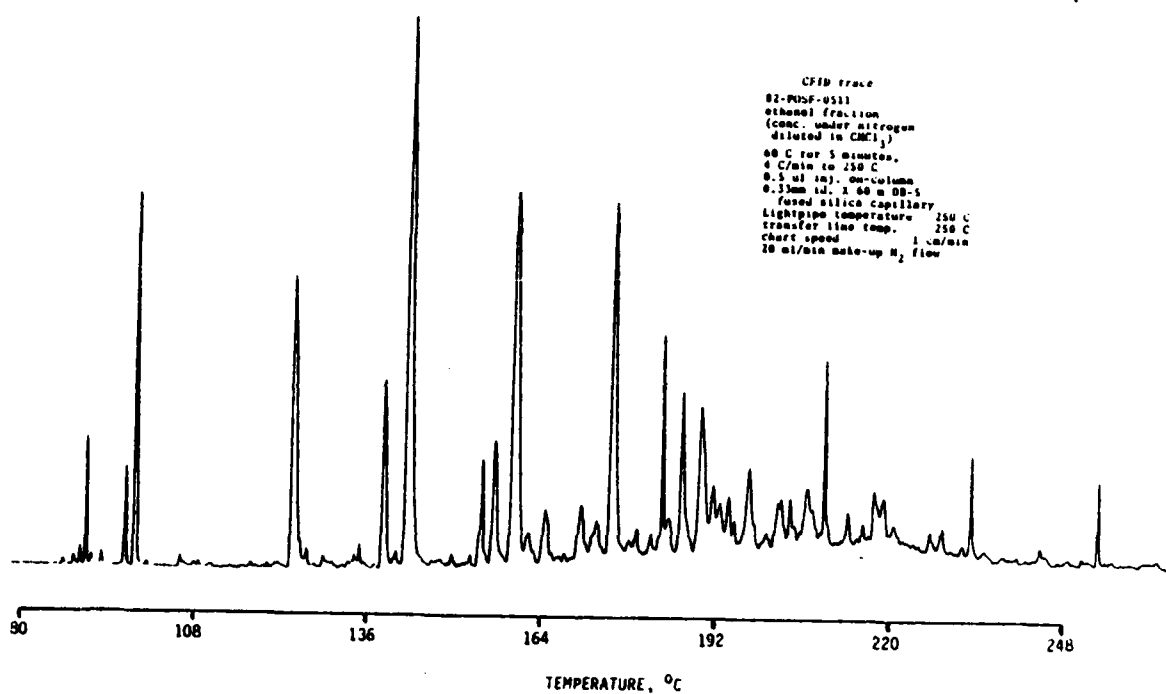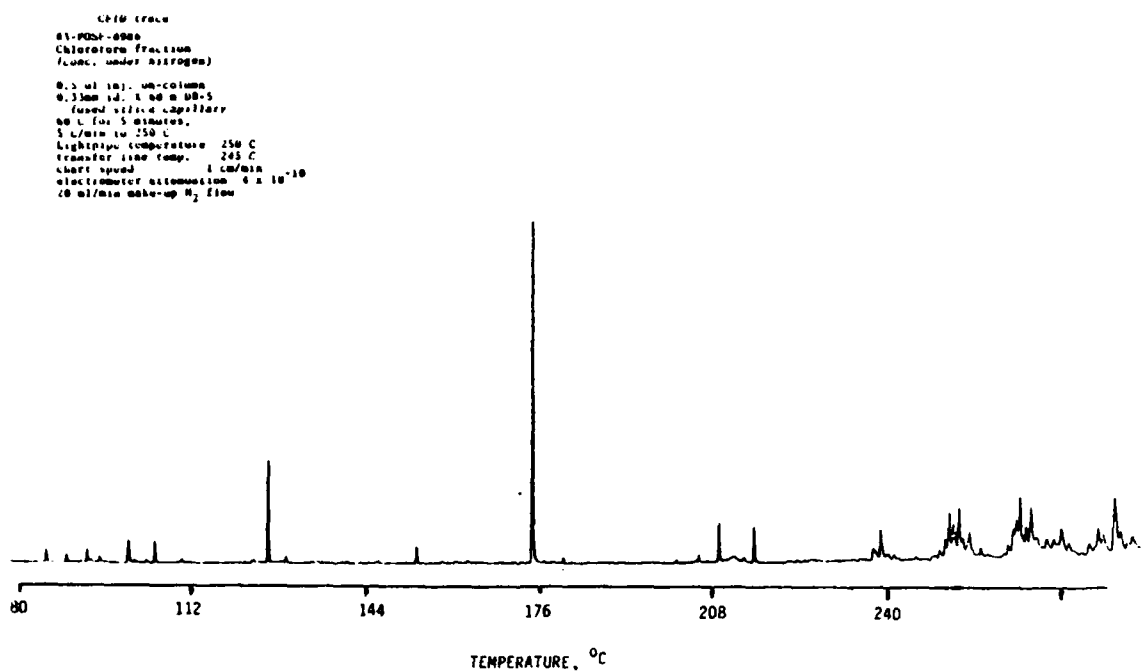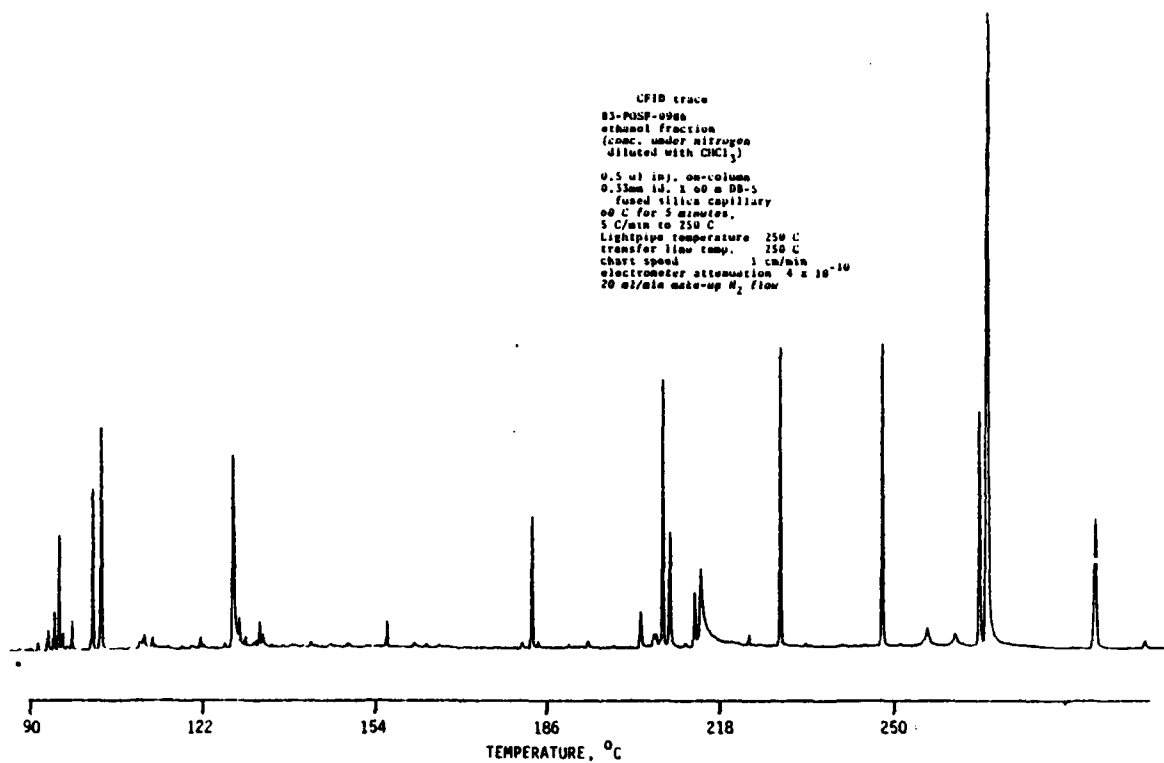
96

prevented from tipping over. Two other possible, yet unlikely, sources of contamination are the silicone rubber seals used within the lightpipe KBr windows and the vacuum grease present in the dry nitrogen manifold that was employed. The lightpipe source is unlikely since it is maintained at 250°C and the vacuum grease was never heated above room temperature.

The siloxane compounds found in fraction 005-Eth appear to have an elution scheme similar to a homologous series. The Chemigram for 005-Eth illustrates this elution order (note the absorbances in the 1250-1000 cm^{-1} and 880-730 cm^{-1} traces in Figure 40). Spectra from six files are shown in Figures 41 and 42. Although the absorbance patterns are very similar, the results from a computerized peak-picker routine indicate a trend toward lower wavenumbers as elution time increases (See Table 22).

Several components from the various fractions have been confidently identified by spectral search routines and have been confirmed by visual side-by-side comparisons. Components which have been identified include substituted phenols, substituted azaarenes, etc. The difficulty in positively identifying components which give rise to these spectra comes in large part because the reference infrared library which we have used contains only 3310 spectra. Other spectra have been added to the library via in-house standards in an effort to improve the possibility of identification. These materials have included mainly phenols, ketones and azaarenes. Several of the original EPA spectra were replaced with these spectra. Table 23 lists the components confidently identified among the 8 fractions.

Although a positive identification could not be made on the majority of components within these fractions, a good indication as to the functionality present for several components has been made. Depending on the goal of the work (i.e. actual identity, chemical group determination, etc.) 100% identification may not be necessary. While isomer differentiation can be successfully accomplished using FTIR data, an insufficient reference library may hinder this endeavor. Table 24 provides a list of the components partially or

97
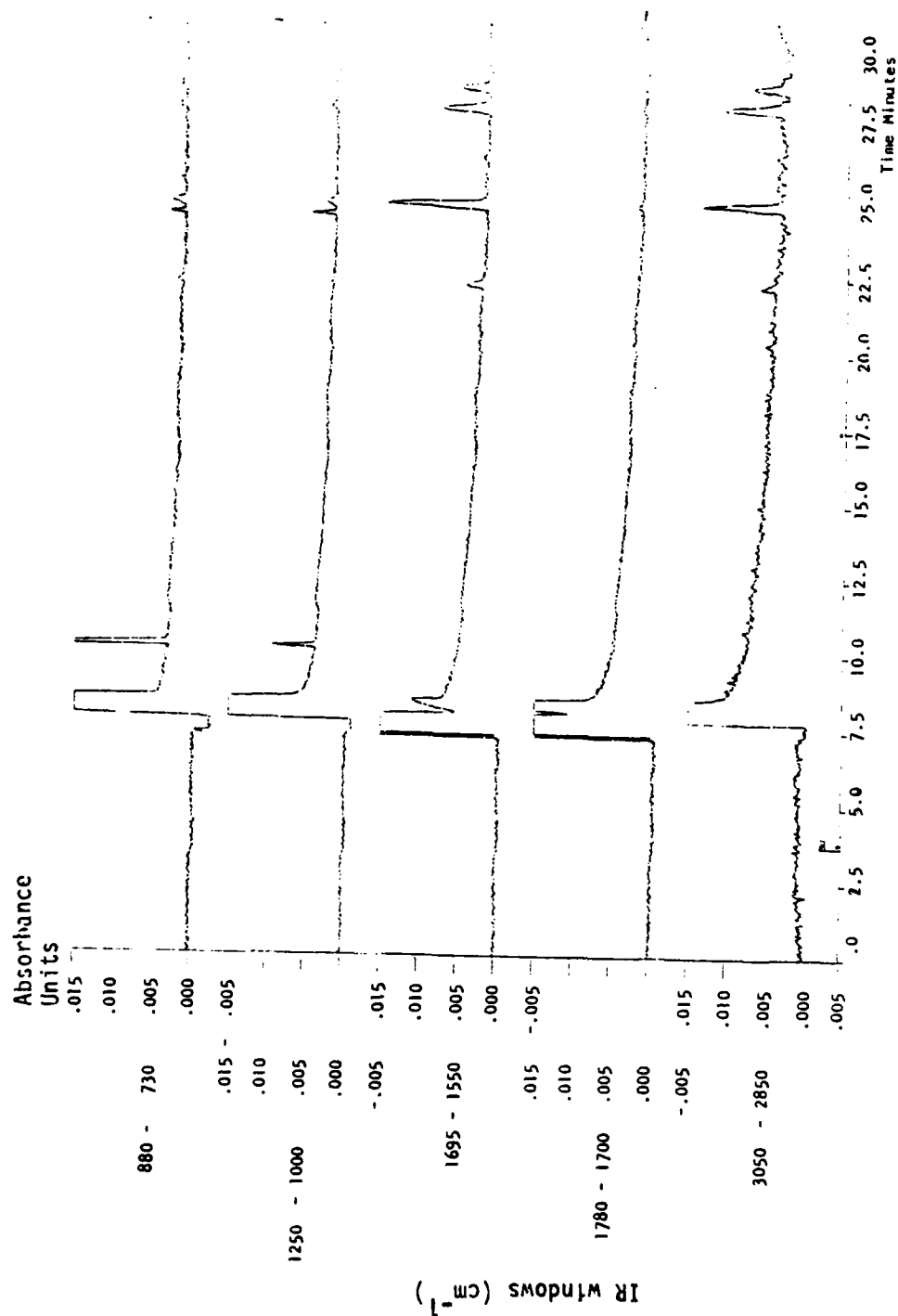
Figure 40. FTIR Chemigram plots for GC separation of 005-Eth. Lightpipe = 250°C, Transfer Line = 250°C, 0.5μL injected, 60°C for 5 minutes followed by 4°C/min up to 250°C.

98

Time(minutes)
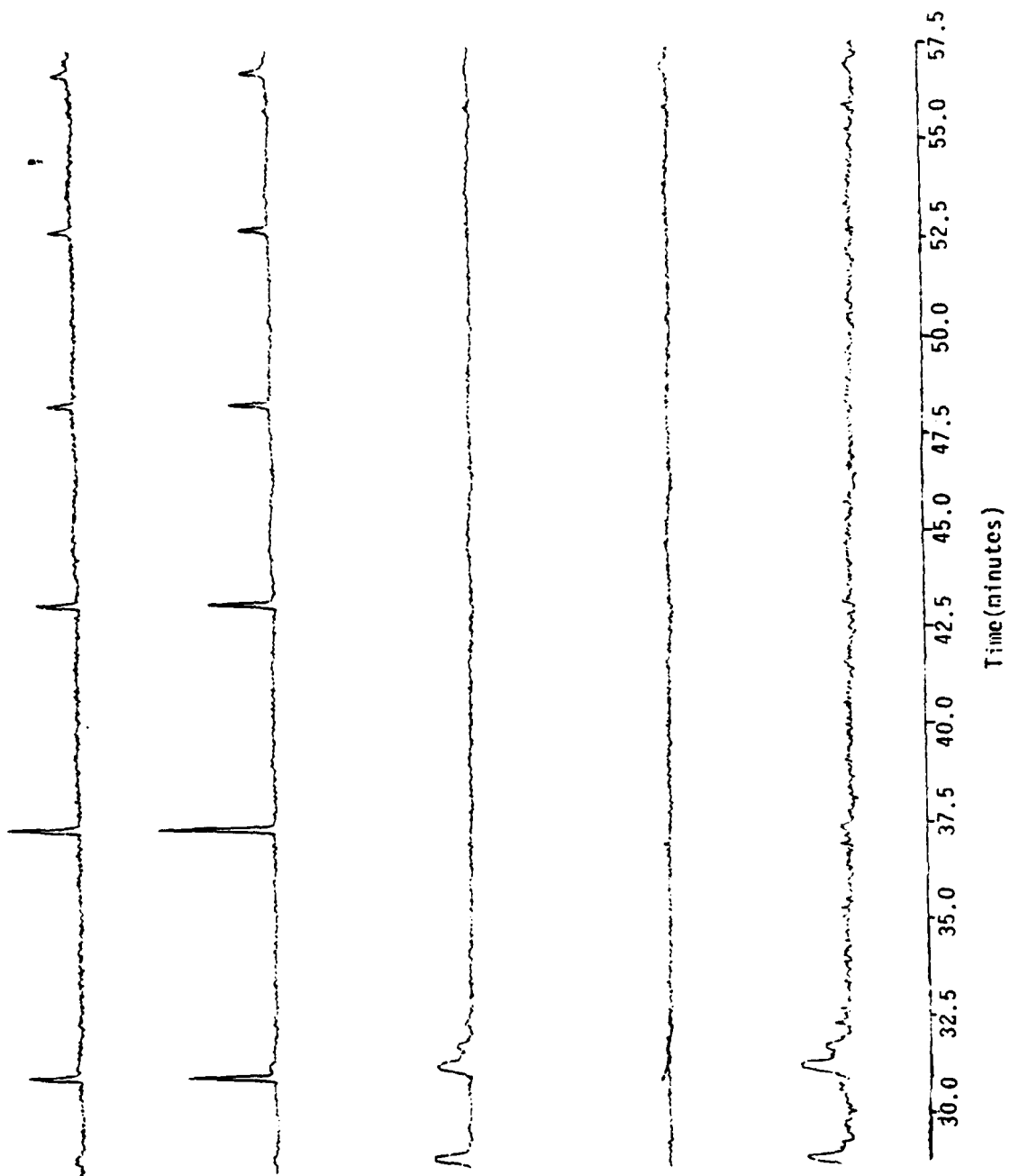
Figure 40. Continued

99
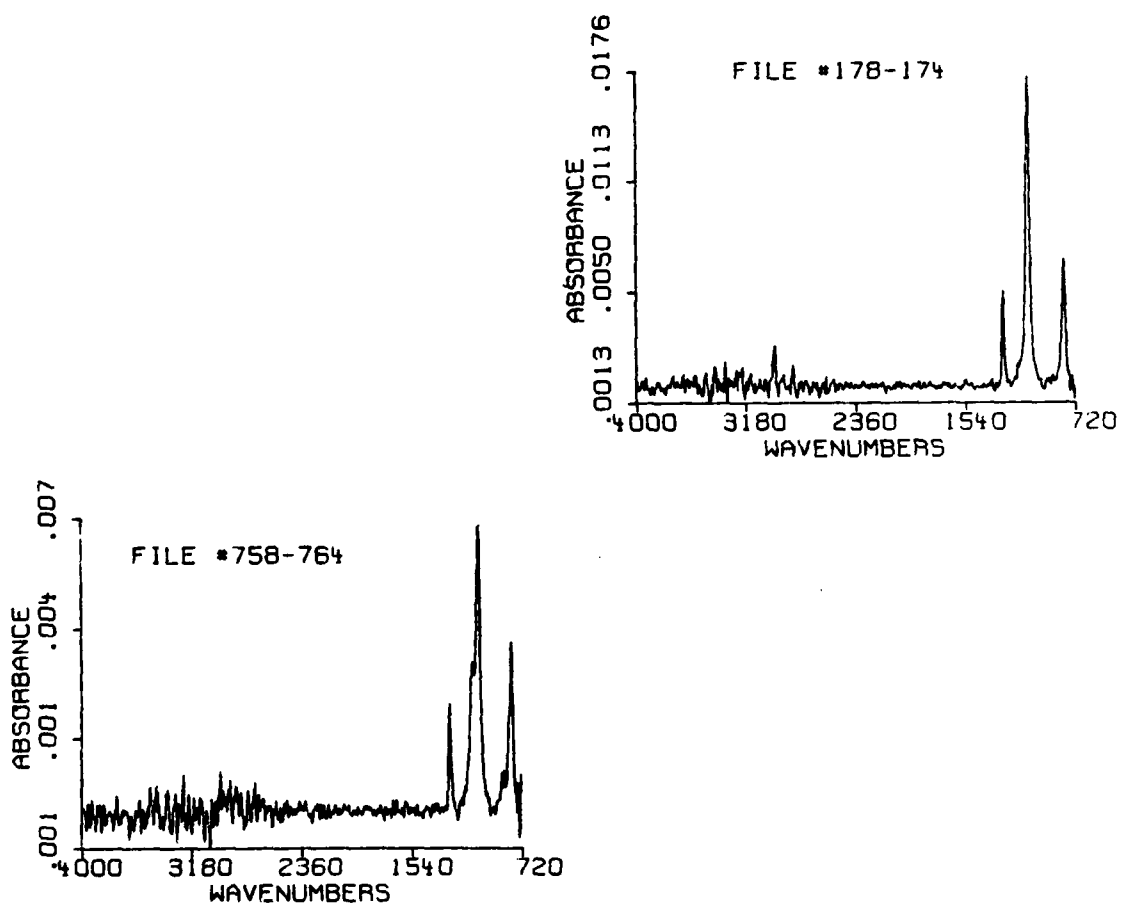
Figure 41.   FTIR file spectra from GC separation of 005-Eth.
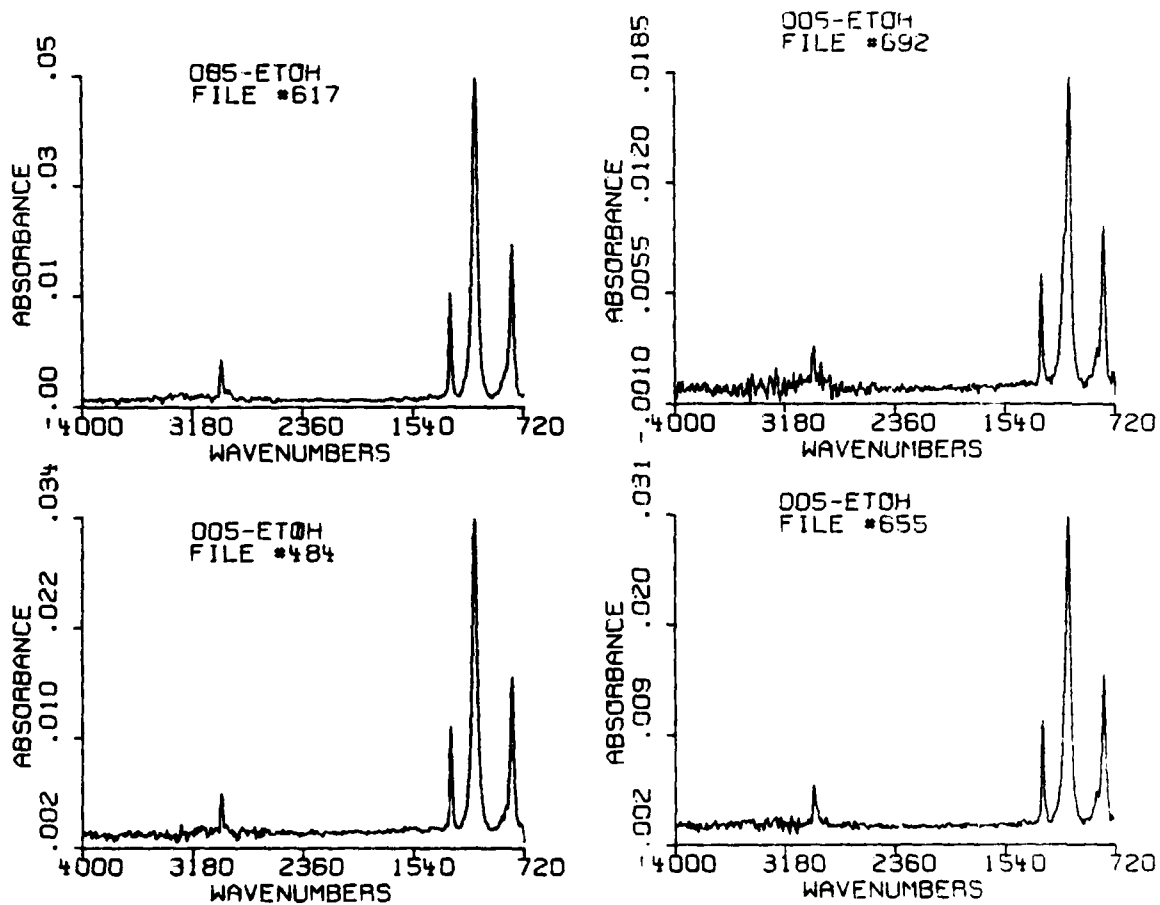
Figure 42.   FTIR file spectra from GC separartion of 005-Eth.

Table 22

Peak-Picker Results for Siloxane Components in 005-Eth

DFN = 178	DFN = 484	DFN = 617
X = 778.262	X = 810.379	X = 808.606
X = 812.894	X = 1087.752	X = 1080.243
X = 1082.829	X = 1265.312	X = 1265.469
X = 1137.543	X = 2969.230	X = 2967.529
X = 1154.644		
X = 1265.884		
X = 2987.149		
24.52 minutes into run	30.91 minutes into run	37.31 minutes into run

DPN = 655	DPN = 692	DFN = 758
X = 806.866	X = 805.803	X = 803.912
X = 860.207	X = 857.201	X = 859.862
X = 1071.062	X = 1063.035	X = 876.108
X = 1265.375	X = 1265.430	X = 1050.438
X = 2966.684	X = 2963.317	X = 1092.871
43.11 minutes into run	48.28 minutes into run	56.79 minutes into run

TABLE 23

Confidently Identified Components in Fuel Fractions Via GC-FTIR

005-Chloro	Retention Time Minutes	EPA Vapor Phase Reference Spectrum No.	Data File
phenanthrene	47.07	1101	763
phenyl ether	37.06	946	304
o-tert-butyl phenol	32.84	232	214
0986-Chloro			
o-tert-butyl phenol	33.30	232	257
phthalic acid, dibutylester	50.60	964	548
2,4-di-tert-butyl-phenol	39.90	294	294
0321-Chloro			
2,6-Lutidine	20.52	783	46
2,4-Lutidine	23.16	56	56
2,4,6-trimethyl pyridine	26.58	218	123
0511-Chloro			
2-nonanone	33.66	556	517
0511-Eth			
2-pentanol	12.99	389	69
2-methoxy ethanol		543	24
0986-Eth			
phthalic acid, dibutylester	48.76	964	659
2,4-dichlorobenzoic acid	38.72		448
2-methoxy ethanol	10.38	543	33

103

TABLE 24

Partially Identified Components in Fractions Via GC-FTIR

005-Chloro	Retention Time Minutes	Data File #
phenol-type	41.85	532
substituted naphthalene	37.36	318
siloxane-type	23.45	158
siloxane-type	33.87	235
0986-Chloro		
aliphatic ketone	18.99	125
siloxane-type	29.14	237
siloxane-type	23.91	215
siloxane-type	39.01	275
0511-Chloro		
substituted phenol	32.96	484
multi-substituted pyridine	28.99	298
multi-substituted pyridine	25.70	144
aliphatic ketone	29.71	332> coelution
multi-substituted pyridine	29.71	332
multi-substituted pyridine	32.55	465
siloxane-type	25.23	122
0321-Chloro		
thiazolo/5,4,3-IJ/Quinolin-2-one		231
substituted pyridine	28.52	204
pyridine-type		31
aromatic	27.40	157
aromatic	30.16	272

TABLE 24 cont'd.

Partially Identified Components in Fractions Via GC/FTIR

0986-Eth	Retention Time Minutes	Data File #
aromatic	27.30	153
aromatic	34.70	461
multi-substituted pyridine	30.71	295
substituted pyridine	31.67	335
tetrahydro quinoline-type	33.93	429
0321-Eth		
multi-substituted pyridine	21.99	151
siloxane-type	36.74	666
substituted pyridine	19.83	61
aromatic	27.16	366
siloxane-type	32.06	570
005-Eth		
multisubstituted pyridine	24.90	196
aromatic	31.15	495
multisubstituted pyridine	28.83	384
multisubstituted pyridine	28.14	351
multisubstituted pyridine	22.21	68
multisubstituted pyridine	31.67	520
siloxane-type	30.90	484
siloxane-type	37.31	617
siloxane-type	43.11	655
siloxane-type	48.28	692
siloxane-type	24.52	178
siloxane-type	56.79	758

TABLE 24 cont'd.

Partially Identified Components in Fractions Via GC/FTIR

0511-Ethanol	Retention Time Minutes	Data File #
substituted phenol	27.97	208
substituted phenol	32.54	331
substituted phenol	36.01	459
substituted phenol	24.73	154
alcohol; aliphatic	12.61	53
substituted phenol	28.78	242
aliphatic ketone	19.15	125

106

nearly identified in the eight fractions.

The computerized spectral subtraction routine has been very useful for interpretation purposes in this work. In many cases the routine was used to smooth-out a baseline or subtract-out background water or carbon dioxide absorbances. Water and CO_2 levels continually change over the course of a long GC/FTIR run even though the spectrometer and lightpipe/detector bench are continually purged with dry nitrogen gas. "Straightening" out of the infrared spectral baseline can greatly improve the results of the library search routines in most cases. The "straightening" (or levelling) is easily done by subtracting a data file in which only background infrared noise exists from the sample spectrum.

Quite often the subtraction technique can be useful in determining whether one chromatographic peak is actually the product of two (or more) coeluting components. A stack plot of one such coelution is presented in Figure 43 which comes from the infrared data obtained on fraction 0511-Chloro. The numbers to the left of each trace are the data file locations. Spectrum file # 332 represents the peak maximum. One will note the appearance of an infrared band at about 1730 cm^{-1} beginning in spectrum file #329 that is not present in file #328. Other minor differences in relative peak heights can be noted throughout the elution scheme, for example, the 3000-2900 cm^{-1} region. The question of whether the spectrum at file #332 is a pure component or not has been answered by doing a series of subtractions to isolate the "second" component. Figure 44 shows the resulting spectrum after multiple subtractions were performed. Note that the left spectrum appears identical to file 328 (as hoped for) but the left spectrum has twice the absorbance intensity. First, file #328 (assumed to be 1 component) was subtracted from the file of interest #332. The amount of #328 subtracted was established by noting when negative absorbance peaks resulted. Figure 45 shows the result of #332 minus #328. The resulting spectrum, corresponding to the coeluting component, has been found to be very similar to an aliphatic straight chain ketone (see Table 25). Again, when the result of #332-#328 was subtracted
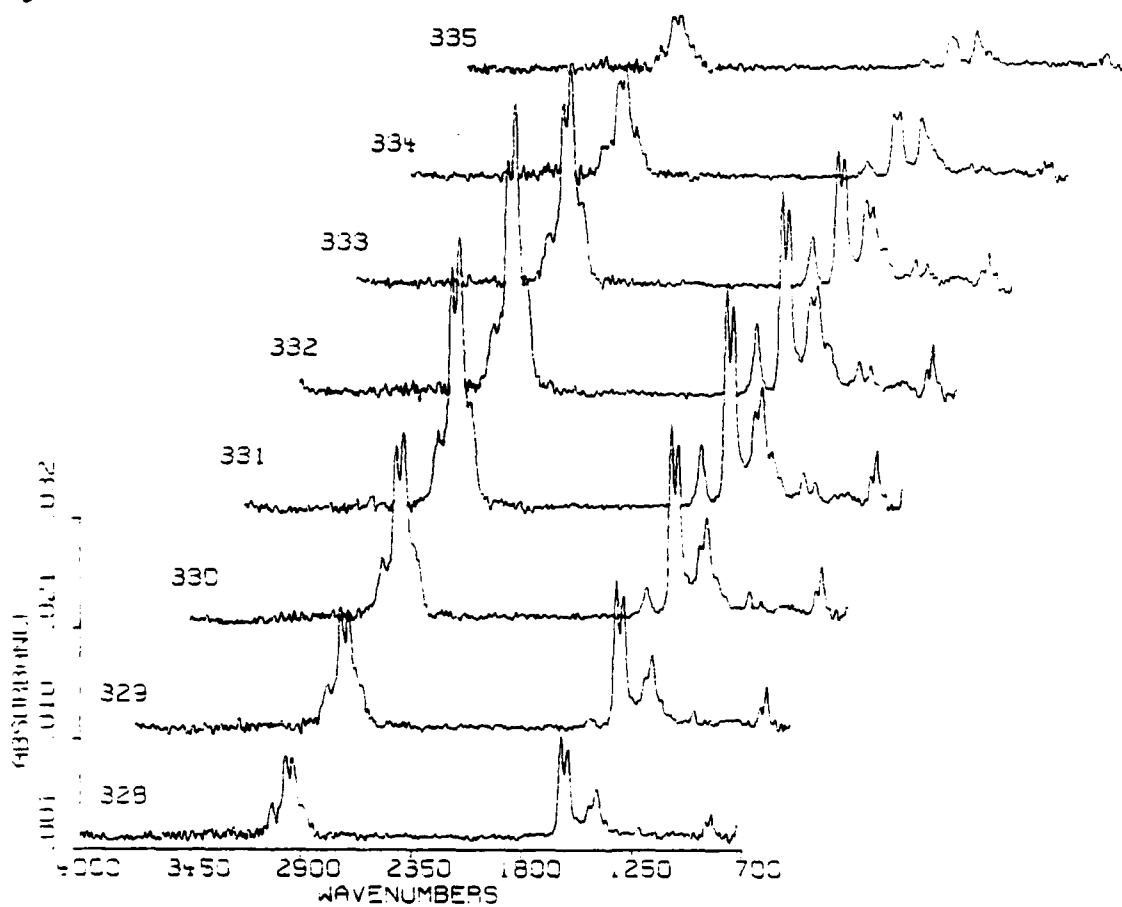
Figure 43.   Stack plot of selected infrared file spectra obtained
during the separation of 0511-Chloro fraction.

108

0511-CHCL3

FILE #332-(332-328)

FILE #328

Figure 44. Difference infrared spectrum (file #322-(#322-#328) and file spectrum #328 obtained during GC-FTIR of 0511-Chloro fraction.

109

0511-CHCL3

FILE #332-328

Figure 45.   Difference infrared spectrum (file #322-#328) obtained
during GC-FTIR of 0511-Chloro fraction.

110

Table 25

Computer Search Routine Results for FTIR File Peak Spectrum in Separation of 0511-Chloro[a]

EPA Vapor Phase Library Number	Possible Hits	Compound[b,c]
3119	455	3-tetradecanone
801	464	2-hendecanone
2174	464	3-hexadecanone
3117	478	3-octadecanone
3295	497	2-nonadecanone
790	534	3-dodecanone
3118	536	10-nonadecanone
2178	547	8-pentadecanone
3152	603	11-hydroxy-10-eicosanone
482	688	2-cyclohexylcyclohexanone

[a]See Figure 45

[b]Squared algorithm used

[c]4000-3700 cm^{-1} and 725-400 cm^{-1} regions skipped

from the original file #332, a spectrum virtually identical to file #328 is produced. Figure 46 illustrates the infrared peak-picker routine for the result of these multiple subtractions. The library search results suggest a substituted pyridine as the most likely match. See compounds listed in Table 26.

6. Capillary Column Efficiency

It would be of interest to know the efficiency of the GC capillary column being used in this study in order to assess whether the chromatography is acting as a limiting factor for analysis of these complex samples. Three flow rates of helium were used at a 140°C oven temperature. Linear gas flow velocities were 25.3, 33.0 and 41.7 cm/sec. o-xylene was used as the solvent in order to minimize solvent flash evaporation since on-column injection was used. Three hydrocarbons (C_{12}-C_{14}) were diluted in o-xylene and injected, although only C_{13} and C_{14} materials were used for calculation purposes. The flame ionization detector traces for these three runs appeared normal and showed base-line separation of dodecane, tridecane and tetradecane. Table 27 lists the data obtained from these chromatographic runs. At a linear velocity of 33.0 cm/sec, almost 169,000 plates can be generated for the 0.33 mm i.d. x 57.6 m DB-5 column. (Note: the outlet of the column was directed straight into the FID flame tip area.) A Van-Deemter plot (Figure 47) indicates that at 33.0 cm/sec the HETP=0.33 mm. As a compromise to both efficiency and reasonable chromatographic retention times, a linear helium velocity of 33.0 cm/sec was chosen for the separation of these jet fuel fractions.

7. Summary

The data presented on these jet fuel product fractions represent a sampling of the type of data and information which can be generated by the capillary GC/FTIR method. Certainly, some of the parameters of the chromatography and/or the IR spectrometry could
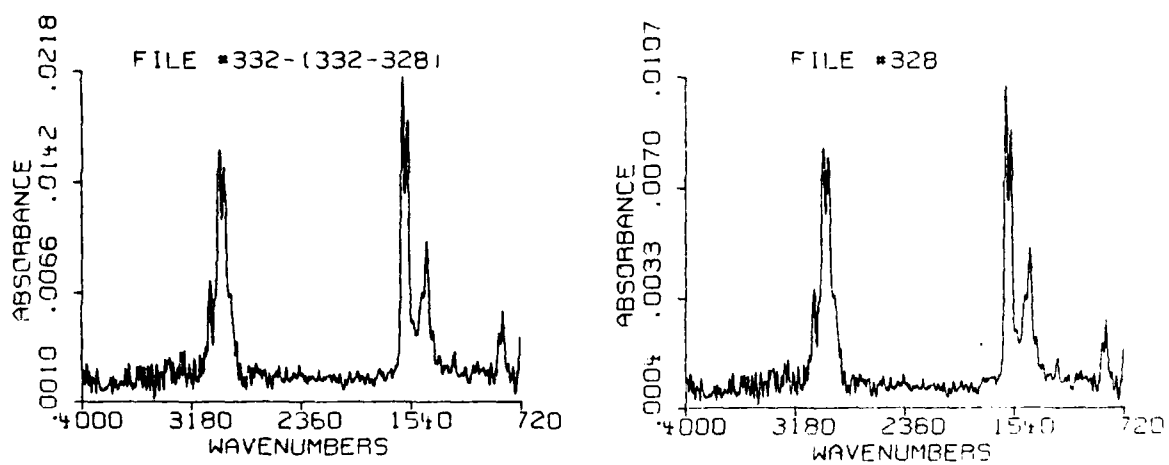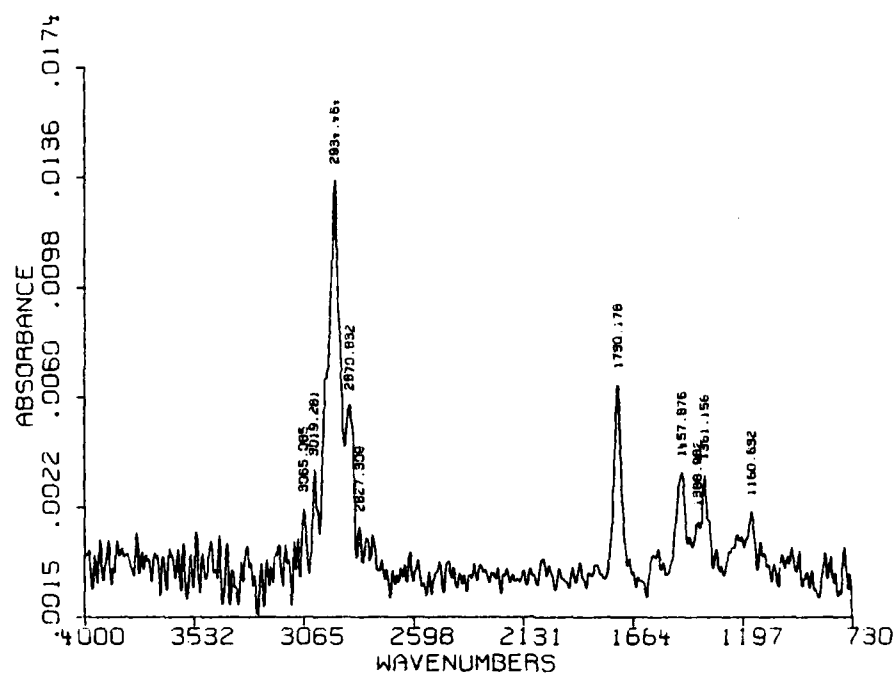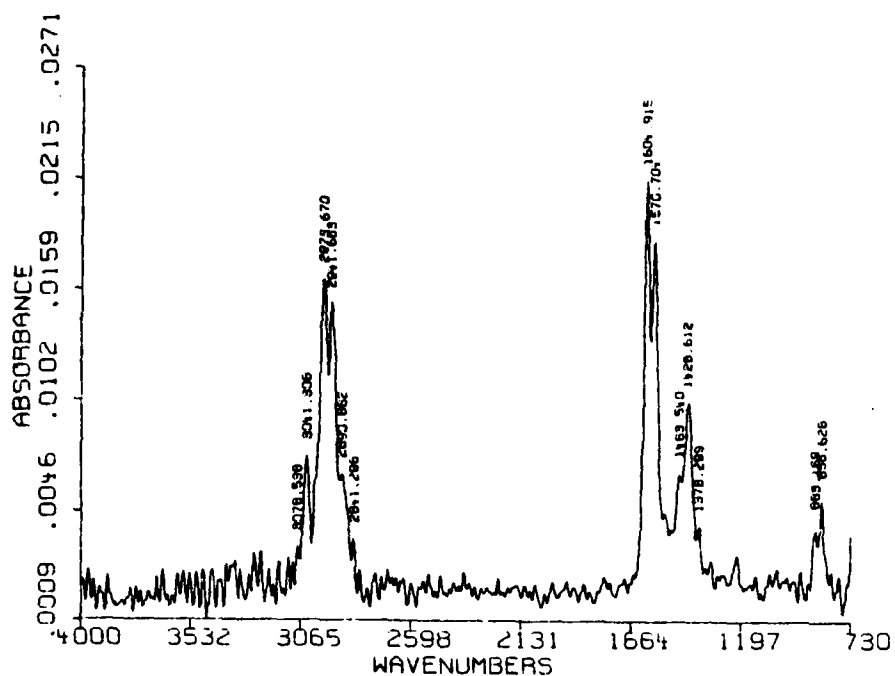
Figure 46. Difference infrared spectrum (file #322-(#322-#328) obtained during GC-FTIR of 0511-Chloro fraction.

113

Table 26

Computer Search Routine Results for FTIR File
Peak Spectrum in Separation of 0511-Chloro[a]

EPA Vapor Phase Library Number	Match Values	Compound[b,c]
567	1461	4-isopropylpyridine
1655	1531	4-t-butylpyridine
2442	1610	di-3,5-xylylamine
77	1693	2,4-lutidine
312	1711	3-t-butyl-5-ethyltoluene
604	1738	5-t-butylbenzene
2418	1774	3,5-di-t-butylphenol
1600	1811	3,5-dimethylcumene
1028	1812	3,5-diisopropyltoluene
2616	1813	2,6-di-t-butylpyridine

[a]See Figure 46

[b]Absolute difference algorithm used

[c]4000-3700 cm^{-1} and 725-400 cm^{-1} regions skipped

114

Table 27

Column Efficiency Calculations[a]

	linear velocity	plates	plates/meter	HETP	$W_{1/2}$	K	K'	t°
C_{13}	25.3 cm/sec	190,729	3311	0.302 mm	0.128 cm	6.25	5.25	3.8 min
C_{14}	25.3 cm/sec	189,607	3292	0.304 mm	0.20 cm	9.74	8.74	3.8 min
C_{13}	33 cm/sec	173,563	3013	0.332 mm	0.10 cm	6.1	5.1	2.9 min
C_{14}	33 cm/sec	168,738	2929	0.341 mm	0.157 cm	9.45	8.45	2.9 min
C_{13}	41.7 cm/sec	117,283	2036	0.491 mm	0.10 cm	6.33	5.33	2.3 min
C_{14}	41.7 cm/sec	138,987	2413	0.414 mm	0.143 cm	9.85	8.85	2.3 min

[a]100 µg of C_{13} and C_{14} injected
o-xylene solvent
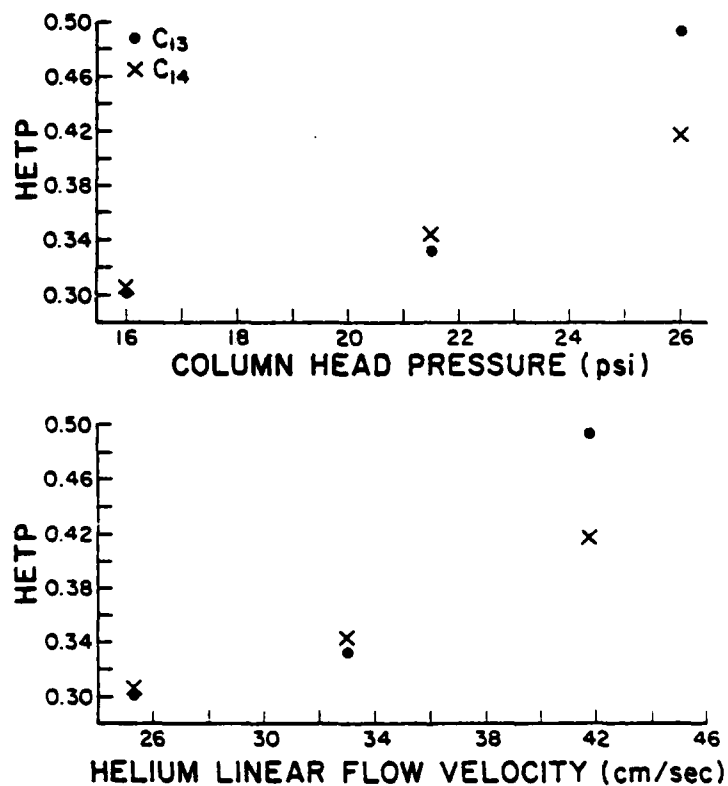140°C oven temperature

115

Figure 47.   Plot of column efficiency versus column head pressure
             and He linear flow velocity.

have been changed to give more information concerning each sample. An increased amount of sample injected combined with a slower temperature program rate may have increased the detection possibilities and better resolved closely eluting components. Also, a more rapid data acquisition rate (i.e. seconds/file) may have aided in resolving some chromatographically coeluting peaks. Given enough experimental time, the optimum parameters for each sample could be generated. Those fractions which have been provided represent a good chromatographic distribution of components. The wide boiling ranges of each fraction have shown that relatively high lightpipe temperatures can be employed successfully in GC/FTIR. Also, the many functional group characteristics found within each sample have given some insight as to problems faced when analyzing real world samples. Those problems include tailing components (obviously polar) and analysis of components with varying degrees of infrared vibrational activity. Such samples are definitely a step-up from simple hydrocarbons or standard compounds which are highly IR active.

REFERENCES

1. B. Katlafsky, M.W. Dietrich, Appl. Spectros. $\underline{29}$, 24 (1975).

2. D.F. Gurka, P.R. Laska, R. Titus, J. Chromatogr. Sci. $\underline{20}$, 145 (1982).

3. K.H. Shafer, S.V. Lucas, R.J. Jakobsen, J. Chromatogr. Sci. $\underline{17}$, 464 (1979).

4. R.W. Crawford, T. Hirschfeld, R.H. Sanborn, C. M. Wong, Anal. Chem. $\underline{54}$, 817 (1982).

5. D. Kuehl, G.J. Lemeny, P.R. Griffiths, Appl Spectros. $\underline{34}$, 222 (1980).

6. L.V. Azarraga, C.A. Potter, J. High Resol. Chromatogr. and Chromatogr. Comm. $\underline{4}$, 60 (1981).

7. C.L. Wilkins, G.N. Giss, R.L. White, G.M. Brissey, E.C. Onyiriuka, Anal. Chem. $\underline{54}$, 2260 (1982).

8. Azarraga, L.V. "Improved Sensitivity of on-the-fly-GCIR Sensitivity: Paper No. 334,"1976 Pittsburgh Conference.

9. K.H. Shafer, A.J. Bjorseth, J. High Resol. Chromatogr. and Chromatogr. Comm. $\underline{3}$, 87 (1980).

10. K.H. Shafer, M. Cooke, R. DeRoos, R.J. Jakobsen, O. Rosario, J.D. Mulik, Appl. Spectros. $\underline{35}$, 469 (1981).

11. K. Krishnan, R.H. Brown, S.L. Hill, S.C. Simonoff, M.L. Olson, D. Kuehl, Amer. Lab. $\underline{13}$(3), 122 (1981).

12. R.D. Dandeneau, E.H. Zerenner, J. High Resol. Chromatogr. and Chromatogr. Comm. $\underline{2}$, 351 (1979).

13. J & W Scientific, Inc., Rancho Cordora, CA, Private Communication.

14. P.R. Griffiths, "The Present State-of-the-Art of GC/FTIR and HPLC/FTIR," Presented at 1982 Pittsburgh Conference, No. 204, Atlantic City, NJ, March 8-13, 1982.

15. K.H. Shafer, R.J. Jakobsen, "Applications of GC/FTIR to Environmental Pollution Sample Analysis," Presented at 1982 Pittsburgh Conference No. 029, Atlantic City, NJ, March 8-13, 1982.

16. S.L. Smith, S.E. Garlock, G.E. Adams, Appl. Spectros. $\underline{37}$, 192 (1983).

17. S.R. Lowry, D.A. Huppler, Anal. Chem. $\underline{53}$, 889 (1981).

18. K. Grob, K. Grob, Jr., J. Chromatography $\underline{151}$, 311 (1978).

19. V. Rossiter, "Capillary GC/FTIR", Amer. Lab. $\underline{14}$, (June 1982), pp. 71-79.

20. S.E. Garlock, G.E. Adams, S.L. Smith, Amer. Lab. $\underline{14}$ (Dec. 1982), pp.48-55.

21. S.R. Lowry, D.A. Huppler, Anal. Chem. $\underline{55}$, 1288 (1983).

APPENDIX A

SPECTRAL COMPARISONS BETWEEN PEAK FILE AND
EPA VAPOR PHASE LIBRARY FOR
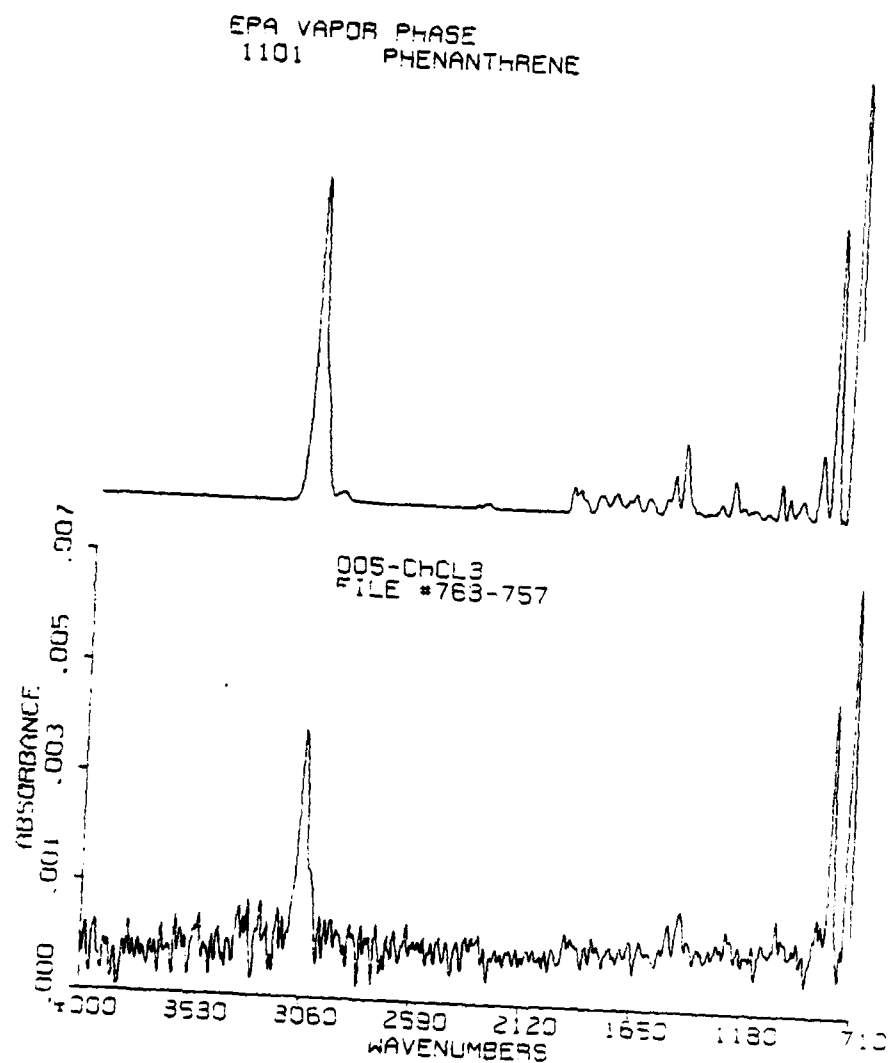CONFIDENT MATCHES IN JET FUEL SEPARATIONS

119

Figure A-1. FTIR peak file spectrum less background compared with
EPA vapor phase spectrum of phenanthrene. See Table
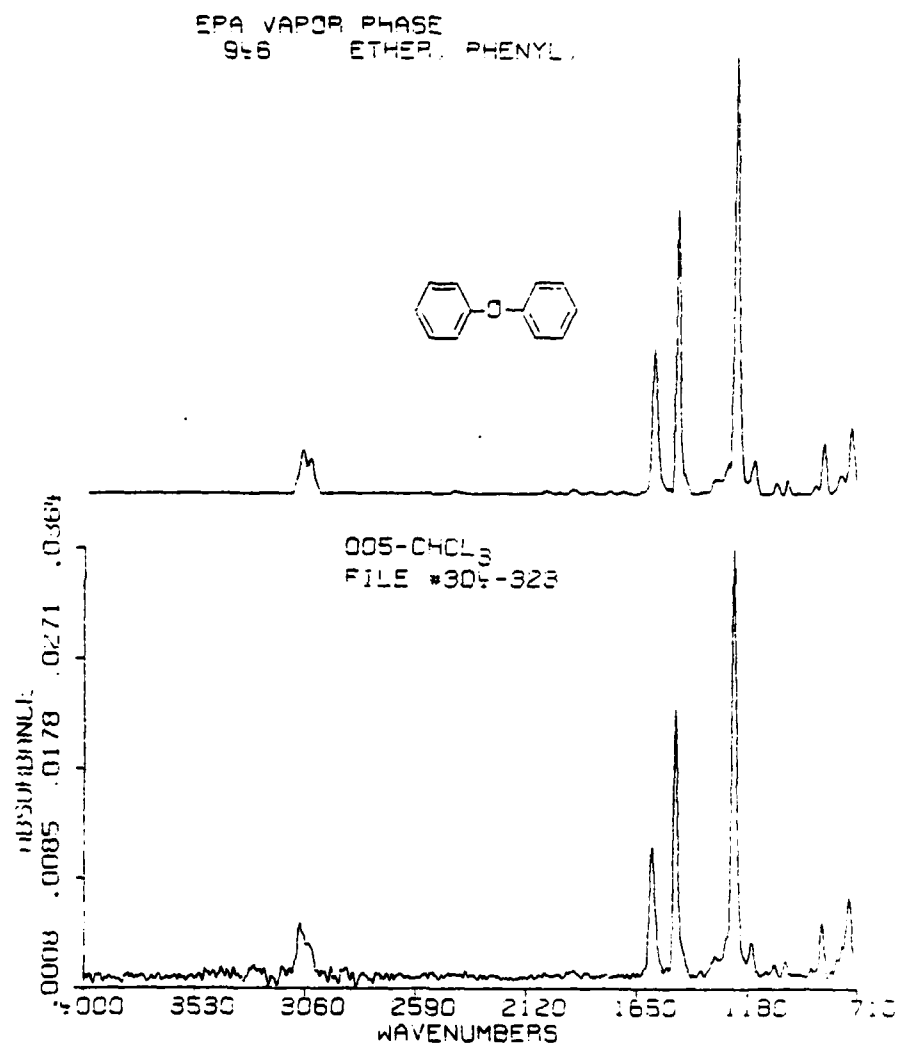B-1 for match values.

120

Figure A-2. FTIR peak file spectrum less background compared with EPA vapor phase spectrum of phenyl ether. See Table B-2 for match values.
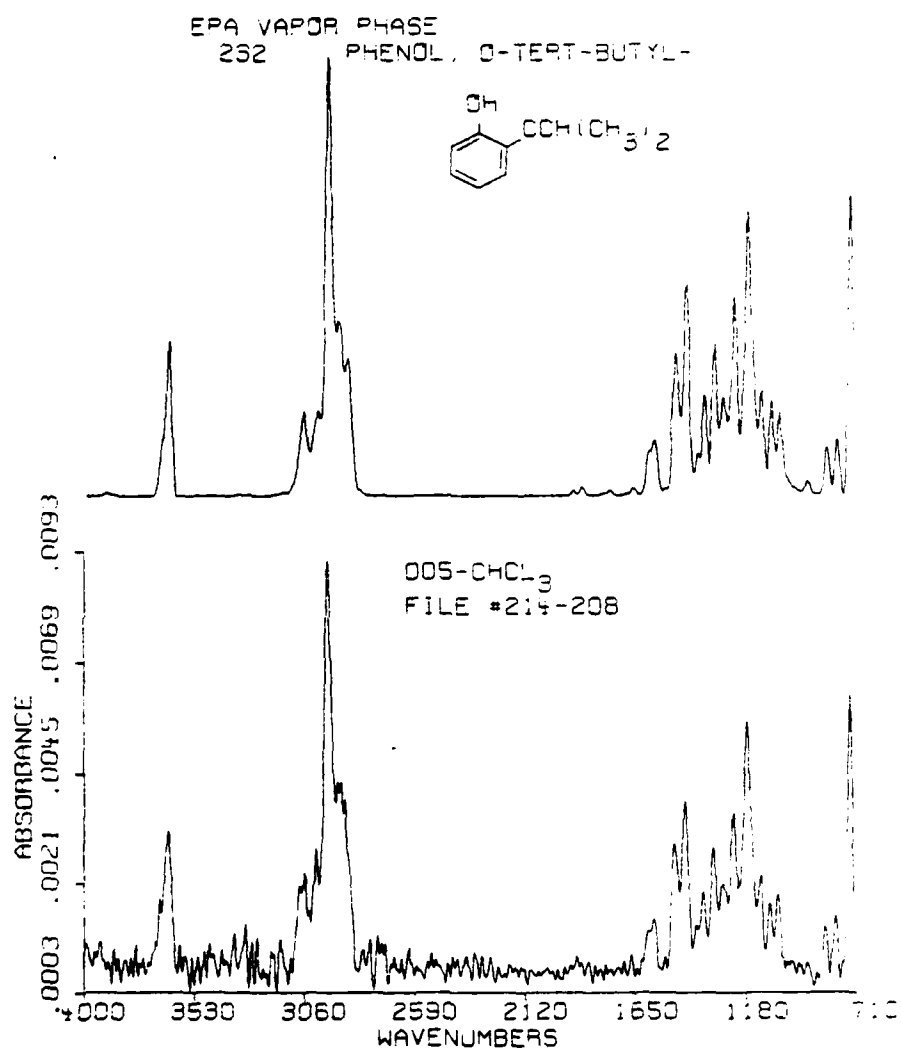
121

Figure A-3. FTIR peak file spectrum less background compared with EPA vapor phase spectrum of o-tert-butyl phenol. See Table B-3 for match values.
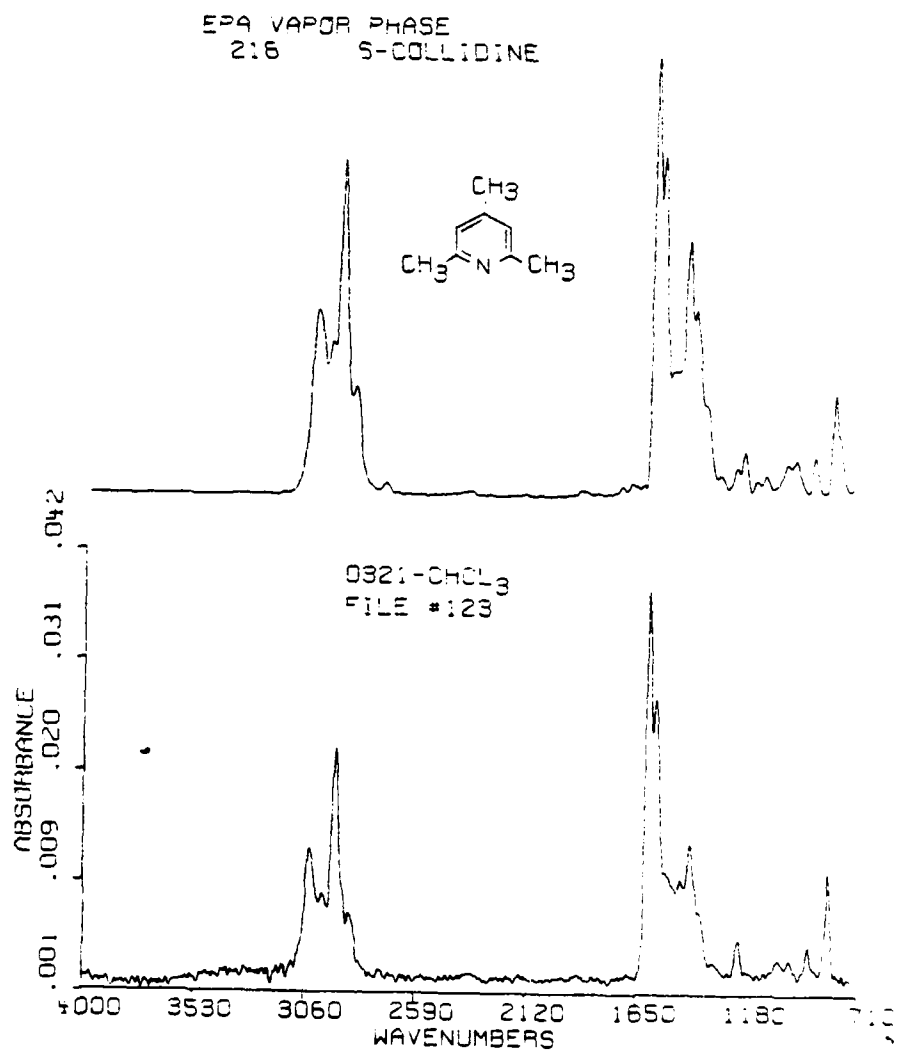
122

Figure A-4. FTIR peak file spectrum less background compared with
EPA vapor phase spectrum of s-collidine. See Table
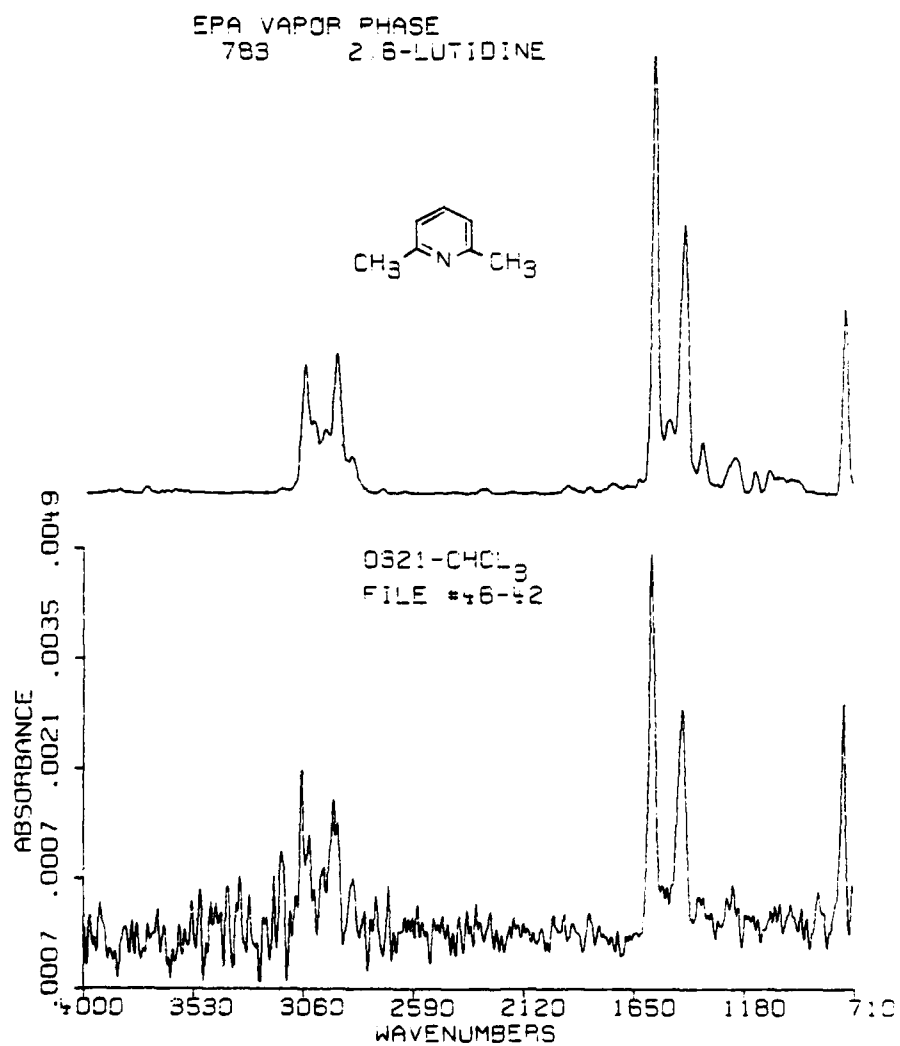B-4 for match values.

123

Figure A-5. FTIR peak file spectrum less background compared with EPA vapor phase spectrum of 2,6-lutidine. See Table B-5 for match values.

Figure A-6. FTIR peak file spectrum less background compared with EPA
vapor phase spectrum of 2,4-Lutidine. See Table B-6 for
match values.

125

EPA VAPOR PHASE
556   2-NONANONE

OS11-CHCL$_3$
FILE #517

ABSORBANCE

.0141
.0104
.0067
.0030
.0007
.0000

4000   3530   3060   2590   2120   1650   1180   710
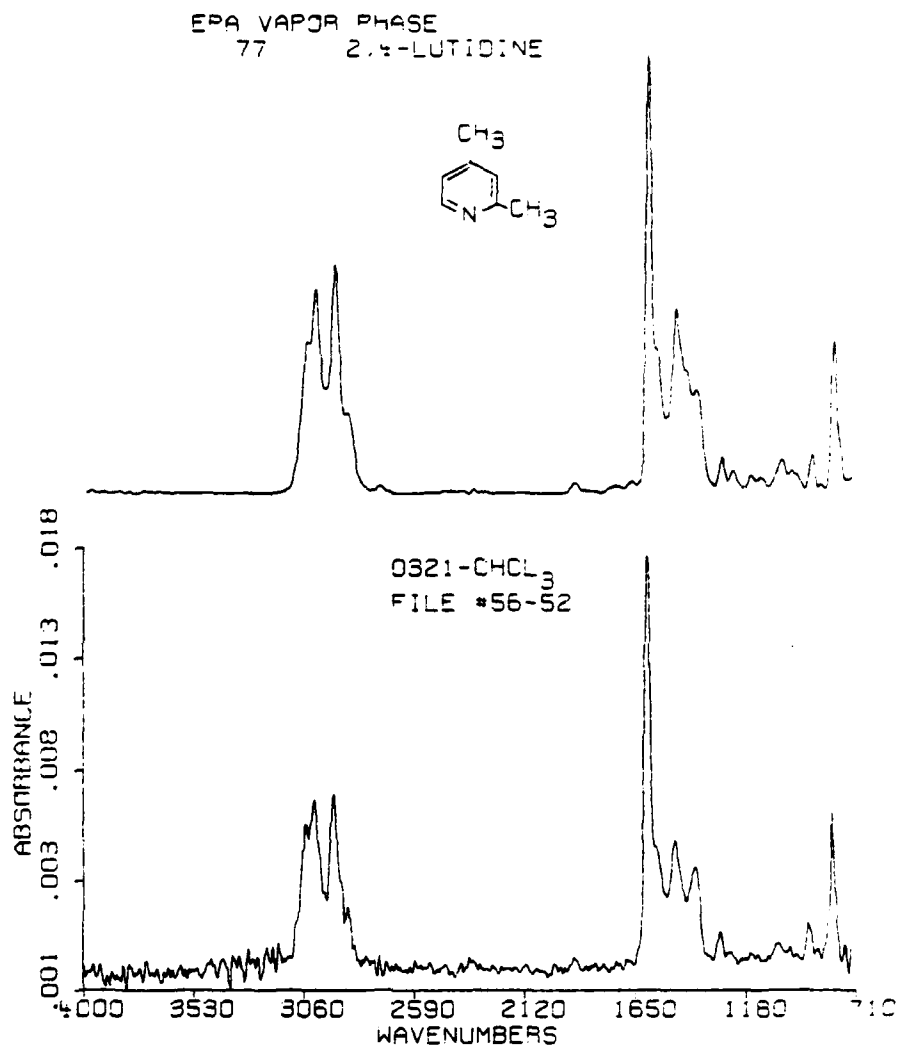WAVENUMBERS

Figure A-7. FTIR peak file spectrum less background compared with
EPA vapor phase spectrum of 2-nonanone. See Table B-7
for match values.

126

Figure A-8. FTIR peak file spectrum less background compared with EPA vapor phase spectrum of 2-methoxy ethanol. See Table B-8 for match values.

127

Figure A-9. FTIR peak file spectrum compared with EPA vapor phase
spectrum of 2-pentanol. See Table B-9 for match values.

EPA VAPOR PHASE
964   PHTHALIC ACID   DIBUTYL ESTER

0986-CHCL3
FILE #548-340

Figure A-10.   FTIR peak file spectrum less background compared with
EPA vapor phase spectrum of dibutyl phthalate. See
Table B-10 for match values.

129

EPA VAPOR PHASE
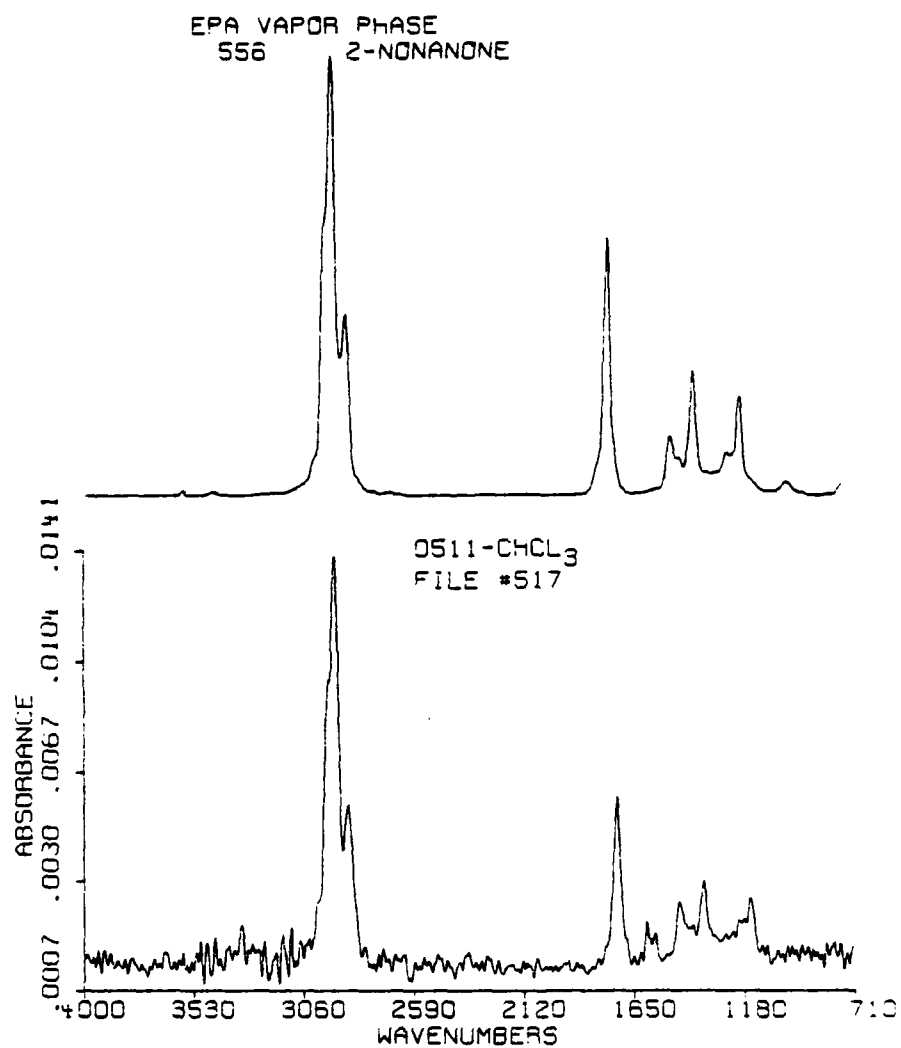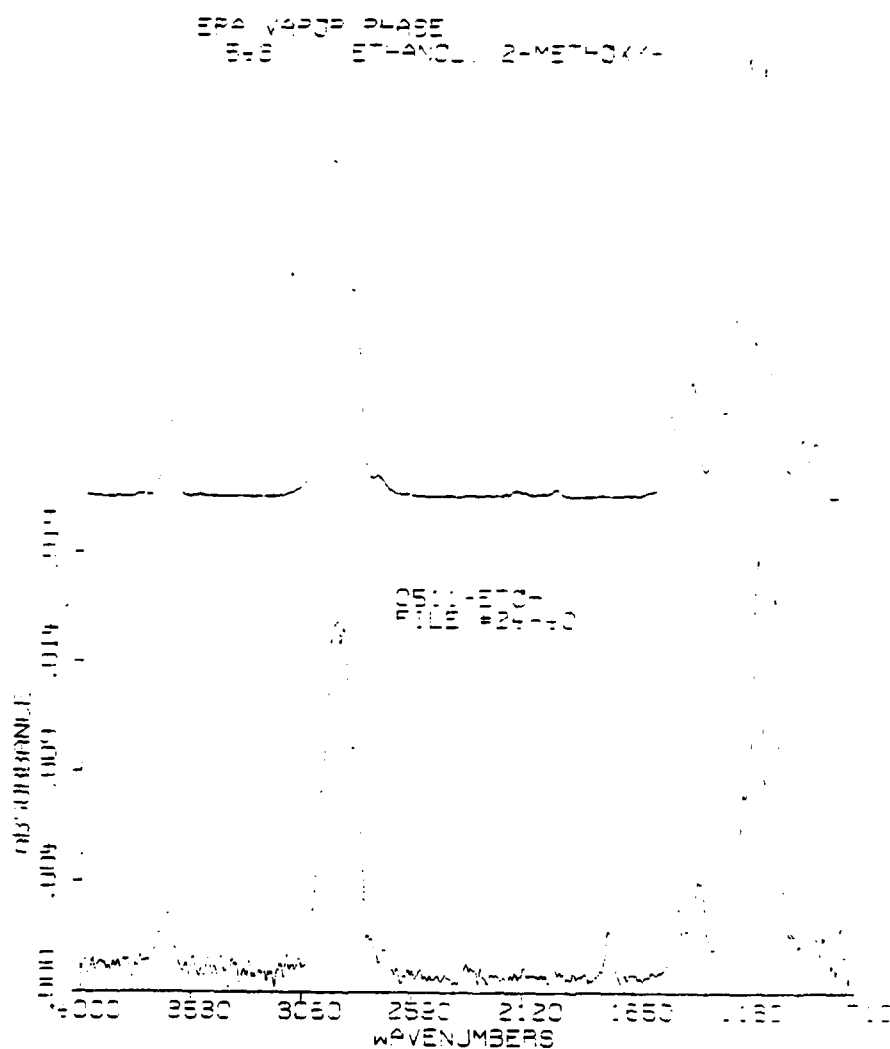543   ETHANOL, 2-METHOXY-,

0986-ETOH
FILE #33-21

Figure A-11. FTIR peak file spectrum less background compared with
EPA vapor phase spectrum of 2-methoxy ethanol. See
Table B-11 for match values.

130

Figure A-12. FTIR peak file spectrum less background compared with EPA vapor phase spectrum of 2,4-dichloro benzoic acid and o-iodo benzoic acid. See Table B-12 for match values.

131

Figure A-13. FTIR peak file spectrum less background compared with
EPA vapor phase spectrum of o-tert-butyl phenol. See
Table B-13 for match values.

132

Figure A-14. FTIR peak file spectrum less background compared with EPA vapor phase spectrum of 2,4-di-tert-butyl phenol. See Table B-14 for match values.

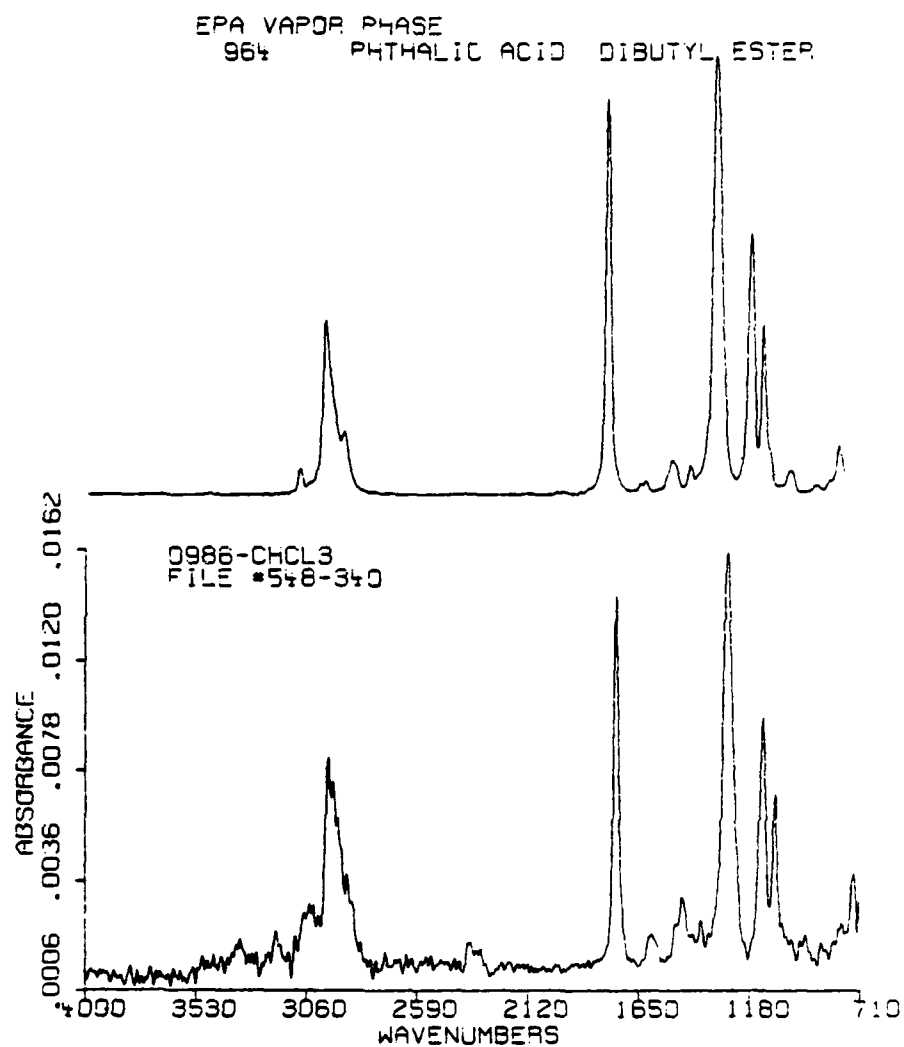133

EPA VAPOR PHASE
96%   PHTHALIC ACID, DIBUTYL ESTER
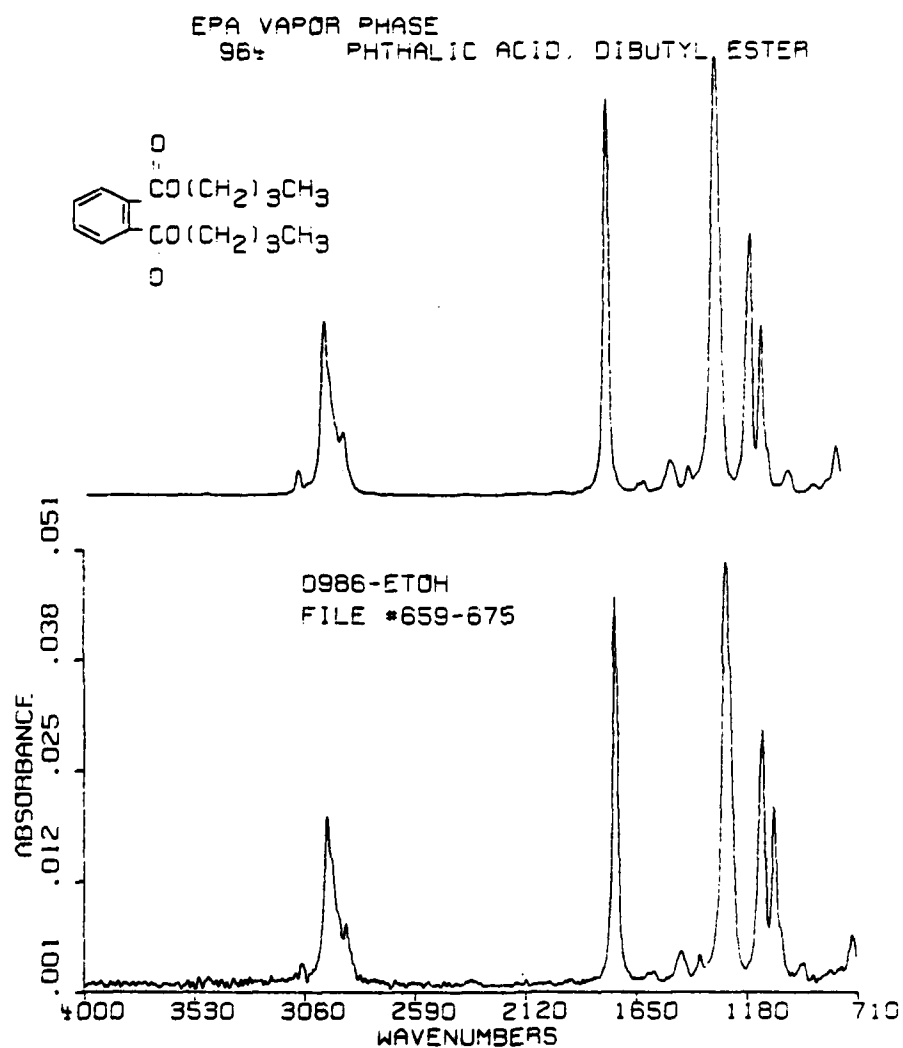
Figure A-15. FTIR peak file spectrum less background compared with
EPA vapor phase spectrum of dibutyl phthalate. See
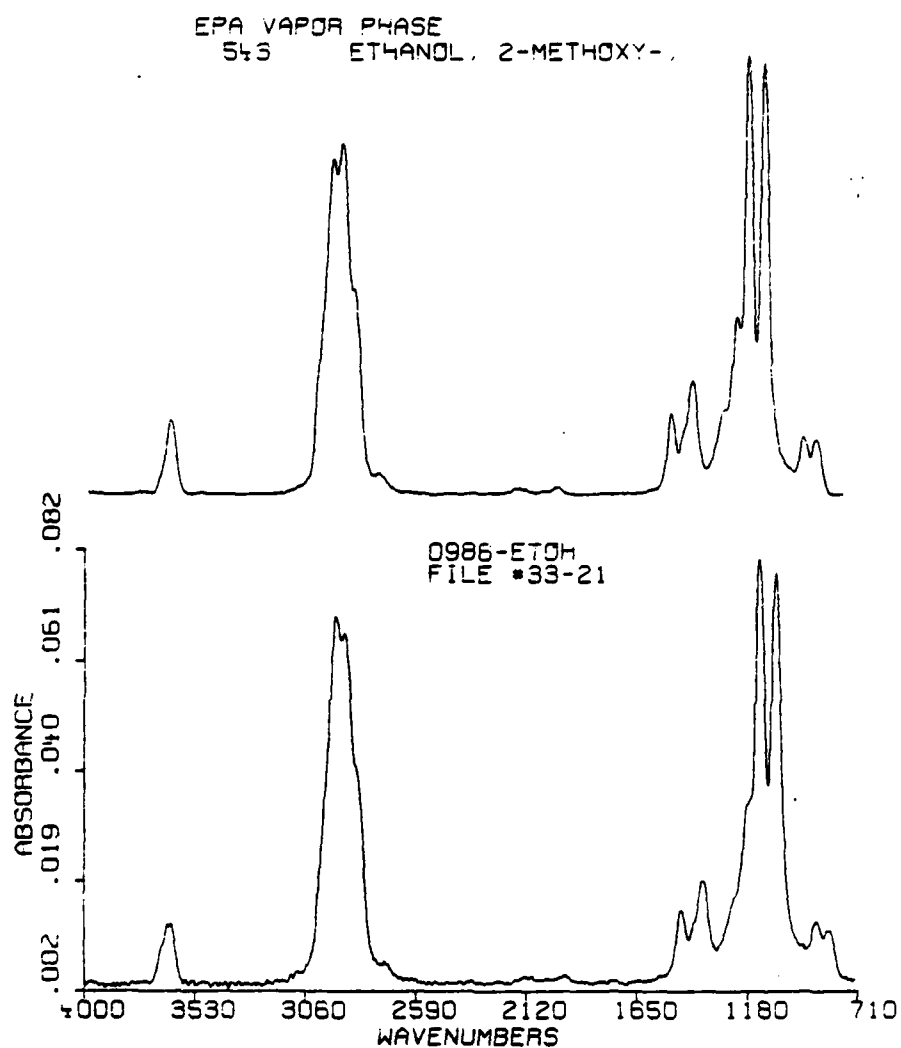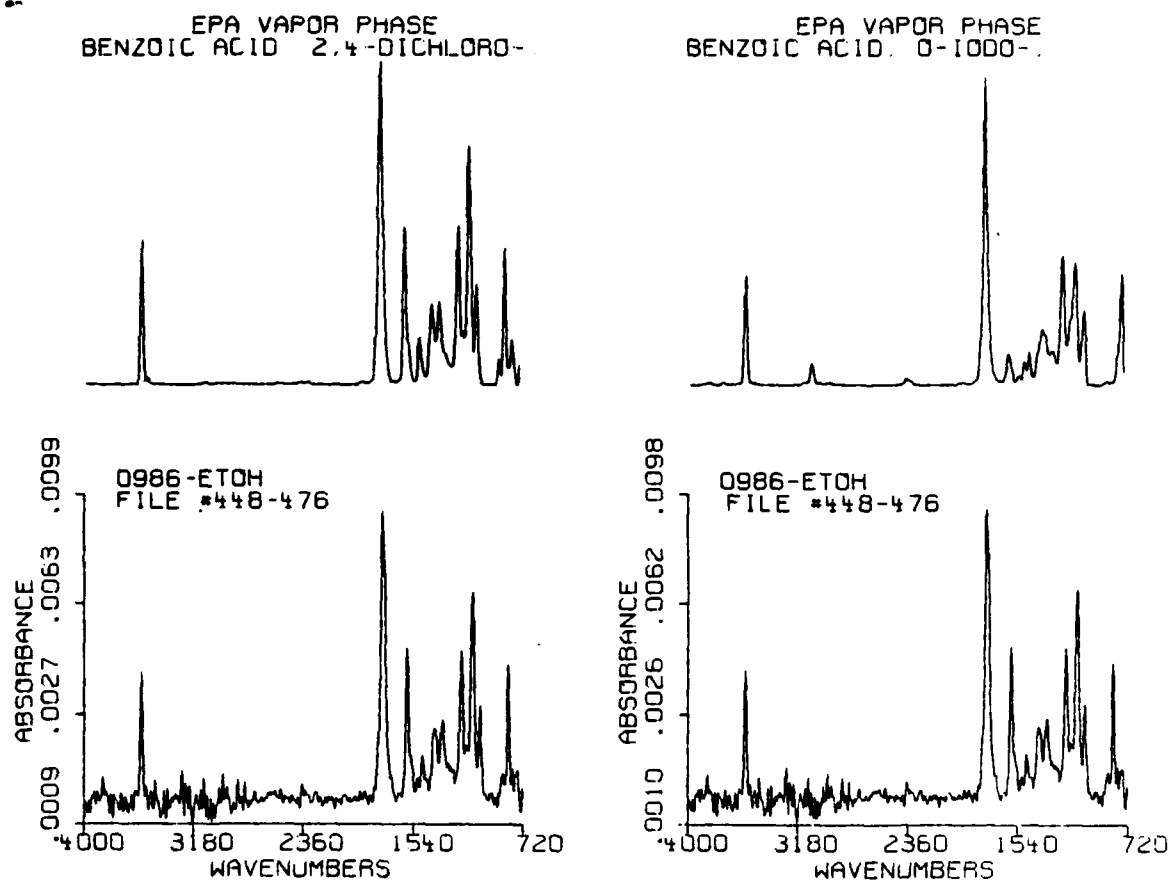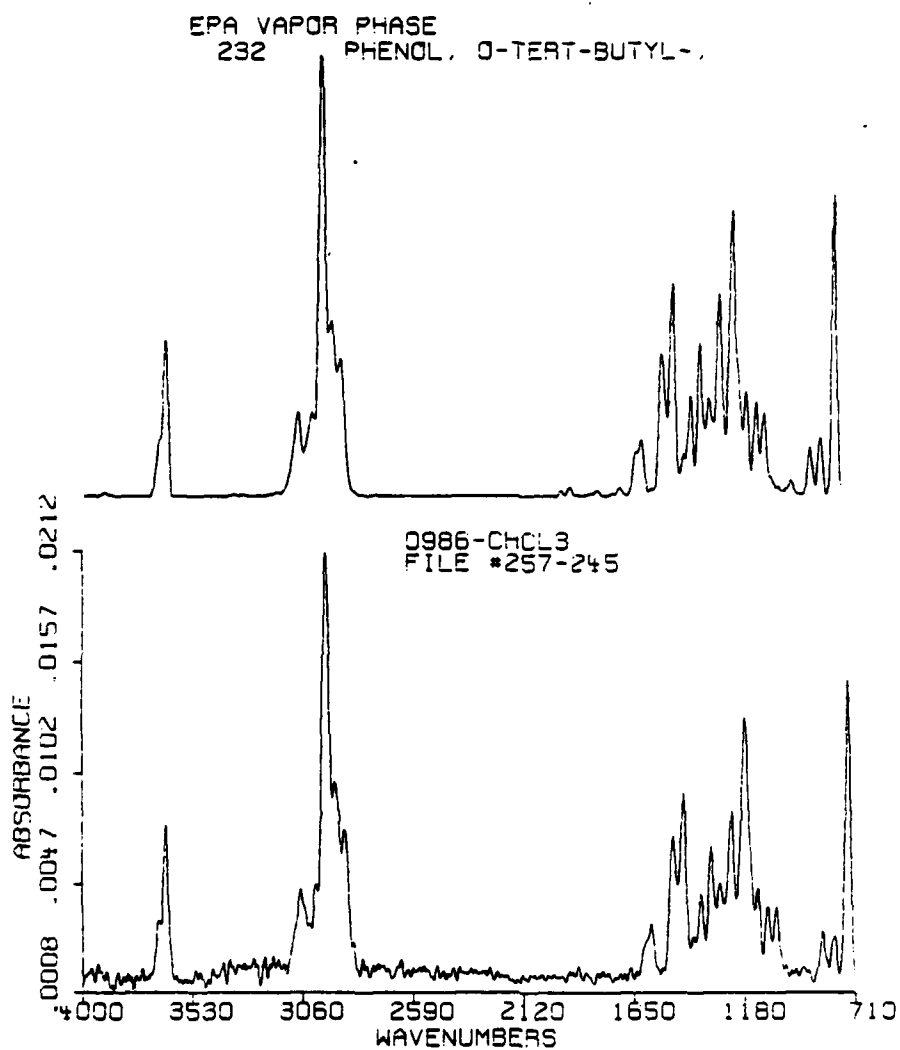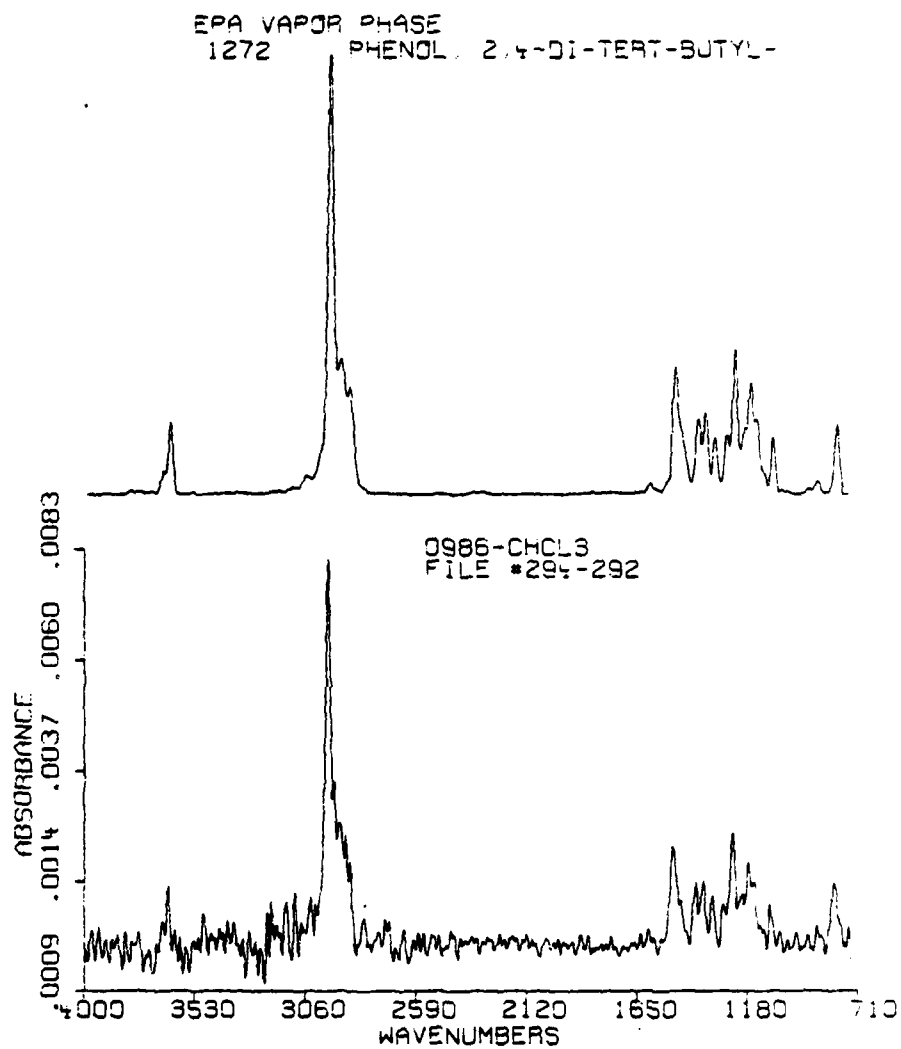Table B -15 for match values.

134

APPENDIX B

COMPUTER SEARCH ROUTINE RESULTS
FOR CONFIDENT MATCHES IN JET
FUEL SEPARATIONS

135

TABLE B-1

Computer Search Routine Results For
File (763-757) in the Separation of 005-Chloro[a]

EPA Vapor Phase Library Number	Match Value	Compound
1107	336	phenanthrene
2280	345	2-benzylpyridine
371	356	bromoform
3306	358	3-phenylpyridine

[a]See Figure A-1.

TABLE B-2

Computer Search Routine Results For
File (304-323) in the Separation of 005-Chloro[a]

EPA Vapor Phase Library Number	Match Value	Compound
946	86	phenyl-ether
1469	241	4-phenoxybiphenyl
949	323	p-bromophenyl phenylether
1699	705	p-bromophenetole

[a]See Figure A-2.

136

TABLE B-3
Computer Search Routine Results For
File (214-208) in the Separation of 005-Chloro[a]

EPA Vapor Phase Library Number	Match Value	Compounds
232	444	o-tert-butyl phenol
2210	671	o-sec-butyl phenol
2102	708	o-sec-pentyl phenol
3303	945	2-tert-butyl-6-methyl phenol

[a]See Figure A-3.

TABLE B-4
Computer Search Routine Results For
File #123 in the Separation of 0321-Chloro[a]

EPA Vapor Phase Library Number	Match Value	Compounds
218	718	s-collidine
77	1169	2,4-lutidine
2442	1689	di-3,5-xylylamine
2808	2374	8-aminoquinaldine

[a]See Figure A-4.

137

TABLE B-5
Computer Search Routine Results For
File (46-42) in the Separation of 0321-Chloro[a]

EPA Vapor Phase Library Number	Match Value	Compounds
783	917	2,6-lutidine
1239	1518	m-chloro-α,α-dibromo toluene
60	1562	1-chloro-1-nitropropane
832	1708	α-chlorotoluene

[a]See Figure A-5.

TABLE B-6
Computer Search Routine Results For
File (56-52) in the Separation of 0321-Chloro[a]

EPA Vapor Phase Library Number	Match Value	Compounds
77	299	2,4-Lutidine
2235	1294	4-picoline
2442	1422	di-e,t-xylylamine
29-9	1751	8-aminoquinaldine

[a]See Figure A-6.

TABLE B-7
Computer Search Routine Results For
File (517) in the Separation of 0511-Chloro[a]

EPA Vapor Phase Library Number	Match Value	Compounds
556	281	2-nonanone
654	31?	4-dodecanone
734	333	3-undecanone
2179	342	7-tridecanone

[a]See Figure A-7.

TABLE B-8
Computer Search Routine Results For
File (24-40) in the Separation of 0511-Eth[a]

EPA Vapor Phase Library Number	Match Value	Compounds
543	311	2-methoxy ethanol
1731	1675	diethylene glycol
3016	1942	2-ethoxy ethanol
1058	1991	butyl cellosolve

[a]See Figure A-8.

TABLE B-9
Computer Search Routine Results For
File (69) in the Separation of 0511-Eth[a]

EPA Vapor Phase Library Number	Match Value	Compounds
389	253	2-pentanol
600	353	3-hexanol
439	412	2-hexanol
2021	433	3-methyl-5-ethyl-2,4-nonanediol

[a]See Figure A-9.

TABLE B-10
Computer Search Routine Results For
File (548-340) in the Separation of 0986-Chloro[a]

EPA Vapor Phase Library Number	Match Value	Compounds
964	572	dibutyl phthalate
970	719	benzyl butyl phthalate
968	720	ethoxy 2-butoxy phosphate
198	734	dipropyl phthalate

[a]See Figure A-10.

TABLE B-11
Computer Search Routine Results For
File (33-21) in the Separation of 0986-Eth[a]

EPA Vapor Phase Library Number	Match Value	Compounds
543	173	2-methoxyethanol
1731	1363	diethylene glycol
3016	1838	2-ethoxy ethanol
1058	1930	butyl cellosolve

[a]See Figure A-11.

TABLE B-12
Computer Search Routine Results For
File (448-476) in the Separation of 0986-Eth[a]

EPA Vapor Phase Library Number	Match Value	Compounds
1097	694	2,4-dichloro benzoic acid
1424	950	o-iodo benzoic acid
1086	991	niacin benzoic acid
1422	1051	o-bromo benzoic acid

[a]See Figure A-12.

141

TABLE B-13
Computer Search Routine Results For
File (257-245) in the Separation of 0986-Chloro[a]

EPA Vapor Phase Library Number	Match Value	Compounds
3264	750	2,6-di-sec-butyl phenol
231	760	2,6-diisopropyl phenol
232	843	o-tert-butyl phenol
2210	883	o-sec-butyl phenol

[a]See Figure A-13.

TABLE B-14
Computer Search Routine Results For
File (294-292) in the Separation of 0986-Chloro[a]

EPA Vapor Phase Library Number	Match Value	Compounds
879	539	m-diisopropyl benzene
935	550	p-diisopropyl benzene
3120	606	p-di-tert-butyl benezene
1026	625	3,5-diisopropyl toluene

[a]See Figure A-14.

TABLE B-15
Computer Search Routine Results For
File (659-675) in the Separation of 0986-Eth[a]

EPA Vapor Phase Library Number	Match Value	Compounds
964	19	dibutyl phthalate
198	124	dipropyl phthalate
968	152	ethoxy-2-butoxy phosphate
970	210	benzyl butyl phthalate

[a]See Figure A-15.

143

END

FILMED

1-85

DTIC